MATTHIAS SCHULTZE-KRAFT

BRAIN-COMPUTER INTERFACES FOR COGNITIVE NEUROSCIENCE AND ADVANCED MENTAL STATE ASSESSMENT

BRAIN-COMPUTER INTERFACES FOR COGNITIVE NEUROSCIENCE AND ADVANCED MENTAL STATE ASSESSMENT

vorgelegt von
M.Sc.
Matthias Schultze-Kraft
geboren in Cali, Kolumbien

von der Fakultät IV - Elektrotechnik und Informatik
der Technischen Universität Berlin

zur Erlangung des akademischen Grades
Doktor der Naturwissenschaften (Dr. rer. nat.)

Genehmigte Dissertation

Prüfungsausschuss:

Vorsitzender:	Prof. Dr. Olaf Hellwich
Gutachter:	Prof. Dr. Benjamin Blankertz
	Prof. Dr. John-Dylan Haynes
	Prof. Dr. Klaus-Robert Müller

Tag der wissenschaftlichen Aussprache: 23.09.2016

Berlin, 2016

To my son, Emil

ABSTRACT

Advancements in machine learning in combination with fundamental research in cognitive neuroscience have put forth application areas for brain-computer interfaces (BCIs) that go beyond communication and control. The ability to decode covert mental states and intentions from the electroencephalogram (EEG) in real-time – hence, to study the "brain at work" – establishes the basis for multifaceted applications of non-control BCIs. In this thesis, the use of such BCIs is demonstrated with two independent studies which both have different research directions and serve different purposes. While the first study follows what has been the traditional path of BCI research, namely the development of an application for people, the second study strikes a new path by engaging in the hitherto unsought approach to use a closed-loop BCI as a research tool for cognitive neuroscience.

The first study aims for the classification of operator workload as it is expected in many real-life workplace environments. Brain-signal based workload predictors, based on modulations of the power of theta and alpha oscillations in the EEG associated with workload changes, were explored. The predictors differed with respect to the level of label information required for training, including an entirely unsupervised approach. This was made possible by employing state-of-the-art EEG spatial filtering methods from machine learning. Mean classification accuracies above 90% were achieved with the supervised predictors and 82% with the unsupervised approach. The findings show that workload states can be successfully differentiated from brain signals, even when less and less information from the experimental paradigm is used, thus paving the way for real-world applications in which label information may be noisy or entirely unavailable.

The second study investigates the role of the readiness potential (RP), a slow cortical potential that starts more than 1 second before spontaneous, voluntary movements. Despite decades-long research in cognitive neuroscience, it has yet remained unclear whether the onset of the RP triggers a chain of events that unfolds in time and cannot be cancelled or whether people can cancel movements after onset of the RP. In this study, this question was addressed in a real-time experiment in which subjects were required to terminate their decision to move upon seeing a stop signal. This signal was elicited by a BCI that had been trained to detect RPs in the ongoing EEG. It was found that subjects could indeed cancel intended movements after the onset of the RP, however only up to a point of no return at approximately 200 ms before movement onset. The finding that the onset of the RP does not trigger a ballistic process that cannot be stopped throws some light on the controversial debate regarding the role of the RP in movement preparation.

ZUSAMMENFASSUNG

Fortschritte im Maschinellen Lernen und Erkenntnisse in den Kognitiven Neurowissenschaften haben neue Anwendungsmöglichkeiten für Hirn-Computer-Schnittstellen (HCS) hervorgebracht, die über die gängigen Kommunikationsanwendungen hinaus gehen und auf der Echtzeit-Erkennung verdeckter mentaler Zustände und Absichten im Elektroenzephalogramm (EEG) basieren. Diese Dissertation demonstriert dies anhand von zwei unabhängigen Studien, die jeweils unterschiedliche Forschungsziele haben. Während sich die erste Studie mit der traditionellen Entwicklung einer personenbezogenen Anwendung beschäftigt, schlägt die zweite Studie einen neuen Pfad ein und verfolgt das Ziel, HCS direkt als Werkzeug für Forschung in den Kognitiven Neurowissenschaften einsetzen zu können.

Die erste Studie strebt die Klassifizierung von Arbeitslast an, wie sie in vielen Arbeitsplatzumgebungen zu erwarten ist. Dazu wurden verschiedene Arbeitslast-Prädiktoren untersucht, die auf Energiemodulationen von theta- und alpha-Oszillationen im EEG beruhen, welche mit Änderungen von Arbeitslast einhergehen, einschliesslich eines komplett nicht-überwachten Prädiktors. Um dies zu ermöglichen, wurden allerneueste Methodenentwicklungen aus dem Maschinellen Lernen benutzt. Mit den überwachten Methoden wurden durchschnittliche Klassifizierungsgenauigkeiten von über 90% erreicht, mit dem nicht-überwachten Ansatz 82%. Diese Ergebnisse zeigen, dass Arbeitslast-Zustände anhand von Hirnsignalen erfolgreich differenziert werden können, selbst wenn zunehmend weniger Information über das experimentelle Paradigma benutzt wird. Damit ist der Weg geebnet für Praxisanwendungen, wo Kennsatz-Information oft verrauscht oder erst gar nicht vorhanden ist.

Die zweite Studie untersucht die Funktion des Bereitschaftspotentials (BP), ein EEG-Signal, das mehr als 1 Sekunde vor spontanen, absichtlichen Bewegungen beginnt. Trotz jahrzentelanger Forschung herrscht noch Unklarheit darüber, ob das Einsetzen des BP eine Ereignisskette in Gang setzt, die sich nicht mehr aufhalten lässt oder ob Menschen eine Bewegung selbst nach Einsetzen des BP stoppen können. Diese Frage wurde in einem Echtzeit-Experiment untersucht, in dem Versuchsteilnehmer aufgefordert wurden, eine Entscheidung für eine Bewegung zurück zu ziehen, sobald ein Stoppsignal erschien. Dieses Signal wurde von einer HCS gesteuert, die zuvor darauf trainiert worden war, das Einsetzen von BPs im EEG zu erkennen. Das Experiment ergab, dass Versuchsteilnehmer Bewegungen selbst nach Einsetzen des BP stoppen konnten, jedoch nur bis zu einem Umkehrgrenzpunkt, der bei ungefähr 200 ms vor Einsetzen der Bewegung lag. Die Erkenntniss, dass das Einsetzen des BP nicht einen ballistischen, d.h. unaufhaltbaren, Prozess in Gang setzt, leistet einen Beitrag zur Aufklärung der kontroversen Debatte bezüglich der Rolle des BP.

ACKNOWLEDGMENTS

The completion of this thesis and the realization of the involved studies would have never been possible without the help from many people around me. Above all, I would like to thank my supervisor Prof. Dr. Benjamin Blankertz, who introduced me to the world of brain-computer interfaces, already during my time as a Masters student, and eventually headhunted me for a PhD position in his wonderful BBCI group. During all my years in that group he supported me in every possible way, was a thorough and patient mentor and gave me the freedom to pursue my own scientific interests. I further owe many thanks to Prof. Dr. Klaus-Robert Müller for his support, for providing me with the first position at the BBCI group and giving me the freedom to complete the two projects that I had started before (whose resulting papers did not make it into this thesis, unfortunately).

I am very grateful to Prof. Dr. John-Dylan Haynes for motivating and supervising the research project that eventually became the PNAS paper, as it were, the crown jewel of my thesis. His captivating and incessant interest in the matter and many fruitful discussions were an important drive for the success of this project. I also would like to thank Dan Birman, who contributed considerably to the recording and analysis of the data and writing of the manuscript and with whom I had many crucial discussions during essential stages of the project. I would like to thank Dr. Sven Dähne, who substantially contributed to the success of the second study that eventually became the JNE paper. Together we developed the main ideas for the analysis of the in parts nasty workload data, using methods he developed in our group. Many thanks also go to Prof. Dr. Gabriel Curio, who contributed numerous significant discussions and ideas at the beginning of this project. I also thank Manfred Gugler for his help in recording the data. Finally, I thank all my co-authors for allowing me to include parts of the manuscripts in this thesis.

Obviously, I also owe many thanks to many colleagues with whom I had the priviledge to work with, travel to distant conference destinations, enjoy many cheerful activities outside of science and share countless laughs. Since I don't have the space here to mention every one of you, I will do my best to catch up on that. A special thank you is reserved for Imke and Dominik for all the organizational and technical support, often in times of despair.

Last but not least, I would like to thank my mother for her moral support and love, my siblings for being always there for me, my father for his constant encouragement and proofreading of this thesis, and my friends for fulfilling the vital role of distracting me from my work to enjoy life at the fullest. Finally, I owe my greatest gratitude to my son Emil: Danke, daß du in meinem Leben bist, bleib der kluge, fröhliche Rabauke, der du bist, einer der tollsten Menschen auf diesem Planeten und mein bester Kumpel.

CONTENTS

1 INTRODUCTION 1
- 1.1 Contributions in this Thesis 2
- 1.2 Outline of this Thesis 3
- 1.3 List of Publications 4
  - 1.3.1 Included Publications 4
  - 1.3.2 Not Included Publications 5

2 FUNDAMENTALS 7
- 2.1 Measuring Brain Activity 7
  - 2.1.1 Electroencephalography 7
  - 2.1.2 Event-Related Potentials 8
  - 2.1.3 Oscillatory Activity 9
- 2.2 Brain-Computer Interfaces 10
  - 2.2.1 BCIs for Communication and Control 10
  - 2.2.2 BCIs beyond Control 11
- 2.3 Methods in BCI Research 11
  - 2.3.1 Classification and Regression 12
  - 2.3.2 EEG Spatial Filtering 14
  - 2.3.3 Removal of EOG Activity 18
  - 2.3.4 Model Selection 20

3 ADVANCING THE ASSESSMENT OF OPERATOR WORKLOAD WITH BCIS 21
- 3.1 Background and Motivation 21
  - 3.1.1 The Concept of Workload 21
  - 3.1.2 Motivation for Workload Assessment 22
  - 3.1.3 Assessment of Mental States from EEG 23
- 3.2 Goal and Challenges 23
  - 3.2.1 Challenge 1: Assess Workload from Multiple Modalities 24
  - 3.2.2 Challenge 2: Use Exclusively Brain Signals 24
  - 3.2.3 Challenge 3: Reduce Training Requirements 25
  - 3.2.4 Challenge 4: Explore the Added Value of Peripheral Physiology 26
- 3.3 Procedures 27
  - 3.3.1 The Experiment: Mimicking an Industrial Workplace 27
  - 3.3.2 Data Analysis 29
  - 3.3.3 Prediction Models 31
- 3.4 Results 34
  - 3.4.1 Impact of Task on Error Metrics and Physiology 34
  - 3.4.2 Performance of Predictive Models 35
  - 3.4.3 Inspection of Model Components 40
  - 3.4.4 Added Value of Physiological Measures 43
- 3.5 Discussion 43
  - 3.5.1 Performance Loss Due to Label Degradation 43
  - 3.5.2 The Advantage of Spatial Filtering 45

3.5.3 Interpretation of Model Components 46
3.5.4 Added Value of Peripheral Physiology 47
3.6 Critical Assessment of Challenges 47
3.6.1 Assessment of Challenge 1 47
3.6.2 Assessment of Challenge 2 48
3.6.3 Assessment of Challenge 3 49
3.6.4 Assessment of Challenge 4 49
4 INVESTIGATING THE ROLE OF THE READINESS POTENTIAL 51
4.1 The Objective of Investigation 52
4.1.1 The Readiness Potential 52
4.1.2 Is there a Point of no Return? 52
4.1.3 Can a Person Override the RP? 54
4.1.4 A Man–Machine Duel 54
4.2 Procedures 55
4.2.1 The "Duel Game" 55
4.2.2 Data Acquisition 57
4.2.3 Online BCI Predictor 57
4.2.4 Offline Analyses 58
4.3 Results 58
4.3.1 Behavioral Results 58
4.3.2 Readiness Potential 59
4.3.3 Possible Trial Outcomes 60
4.3.4 Timing of Predictions 64
4.3.5 In Search of Early Cancellations 65
4.3.6 Questionnaire 68
4.4 Discussion 69
4.4.1 Model of Results 69
4.4.2 Assessment of Hypotheses 70
5 GENERAL DISCUSSION AND CONCLUSIONS 73
5.1 Characteristics of BCIs for Applications Beyond Control 73
5.2 A BCI for Advanced Assessment of Operator Workload 74
5.3 A Closed-Loop BCI for Cognitive Neuroscience 75
5.3.1 The Role of the Readiness Potential 76
5.3.2 The Ability to "Veto" Voluntary Movements 77
5.3.3 BCIs for Movement Prediction 78
5.4 Conclusions 79
A APPENDIX 81
References 91

1 INTRODUCTION

Despite being far from providing a complete and coherent understanding, neuroscience has delivered a plethora of findings that have established a large corpus of knowledge about the function of the human brain (Kandel et al., 2000). Cognitive neuroscience in particular has so far strengthened the notion that virtually all human behavior and cognition have a neuronal correlate in the brain (Gazzaniga, 2004; Raichle, 2009). While brain processes can often be directly linked to overt behavior, it is the realm of covert mental states and intentions that is hidden in the inaccessible mind of a person and therefore eludes a forthright investigation. Often in research, the prevalent approach to overcome this handicap is to link recorded brain activity to subsequently obtained subjective reports (Hebb, 2005). And yet, it seems most intriguing to depart from such retrospective analyses and study the relationship between brain processes and covert mental states in *real-time*, that is to study the "brain at work".

In humans, this endeavor was pioneered by brain-computer interfaces (BCIs) based on the electroencephalogram (EEG) (Berger, 1929). The original motivation for the development of BCIs was to provide paralyzed patients with a direct communication and control channel through thought (Birbaumer et al., 1999; Wolpaw et al., 2002), making the use of efferent pathways obsolete. The BCI achieves this by converting brain activity patterns, which are associated with the willful generation of mental states by the user, into meaningful control signals (Dornhege, 2007; Wolpaw and Wolpaw, 2012). One of the principles for such BCIs, the detection motor imagery-induced modulation of the sensorimotor rhythm (Pfurtscheller and Da Silva, 1999), represents one of the first covert mental states being detected in real-time from ongoing neural activity. This endeavor has been consistently fostered by advancements in and contributions from the machine learning community which have substantially improved signal processing approaches, allowing to decode relevant information from the intrinsically noisy and convoluted measurements of brain activity (Dornhege et al., 2007; Blankertz et al., 2008; Tomioka and Müller, 2010; Dähne et al., 2014a; Dähne et al., 2014b).

While BCI research has primarily been focused on its use as an assistive technology in the medical context, since the turn of the century research has expanded towards BCI applications that go beyond control (Blankertz et al., 2010) and entails the use of BCIs for the assessment of a variety of covert mental states and intentions (Kohlmorgen et al., 2007; Müller et al., 2008; Schubert et al., 2008; Abbass et al., 2014; Haufe et al., 2014b).

1.1 CONTRIBUTIONS IN THIS THESIS

At the core of this thesis is the use of such BCIs that allow a person to engage with a self-paced task, while the BCI silently analyses the ongoing EEG in the background and infers intentions or mental states from it. This implicit information can then be used by the BCI to interact with the individual based on specific purposes. The versatile scope of application is exemplified in two independent studies which both have different research directions and serve different purposes, and yet both exploit the virtues of such BCI, namely the ability of real-time decoding of information from and interaction with the "brain at work".

Advancing the Assessment of Operator Workload with BCIs

The first contribution follows what has been the traditional path of BCI research in the last decades, namely the development of an application for people, and is concerned with enhancing the interaction of humans with a machine, computer or work environment. This idea is described well by neuroergonomics (Parasuraman, 2003) which suggests to augment the development of human-machine interaction frameworks, traditionally based solely on the measurement of overt performance or subjective reports, by using neurophysiological markers related to human cognition and behavior. Given that our modern world has created many fields of activity in which humans are engaged as operators in attention-demanding and safety-critical activities (Wilde, 1982), the idea emerges to employ BCIs that monitor particular cognitive states of the operator in real-time, such as vigilance and workload, thus providing the possibility of enhancing the interaction of the operator with a machine, computer or work environment (Parasuraman and Wilson, 2008). To date, this approach has been explored in various contexts such as driving (Kohlmorgen et al., 2007; Haufe et al., 2011; Dijksterhuis et al., 2013; Haufe et al., 2014b), air traffic control (Abbass et al., 2014), piloting (Borghini et al., 2014) and industrial work environments (Venthur et al., 2010a).

The contribution in this thesis aims for the development of a BCI that assesses the level of cognitive workload of a human operator in the context of an industrial work environment by analyzing the ongoing EEG in real-time. In a study with ten participants, the ability of a BCI to differentiate different levels of operator workload from the EEG is demonstrated. Of particular importance was to reduce as much as possible the requirements that the BCI needs to achieve this goal. To this end, novel, state-of-the-art machine learning methods for the analysis of EEG data are employed (Dähne et al., 2014a; Dähne et al., 2014b). This contribution thus endeavors the advancement of workload assessment with a BCI and aims to pave the path for its application in non-laboratory conditions.

Investigating the Role of the Readiness Potential

The second contribution strikes a new path that fundamentally departs from the traditional goal of BCIs and demostrates the use of a BCI as a research tool to address a question in cognitive neuroscience. The object of investigation is the readiness potential (RP), a slow cortical potential that starts more than one second before spontaneous, voluntary movements (Kornhuber and Deecke, 1965). Although it has been suggested that the RP may constitute a part of a general mechanism of movement preparation, to date the exact nature and causal role of the RP in voluntary movements is debated controversially (Libet, 1985; Haggard, 2008; Schurger et al., 2012). This contribution aims to follow up this line of research by investigating the role of the RP and study how much the presence of the RP undermines the *degree of control* that a person exerts in the generation of voluntary movements. We therefore asked two questions: (i) Does the onset of the readiness potential trigger a chain of events that unfolds in time and cannot be cancelled, and if not, is there a *point of no return* after which an intended movement can no longer be aborted? And (ii) can individuals behave unpredictably by intentionally *overriding* the readiness potential?

One obvious and intriguing way to test the underlying hypotheses is if a person is provided with an immediate notification that a readiness potential has just started in their EEG, but *before* they have started the intended movement, thus potentially giving them the opportunity to stop the movement (Haynes, 2011). Here, the use of a BCI comes into play in a unique way: It can track the ongoing EEG, detect the occurence of a readiness potential and immediately provide this information to the subject with high temporal precision as a signal to withhold the intended movement. In this part of the thesis, the exellence of a BCI to be used in an experimental paradigm in order to investigate the outlined questions is demonstrated, thereby fostering the study of human volition with a novel approach.

1.2 OUTLINE OF THIS THESIS

Following this introduction the thesis is structured as follows. Chapter 2 is on fundamentals and provides the technical and scientific scope of the two studies. It introduces the concepts of neurophysiological measures and of several machine learning techniques used to decode information from them as well as the current state of BCI technology. Chapter 3 deals with the first study and first formulates the motivation and challenges for the development of a system capable of real-time detection of operator workload from brain signals. It then continues to present an experiment that aimed at mimicking the circumstances under which such a system would ultimately be employed and suggests a workflow for the analysis of the EEG signals recorded during the experiment, including the use of state-of-the-art machine learning methods. Eventually, the analysis results are pre-

sented, interpreted and discussed. Chapter 4 presents the second contribution. After formulating two hypotheses concerning the role of the readiness potential, an experiment is described to test these hypotheses. Subsequently, the results from the experiment are presented and the hypotheses evaluated. Finally, Chapter 5 consists of a general discussion of the two presented studies and provides a final conclusion.

1.3 LIST OF PUBLICATIONS

1.3.1 *Included Publications*

The two core parts of this thesis amount to the two aforementioned studies which were published in peer-reviewed journals and furthermore presented in parts at conferences. This thesis closely follows those publications.

Remark: In the first of the publications listed below under *Journal Articles*, the first-authorship was shared with Daniel Birman (DB). We both contributed equally to the design of the study, the recording and analysis of the data and the writing of a first version of the manuscript. When DB left the research group, the final design of the presentation of our research results, including the generation of some additional data, and all final steps of manuscript preparation and submission, was my sole responsibility.

Journal Articles

M. Schultze-Kraft, D. Birman, M. Rusconi, C. Allefeld, K. Görgen, S. Dähne, B. Blankertz, and J.-D. Haynes (2016a). The point of no return in vetoing self-initiated movements. *Proceedings of the National Academy of Sciences* 113.4, pp. 1080–1085. DOI: 10.1073/pnas.1513569112

M. Schultze-Kraft, S. Dähne, M. Gugler, G. Curio, and B. Blankertz (2016b). Unsupervised classification of operator workload from brain signals. *Journal of Neural Engineering* 13.3, p. 036008. DOI: 10.1088/1741-2560/13/3/036008

Conference Abstracts

M. Schultze-Kraft, S. Dähne, G. Curio, and B. Blankertz (2013a). „Temporal and spatial distribution of workload-induced power modulations of EEG rhythms." In: *5th International BCI Meeting, Asilomar, USA*

M. Schultze-Kraft, D. Birman, M. Rusconi, C. Allefeld, K. Görgen, S. Dähne, B. Blankertz, and J.-D. Haynes (2014a). „A man vs. machine shootout duel: Do we have control over our choice-predictive brain signals?" In: *12th International Conference on Cognitive Neuroscience (ICON), Brisbane, Australia*

M. Schultze-Kraft, S. Dähne, G. Curio, and B. Blankertz (2014b). „Classification of visuomotor workload: A comparison of state-of-the-art spatial filtering methods." In: *Annual Meeting of the Organization for Human Brain Mapping (OHBM), Hamburg, Germany*

M. Schultze-Kraft, D. Birman, M. Rusconi, C. Allefeld, K. Görgen, S. Dähne, B. Blankertz, and J.-D. Haynes (2015). „Predicting and interrupting movement intentions with a closed loop BCI." in: *Annual Meeting of the Organization for Human Brain Mapping (OHBM), Honolulu, USA*

1.3.2 *Not Included Publications*

Two further studies that were published in peer-reviewed journals and presented at conferences were conducted at the beginning of my work on this thesis and are listed below. However, they ultimately did not find their way into this thesis.

Journal Articles

M. Schultze-Kraft, R. Becker, M. Breakspear, and P. Ritter (2011a). Exploiting the potential of three dimensional spatial wavelet analysis to explore nesting of temporal oscillations and spatial variance in simultaneous EEG-fMRI data. *Progress in biophysics and molecular biology* 105.1, pp. 67–79

M. Schultze-Kraft, M. Diesmann, S. Grün, and M. Helias (2013b). Noise suppression and surplus synchrony by coincidence detection. *PLoS Comput Biol* 9.4, e1002904

Conference Abstracts

M. Schultze-Kraft, M. Diesmann, S. Grün, and M. Helias (2011b). Correlation transmission of spiking neurons is boosted by synchronous input. *BMC Neuroscience* 12.1, p. 1

M. Schultze-Kraft, M. Diesmann, S. Grün, and M. Helias (2011c). „How much synchrony would there be if there was no synchrony?" In: *Ninth Göttingen Meeting of the German Neuroscience Society, Göttingen, Germany*

2

FUNDAMENTALS

2.1 MEASURING BRAIN ACTIVITY

The first prerequisite for the study of the human brain is the ability to quantify neural activity. Technological advances in the course of the last hundred years have provided increasingly refined methods that measure neural activity at multiple temporal and spatial scales (Hodgkin and Huxley, 1952; Cohen et al., 1968; Jobsis, 1977; Wyler et al., 1984; Kwong et al., 1992; Scanziani and Häusser, 2009). Being the primary method of choice for use in BCIs, this thesis focuses on the electrophysiological measure called electroencephalogram (EEG) (Berger, 1929). The following sections provide a basic understanding of the generation of EEG signals and introduce the two most important neurophysiological phenomena observed in EEG signals, event-related potentials and oscillatory activity.

2.1.1 *Electroencephalography*

The human EEG, first described by Berger (1929), measures changes in electrical potentials between electrodes placed on the scalp. There are three types of signal sources that contribute to its formation: Electrical activity of large numbers of (mostly) cortical neurons, physiological artifacts of non-cerebral origin such as muscle and ocular activity, and non-physiological artifacts from the measurement apparatus. While the two latter contributions are not entirely unavoidable, EEG experiments take precautions to keep them to a minimum.

The cerebral contribution to the EEG is a result of the synchronous activity of approximately one hundred billion heavily interconnected neurons. Closely following Baillet et al. (2001), Nunez and Srinivasan (2005), and Wolters and Munck (2007), the generating mechanism can be summarized as follows. Neurons are specialized cells which communicate with each other via short electrical pulses and chemical processes. By means of ionic pumps, a high concentration of potassium ions is maintained inside the cell, while a high concentration of sodium and calcium ions is maintained in the extracellular matrix. This creates an electrical gradient that keeps the membrane of neurons electrically charged. Neurons can be subdivided into three main compartments: the cell body (soma), the dendrites and the axon. Signal transmission between neurons can be roughly described by the following process: By means of synapses, neurotransmitters are released from the presynaptic cell and enter the postsynaptic cell at their dentritic tree. This causes a small, transient change in polarization of the postsynaptic cell called a postsynaptic potential (PSP). These PSPs travel along the dentrites to the soma where they are in-

tegrated and depolarize the cell membrane. If this depolarization reaches a certain threshold various voltage-dependent ion channels are activated in succession, which creates an action potential. This electric pulse, mediated through an ion current flow and chemical transmission at the synapses, travels along the axon of the cell and via synapses in turn excites the next postsynaptic cell. This current flow is called the primary current.

However, the rule of conservation of electric charges implies that there is also current flow in the opposite direction. This secondary volume current travels through the extracellular matrix of the neuron. Given the geometric and conductive properties of the traversed media, which are the brain, the cerebrospinal fluid, the scull and scalp tissue, the volume current of a single neuron would not be measureable at the scalp. However, here two important properties of brain anatomy and function come into play. First, the most prominent type of neurons in the cortex, the pyramidal cells, are organized in layers and have an apical dendrite that is oriented perpendicularly to the scalp. And second, due to their heavy interconnected nature, neurons tend to be synchronously activated in large ensembles. Therefore, their primary currents add and the corresponding secondary currents, which spread over the whole volume conductor, are strong enough to be measurable as scalp potentials. The dynamics observed in the EEG signals is assumed to be caused by interacting networks of such active cortical patches. EEG is usually recorded unipolar, that is by recording all channels against a single or a pair of reference electrodes. For reproducibility, recording electrodes are placed on the scalp according to a fixed scheme, for which the extended 10-20 international system is commonly used.

2.1.2 *Event-Related Potentials*

Event-related potentials (ERPs) are characteristic deflections in the EEG following internally or externally triggered events (Luck, 2014). They exhibit a spatio-temporal signature that depends on the location of the active cerebral current sources involved in the processing of the event and the spatio-temporal dynamics of source activition. The amplitude of ERPs typically lies in the range of 1-20 μV, which is approximately 1-2 orders of magnitude below the background activity level. However, because they are both time and phase-locked to the event, each component of the complex has a latency and polarity that is approximately the same for repetitions of the event. Therefore, ERPs are usually estimated from multiple repetitions of the same event by averaging the respective event-locked EEG segments. This procedure increases the signal-to-noise ratio (SNR) of ERPs by cancelling out EEG activity that is unrelated to the task.

External events that elicit ERP responses have long since been reported as triggered by visual (Spehlmann, 1965; Jeffreys and Axford, 1972), auditory (Davis, 1939) or tactile and electrical (Penfield and Boldrey, 1937) stimuli. An ERP is typically considered a complex

that consists of several components that exhibit a characteristic spatio-temporal shape. While early components (w.r.t. stimulus onset) reflect the processing of physical properties of the stimulus (Polich, 1989), later components are increasingly cognitive in nature, that is they can be modulated by top-down processes such as attention (Hillyard et al., 1973), semantic processing (Falkenstein et al., 2000) and expectation (Walter et al., 1964). The study of event-related potentials has widespread applications in clinical diagnosis and psychophysiology (Fabiani et al., 2000).

More importantly, ERPs have proven to be excellent signals to be used for the control of brain-computer interfaces (Blankertz et al., 2011), as already suggested by Vidal (1973). Among the various types of ERPs used for BCIs are visually evoked potentials (Müller-Putz et al., 2005), auditory evoked potentials (Schreuder et al., 2010) and the P300 (Farwell and Donchin, 1988). The most promiment example of an internally triggered ERP is the readiness potential (RP), first described by Kornhuber and Deecke (1965) (see Section 4.1.1).

2.1.3 *Oscillatory Activity*

The EEG power spectrum typically exhibits a characteristic $1/f$ shape (Penttonen and Buzsáki, 2003). However, this spectrum is often found to be superimposed by one or more spectral peaks representing increased oscillatory activity in particular frequency bands (Buzsaki and Draguhn, 2004). The most prominent is the alpha band which ranges in the frequency 8 to 13 Hz and is often observable with the naked eye in unfiltered EEG data. Other relevant frequency bands include the delta band (1-3 Hz), the theta band (4-7 Hz), the beta band (14-30 Hz) and the gamma band (30 to more than 100 Hz). Modulations of the oscillatory power of all frequency bands are associated with various cognitive and sensory phenomena, including alterness (Jung et al., 1997), attention (Harmony et al., 1996; Klimesch et al., 1998; Bauer et al., 2006), memory encoding (Klimesch, 1999; Jensen and Colgin, 2007), workload (Gevins and Smith, 2003; Holm et al., 2009) and perception (Makeig and Jung, 1996; Thut et al., 2006; Schubert et al., 2009). Alpha power is further modulated by the amount of relaxation of the visual system, is strongest when the eyes are closed and over perieto-occipital areas (Niedermeyer, 1997).

Similarly, the related mu rhythm lies in a similar frequency band, is strongest over central areas and is related to the level of relaxation of the motor system. Its power, as well as that of the beta band, decreases when movements are observed (Babiloni et al., 2002) and executed or even imagined (Pfurtscheller and Da Silva, 1999). This process is called event-related desynchronization (ERD) (Pfurtscheller and Da Silva, 1999) and is utilized in a type of brain-computer interfaces, where the willful modulation of EEG band power via motor imagery is used to control computer applications, such as spelling programs (Blankertz et al., 2007b; Blankertz et al., 2008). Interestingly, this desynchronization is not only observed during movement

but starts up to two seconds before voluntary, self-initiated movements (Pfurtscheller and Aranibar, 1979; Bai et al., 2005).

2.2 BRAIN-COMPUTER INTERFACES

At the Ostler Society of Oxford in 1964, Grey Walter presented an experiment that he never published but that was recounted only much later by Dennett (1993). This experiment, in which a patient was able to advance slides of a slide's projector whenever his brain activity indicated that he intended to press the button, represents the first reported instance of a brain-computer interface. The term BCI was then introduced by Vidal (1973) who suggested to make use of externally triggered event-related potentials in order to control an apparatus or device.

2.2.1 *BCIs for Communication and Control*

Although an array of BCI applications have emerged ever since, so far BCI research has primarily focused on its application as an assistive technology for individuals with complete (or near-complete) paralysis. If all or most motor functions are compromised a BCI can decode information from otherwise intact brain areas and use these to control a computer program or device, thus superseding the brain's natural efferent pathways (Birbaumer et al., 1999; Dornhege, 2007).

The concept of such a communication channel relies on the assumption that a person can willfully alter his brain state to express an intention (Sutton et al., 1965), thus allowing for direct "communication and control" through thought (Wolpaw et al., 2002). Research has shown that BCIs can be controlled using a variety of measurements of brain activity, such as intracortical recordings (Nicolelis, 2003), electrocorticography (ECoG) (Leuthardt et al., 2004; Leuthardt et al., 2006), functional magnetic resonance imaging (fMRI) (Weiskopf et al., 2004), functional near-infrared spectroscopy (fNIRS) (Coyle et al., 2004; Fazli et al., 2012) and magnetoencephalography (MEG) (Mellinger et al., 2007). However, due to its high temporal resolution and cost efficiency, the EEG has been the single most widely used measurement of brain activity in BCI research (Mason et al., 2007). Most BCIs for communication use the user's intention to control a computer programm, typically a speller. Since the turn of the century, progress in BCI research has been accelerated by constant advancements in machine learning (Blankertz et al., 2002; Dornhege et al., 2007; Tomioka and Müller, 2010).

In principle, there exist two basic types of brain-computer interfaces for communication, which differ with respect to the signal they use: event-related potentials (EPRs) and event-related desynchronization (ERD). ERP-based BCIs rely on exogenous stimulation to elicit ERP responses in the user's brain that convey information about their intention. The most widely studied ERP-based BCIs employ the so-called odball-paradigm using visual (Farwell and Donchin, 1988; Sell-

ers et al., 2006; Treder and Blankertz, 2010), auditory (Schreuder et al., 2010; Schreuder et al., 2011) or tactile stimuli (Müller-Putz et al., 2006). Other approaches use steady state visually evoked potential (SSVEP) paradigms which can be based on time modulation (Guo et al., 2008), frequency modulation (Müller-Putz et al., 2005; Allison et al., 2008), and code modulation (Bin et al., 2011). BCIs that use ERD for control employ the motor imagery (MI) paradigm (Wolpaw and McFarland, 2004; Blankertz et al., 2007a) and provide asynchronous, continuous output signals that are optimal for applications such as motor control and object manipulation (Pfurtscheller et al., 2003; Galán et al., 2008).

2.2.2 *BCIs beyond Control*

Early findings that assocciated electrocortical activity with task performance and cognitive states such a vigilance (Beatty et al., 1974; Matousek and Petersén, 1983) laid the foundations for the idea to use ongoing EEG activity in order to infer particular mental states of the users and thus provide the possibility of enhancing the interaction of humans with machines, computers or work environments (Parasuraman, 2003; Parasuraman and Wilson, 2008). Only recently and going hand in hand with advancements in data analysis methods, BCI research beyond control and communication has expanded considerably (Müller et al., 2008; Blankertz et al., 2010; Zander and Kothe, 2011; Erp et al., 2012).

For instance, the interaction with software interfaces can be adapted by a BCI by exploiting implicit information about the cognitive state of its user (Nicolae et al., 2015; Uščumlić and Blankertz, 2016; Wenzel et al., 2016). Furthermore, the design of products can be optimized based on its direct effect on neural processes, such as the quality perception of speech (Porbadnigk et al., 2013) and video (Scholler et al., 2012; Acqualagna et al., 2015). BCIs can also detect specific brain states before they trigger behavioral actions, particularly in safety-critical applications such as in emergency braking situations during driving (Haufe et al., 2014b). Furthermore, BCIs have successfully been used to assess workload as induced by the n-back task (Prinzel et al., 2000; Scerbo et al., 2003), in air traffic control (Abbass et al., 2014), in piloting (Borghini et al., 2014), in a simulated driving environment (Dijksterhuis et al., 2013) or in real traffic conditions (Kohlmorgen et al., 2007).

2.3 METHODS IN BCI RESEARCH

The work with brain-computer interfaces involves the use of several signal processing and analysis methods. The following sections describe the methods that are essential in this thesis. First, the classification and regression methods and their regularization approach are described. Subsequently, four EEG spatial filtering methods and the linear generative model of EEG, on which they are based, is presented. Finally, a method for the removal of EOG activity and the

approach for model selection fundamental to BCI research, namely cross-validation, are described.

2.3.1 *Classification and Regression*

Classification and regression are both instances of supervised learning (Bishop, 2007). The goal of classification is to use the features of an object on order to determine to which class it belongs. By using features from the data, it finds a separating hyperplane such that both classes are maximally separated. From the many methods that exist for classification, in this thesis one is employed that has proven to be a powerful tool for classification of binary classes extracted from EEG data (Friedman, 1989; Blankertz et al., 2011), the Linear Discriminant Analysis (LDA). Given that often the number of observations available for training a classifier is small, it is advisable to regularize the classifier, which is achieved by shrinking the estimated covariance matrix (Ledoit and Wolf, 2004; Schäfer, Strimmer, et al., 2005; Bartz and Müller, 2013). The concepts of LDA and shrinkage are described in the following.

Linear Discriminant Analysis

Given two class-distributions, Linear Discriminant Analysis (LDA) is the optimal classifier in the sense that it minimizes the risk of misclassification for new samples drawn from the same distributions, assuming that the following three criteria are fulfilled: (a) The features of each class are Gaussian distributed, (b) Gaussians of all classes have the same covariance matrix and (c) the true class distributions are known (Friedman, 1989). The first two criteria are largely satisfied by a variety of features extracted from the EEG, such as ERP amplitudes and the magnitude of ERD. The last criterion is obviously never satisfiable with real data, means and covariance matrices of the distributions have to be estimated from those data. The estimation bias that is expected to occur with high dimensional data is dealt with regularization (see section below).

A LDA classifier can be characterized by a projection vector $\boldsymbol{w}$ and a bias term b, which refer to the separating hyperplane $\boldsymbol{w}^\top \boldsymbol{x} + b = 0$. The weight vector of an LDA classifier is defined by

$$\boldsymbol{w} = \hat{\boldsymbol{\Sigma}}^{-1}(\hat{\mu}_2 - \hat{\mu}_1) \tag{1}$$

and the bias

$$b = \boldsymbol{w}^\top \frac{(\hat{\mu}_1 + \hat{\mu}_2)}{2} \tag{2}$$

where $\hat{\mu}_c$ is the mean of class c, and $\hat{\boldsymbol{\Sigma}}$ is the pooled covariance matrix, that is the average of the class-wise covariance matrices. A class label can then be assigned to a data point $\boldsymbol{x} \in \mathbb{R}^N$ according to $\text{sign}(\boldsymbol{w}^\top \boldsymbol{x} - b)$.

Regularization

The class means and class-wise covariance matrices of an LDA classifier both have to be estimated from the data. For the empirical covariance matrix, this may become a problem when only a small number of observations n are available compared to the number of dimensions d of the data. This is particularly the case for $d > n$ and leads to a systematic error where large eigenvalues of the covariance matrix are estimated too large, and small eigenvalues are estimated too small (Bartz and Müller, 2013). Because this error is detrimental for the performance of an LDA classifier, it is essential to mitigate this effect with regularization. Different approaches for regularization exist (Tomioka and Müller, 2010). In an approach called shrinkage, the empirical covariance matrix is shrunk, i.e. made more spherical. This is achieved by replacing $\hat{\mathbf{\Sigma}}$ with

$$\tilde{\mathbf{\Sigma}}(\gamma) = (1-\gamma)\hat{\mathbf{\Sigma}} + \gamma\nu\mathbf{I}, \tag{3}$$

where ν is the average eigenvalue of $\hat{\mathbf{\Sigma}}$. The hyperparameter $\gamma \in [0, 1]$ tunes the degree to which $\hat{\mathbf{\Sigma}}$ is shrunk towards a spherical covariance matrix with $\gamma = 0$ meaning unregularized LDA and $\gamma = 1$ yielding a perfectly spherical covariance matrix. One possible way to define an optimal γ is via cross-validation (see Section 2.3.4), however, such an approach is very time-consuming. Fortunately, an analytical method exists to calculate the optimal shrinkage parameter where large sample-to-sample variance in the empirical covariance are penalized with a stronger shrinkage (Ledoit and Wolf, 2004; Schäfer, Strimmer, et al., 2005). Let $x_1, \ldots, x_n \in \mathbb{R}^d$ be n feature vectors and let $(x_k)_i$ resp. $(\hat{\mu})_i$ be the ith element of the vector x_k resp. $\hat{\mu}$, and define

$$z_{ij}(k) = ((x_k)_i - (\hat{\mu})_i)((x_k)_j - (\hat{\mu})_j), \tag{4}$$

then the optimal shrinkage parameter can be found by

$$\gamma^* = \frac{n}{(n-1)^2} \frac{\sum_{i,j=1}^{d} \mathrm{Var}_k(z_{ij}(k))}{\sum_{i \neq j} s_{ij}^2 + \sum_i (s_{ii} - \nu)^2}, \tag{5}$$

where s_{ij} denotes the element in the ith row and jth column of $\hat{\Sigma}$.

Ridge Regression

The goal of linear regression is to model the relationship of a target variable with a set of explanatory variables. This is achieved by using linear predictor functions whose unknown model parameters are estimated from the data. Linear regression models are often fitted using the least squares approach. LDA has been shown to be equivalent to linear regression with the class label as the output (Duda et al., 2001). Because this approach also suffers from the high dimensionality of data, its regularized version, *ridge regression*, is used in this thesis. Like with LDA, the empirical covariance matrix is shrunk using the above approach.

2.3.2 *EEG Spatial Filtering*

In this thesis, several spatial filtering methods for EEG data were used. In the following sections, first some principles, on which all methods are based, are introduced, followed by a description of the employed methods, and finally some properties and applications are discussed.

Forward Model of EEG

All described methods are based on what is called the generative or *forward model* of EEG. The forward model states that the observed data can be decomposed into a limited set of components. Each component, in turn, is characterized by a fixed spatial activation pattern and a corresponding time course of activity. The physics of electrophysiology implies that the scalp measurements are a linear superposition of the individual component activities. Thus, the mapping of component activity to the EEG recording channels is modeled by the following equation. Let $\mathbf{x}(t) \in \mathbb{R}^d$ denote the d-dimensional EEG recording at time point t, then

$$\begin{aligned} \mathbf{x}(t) &= \sum_{i=1}^{K} \mathbf{a}_i \cdot s_i(t) + \boldsymbol{\epsilon}(t) \\ &= \mathbf{A}\mathbf{s}(t) + \boldsymbol{\epsilon}(t) \,, \end{aligned} \tag{6}$$

where $\mathbf{a}_i \in \mathbb{R}^d$ denotes the spatial activation pattern and $s_i(t)$ the temporal activation of the ith component, for $i \in \{1, ..., K\}$. The matrix $\mathbf{A} = [\mathbf{a}_1, ..., \mathbf{a}_K] \in \mathbb{R}^{d \times K}$ contains the spatial activation patterns of the K components in its columns and the vector $\mathbf{s}(t) = (s_1(t), ..., s_K(t))^\top \in \mathbb{R}^K$ contains the temporal activity of all components at time point t. Activity that is not explained by the K components is captured by $\boldsymbol{\epsilon}(t) \in \mathbb{R}^d$ and considered noise.

Backward Model of EEG

The estimation of components from the data, i.e., the inversion of the generative model, is called backward modeling. In this approach, the estimation of the time courses and spatial activation patterns is parameterized by a so-called spatial filter matrix, here denoted by $\mathbf{W} \in \mathbb{R}^{d \times K}$. An estimate of the component time courses, denoted by $\hat{\mathbf{s}}$, is extracted by projecting the data onto the columns of $\mathbf{W}$. Thus,

$$\hat{\mathbf{s}}(t) = \mathbf{W}^\top \mathbf{x}(t) \,. \tag{7}$$

An estimate of the corresponding spatial activation patterns can be derived from the spatial filters using the filter-pattern transformation

$$\hat{\mathbf{A}} = \mathbf{C}\mathbf{W}\left(\mathbf{W}^\top \mathbf{C}\mathbf{W}\right)^{-1} \,, \tag{8}$$

where $\mathbf{C}$ denotes the covariance matrix of the EEG data $\mathbf{x}$. It is important to note that the neurophysiological interpretability of extracted

components, i.e. their anatomical origin and neurophysiological relevance, is not encoded in the filter coefficients, but is only possible through interpreting the spatial activation patterns (Haufe et al., 2014c).

Four State-of-the-Art Methods

From Eqs. 7 and 8 it follows that the estimation of components is reduced to finding appropriate spatial filters, i.e., columns of matrix $\mathbf{W}$. The following sections present four methods (Koles, 1991; Nikulin et al., 2011; Dähne et al., 2014a; Dähne et al., 2014b) that optimize such spatial filters based on certain assumptions about the statistics of the components that are to be extracted from the data. In particular, these methods make assumptions about the spectral properties of the component time courses. All four methods are examples of backward modeling techniques and they are all based on the linear generative model shown in Eq. (6).

In order to optimize spatial filters that extract oscillatory components it is useful to express the spectral power of a signal in terms of variance. Let $\phi_f^{\hat{s}}$ denote the spectral power of the estimated component time course $\hat{s}$ in a frequency band f. Then $\phi_f^{\hat{s}}$ is well approximated by first bandpass filtering the time-domain signal and then computing its variance, which we denote by $\mathrm{Var}(\hat{s}_f)$. Note that the variance of the (bandpass filtered) component time series can be expressed in terms of the spatial filter $\mathbf{w}$ that is necessary to extract $\hat{s}$ from the data:

$$\phi_f^{\hat{s}} \approx \mathrm{Var}(\hat{s}_f) = \mathbf{w}^\top \mathbf{C}_f \mathbf{w} \,, \tag{9}$$

where $\mathbf{C}_f$ denotes the covariance matrix of the bandpass filtered data.

A time-resolved expression for component bandpower can be derived by simply computing the variance in short consecutive time windows, also called epochs. Let these epochs be indexed by $e \in [1, \ldots, N_e]$, then we have

$$\phi_f^{\hat{s}}(e) \approx \mathbf{w}^\top \mathbf{C}_f(e) \mathbf{w} \,, \tag{10}$$

where $\mathbf{C}_f(e)$ denotes the covariance matrix of the bandpass filtered data within the eth epoch.

Method 1: Spatio-Spectral Decomposition (SSD)

The aim of Spatio-Spectral Decomposition (SSD) is to optimize spatial filters $\mathbf{W}$ for components that concentrate most of their spectral power in a given frequency band (Nikulin et al., 2011). The idea is to separate components with a "peaky" power spectrum from components which exhibit more of a $1/f$ spectrum. While the former is attributed to genuine brain processes, the latter is considered background noise. Thus, it is useful to define the spectral signal-to-noise ratio (SNR) of a component for a given frequency band f as $\frac{\phi_f^{\hat{s}}}{\left(\phi_{f-\delta}^{\hat{s}} + \phi_{f+\delta}^{\hat{s}}\right)}$, where $f-\delta$ and $f+\delta$ denote frequency bands neighboring the band of interest f. Using the variance approximation for spectral power, it is possible to

parameterize the spectral SNR of a component time course $\hat{s}$ in terms of the spatial filter $\mathbf{w}$:

$$\frac{\phi_f^{\hat{s}}}{\left(\phi_{f-\delta}^{\hat{s}} + \phi_{f+\delta}^{\hat{s}}\right)} \approx \frac{\mathbf{w}^\top \mathbf{C}_f \mathbf{w}}{\mathbf{w}^\top \left(\mathbf{C}_{f-\delta} + \mathbf{C}_{f+\delta}\right) \mathbf{w}} . \tag{11}$$

SSD optimizes the above expression for a set of weight vectors under the constrained that the component time courses are decorrelated to each other. Haufe et al. (2014a) have demonstrated the usefulness of SSD as a dimensionality reduction tool for the analysis of oscillatory processes in the EEG.

Method 2: Source Power Co-modulation (SPoC)

The bandpower of neural oscillations changes over time and these power dynamics have been related to switching of mental states. A method that optimizes spatial filters based on a presumed covaration between band power dynamics and an external target signal is the Source Power Co-modulation analysis (SPoC) (Dähne et al., 2014a). Let the variable z denote the target signal and let us further assume that z has zero mean. Then the covariance between the bandpower dynamics of a component $\hat{s}$ and the target signal z can be expressed in terms of the spatial filter $\mathbf{w}$ as

$$\begin{aligned} \mathrm{Cov}\left(\phi_f^{\hat{s}}, z\right) &= \frac{1}{N_e} \sum_{e=1}^{N_e} \phi_f^{\hat{s}}(e) \cdot z(e) \\ &= \mathbf{w}^\top \left(\frac{1}{N_e} \sum_{e=1}^{N_e} \mathbf{C}_f(e) \cdot z(e) \right) \mathbf{w} . \end{aligned} \tag{12}$$

The SPoC algorithm optimizes spatial filters that maximize the above expression under the constraint that extracted source time courses have unit variance and are mutually decorrelated.

Method 3: Common Spatial Patterns (CSP)

If the bandpower dynamics of a component are to be used in a classification setting, one can base the optimization of the spatial filters on the assumed difference of bandpower between classes. This then leads to an algorithm called Common Spatial Patterns (CSP) (Koles, 1991; Blankertz et al., 2008). CSP seeks components that maximize the class difference of bandpower. Let $\phi_{f,i}^{\hat{s}}$ and $\mathbf{C}_{f,i}$ respectively denote the power and covariance of component $\hat{s}$ for class $i \in \{1, 2\}$ and frequency band f. Then the CSP objective function can be formalized as

$$\phi_{f,1}^{\hat{s}} - \phi_{f,2}^{\hat{s}} = \mathbf{w}^\top \left(\mathbf{C}_{f,1} - \mathbf{C}_{f,2}\right) \mathbf{w} , \tag{13}$$

subject to unit variance and mutual decorrelation constraints. Note that CSP can be obtained as a special case of SPoC by encoding the class labels in the SPoC target function z.

Method 4: Canonical Source Power Co-modulation (cSPoC)

While CSP and SPoC use label information for the extraction of relevant components, canonical Source Power Co-modulation (cSPoC) (Dähne et al., 2014b) optimizes spatial filters solely based on assumptions about (positive or negative) co-variation between bandpower dynamics of individual components. In addition to $\phi_f^{\hat{s}}(e)$ let $\phi_{\acute{f}}^{\acute{\hat{s}}}(e)$ denote the time-resolved bandpower dynamics of a separate component $\acute{\hat{s}}$ at a frequency band $\acute{f}$, with $\acute{f} \neq f$. As before, let $\mathbf{C}_{\acute{f}}(e)$ denote the corresponding time series of covariance matrices. With these definitions the notion of bandpower covariance is formalized as

$$\begin{aligned} \mathrm{Cov}\left(\phi_f^{\hat{s}}, \phi_{\acute{f}}^{\acute{\hat{s}}}\right) &= \frac{1}{N_e}\sum_{e=1}^{N_e} \phi_f^{\hat{s}}(e) \cdot \phi_{\acute{f}}^{\acute{\hat{s}}}(e) \\ &= \frac{1}{N_e}\sum_{e=1}^{N_e} \mathbf{w}^\top \mathbf{C}_f(e)\mathbf{w} \cdot \acute{\mathbf{w}}^\top \mathbf{C}_{\acute{f}}(e)\acute{\mathbf{w}}\,. \end{aligned} \tag{14}$$

cSPoC optimizes the above expression for pairs of filters $\mathbf{w}$ and $\acute{\mathbf{w}}$ under unit variance and mutual decorrelation constraints. The algorithm can be set to either maximize or minimize the objective function, thereby searching for components with positive or negative bandpower covariance, respectively.

Properties and Applications

Owing to volume conduction (see Section 2.1.1), raw EEG scalp potentials are known to have a poor spatial resolution. According to the linear generative model of EEG, spatial filtering methods decompose the observed data into a set of components. This decomposition is used in BCI research for different purposes. First, while EEG is usually recorded from 64 or more channels, the number of sources in the brain that generate relevant signals are expected to be much smaller. If scalp measurements are assumed to be a linear superposition (i.e. weighted sum) of the individual component activities, extracting those components that are assumed to have useful properties for a particular BCI application, while removing components that are unrelated to that application, is advantageous for the real-time analysis of EEG data. This procedure is called *dimensionality reduction* and its virtue has been demonstrated by methods such as principal component analysis (PCA) and SSD (Haufe et al., 2014a).

Second, if oscillatory signals of interest – like the central μ-rhythm in motor imagery (MI) – are weak in power, while other sources produce strong signals in similar frequency ranges like the α-rhythm of the visual cortex or movement and muscle artifacts, it becomes essential to calibrate the BCI to the specific characteristics of each user. The problem even increases when the goal is to analyze single trials of EEG for BCI applications. In this context, the calculation of subject-specific spatial filters, which are optimal for the extraction of specific power oscillations, has proven to be useful. Here the most widely used approach is CSP (Blankertz et al., 2008), which has become one

of the corner stones of sensorimotor rhythm based brain-computer interfaces (Sannelli et al., 2011; Fazli et al., 2015).

And finally, unsupervised methods like the independent component analysis (ICA) (Bell and Sejnowski, 1995; Hyvarinen, 1999), whose decomposition principle is based on statistical independence, have been used to analyze the functionality and dynamics of components in the EEG (Makeig et al., 1996; Makeig et al., 1999; Makeig et al., 2002).

Spatial filtering methods can be subdivided into *supervised* and *unsupervised* methods. Supervised methods make use of class membership (e.g. in CSP) or an external target signal (e.g. in SPoC) during the optimization of the parameters. While the use of such methods for the extraction of features from EEG signals is quite common, their requirement for a supervision signal limits their use in BCIs to applications where such a signal or information is necessarily available. Unsupervised methods, on the other hand, don't require a supervision signal as they rely on the statistics of the data alone. Such methods may thus use a-priori information about the BCI experiment that is expected to be reflected in the EEG, such as a specific frequency band of interest (e.g. in SSD) or the anti-correlation of particular frequency bands (e.g. in cSPoC).

2.3.3 *Removal of EOG Activity*

Vertical and horizontal eye movements cause strong scalp deflections in the EEG, called electrooculogram (EOG) activity, which are 1 to 2 orders of magnitude higher than the activity originating from the cortex. These deflections are measured predominantly in frontal EEG electrodes and the direction and magnitude of the deflections are indicative of the orientation and degree of eye motion (Figure 1a). EOG activity is considered as an artifact that is very often removed from the EEG during preprocessing before further analysis. Several methods exist for such a removal.

In experimental paradigms, where the information for a BCI application is conveyed in short segments of EEG data (e.g. in ERP-based spellers), a very common approach consists in removing any such segments that contain deflections caused by eye movements. The detection of these segments is accomplished via a simple criterion that is based on the fact that EOG deflections exhibit a considerably larger amplitude or variance than cortically generated potentials. Other approaches employ unsupervised source separation methods such as ICA in order to identify and remove components that contain artifacts (Vigário, 1997; Jung et al., 2000; Winkler et al., 2011), or use a regression approach that subtracts estimated EOG activity from the EEG Parra et al. (2005). Figure 1b shows two exemplary segments of EEG data, before and after removing EOG activity with this regression approach.

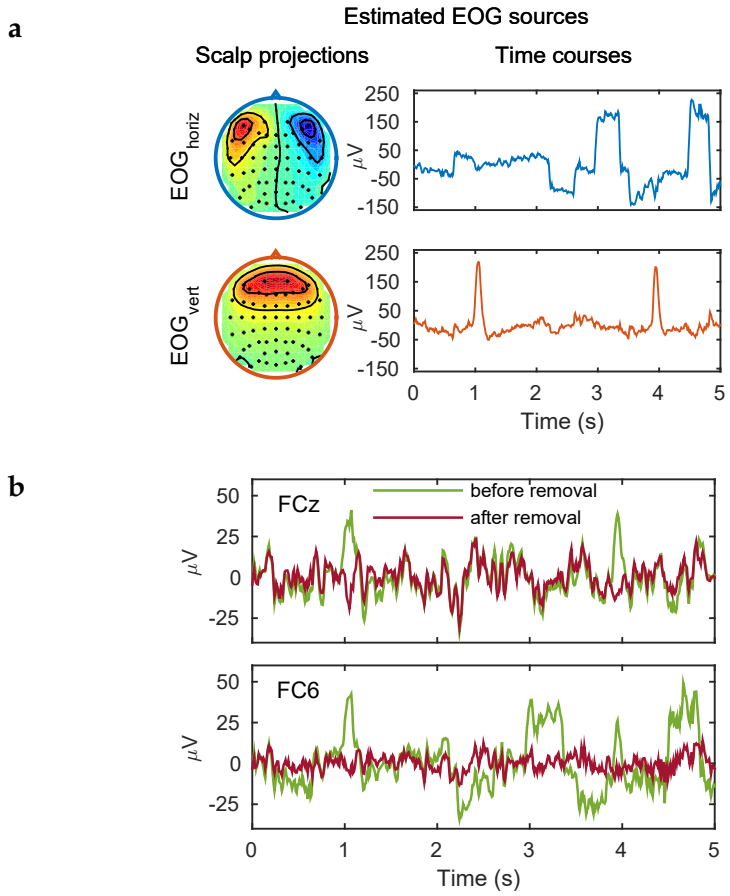

Figure 1: Estimation and removal of EOG activity, demonstrated exemplarily on EEG data from subject *lh* in Chapter 3. (**a**) Estimated scalp projections (left) and time courses (right) of horizontal (top) and vertical (bottom) EOG activity. Horizontal eye movements were estimated from the difference between electrodes *F9* and *F10*, vertical eye movements were estimated from the average of electrodes *Fp1* and *Fp2*. Horizontal eye movements to a particular side cause deflections in the EEG whose polarity is reversed in electrodes placed on opposed sides of the scalp. Hence, they exhibit a topology with a clear amplitude symmetry along the medial axis, but reversed polarity. The topology of vertical eye movements shows a clear central contribution from the most frontal channels that quickly decreases in dorsal direction with a perfect symmetry with respect to amplitude and polarity. The two events observed in the estimated time course are typical for eye blinks. (**b**) Time courses of EEG segments in channels *FCz* (top) and *FC6* (bottom), one time before (green) and one time after (red) removal of EOG activity. While the influence of the eyeblinks is clearly seen in both channels before removal, the impact of horizontal eye movements on central channels (e.g. *FCz*) is very small. Note that the regression approach clearly removes the deflections associated with eye movements without affecting the non eye related EEG signals.

2.3.4 *Model Selection*

Whenever a model, such as a classifier, needs to be selected, it is essential to chose one that generalizes well in the sense that it reasonably explains unseen data (Müller et al., 2001; Bishop, 2007). One well-established technique to estimate the predictive value of a model is called *cross-validation*. In a K-fold cross-validation, the dataset is split into K equal parts. In each fold, the model is fitted on $K-1$ parts (called the *training set*) and applied to the part that was left out (called the *test set*). The average error across all folds then provides a good estimate of the generalization error of the selected model.

If the data are independent and identically distributed this generalization error is unbiased. However, due to the temporal structure of EEG data in most BCI experiments non-stationarities are to be expected, which violates the assumption of independence (Lemm et al., 2011). Therefore, an unbiased validation scheme is *chronological validation*. Here, it is ensured that the training set chronologically precedes the test set. The generalization error in this validation scheme will reflect a failure of the model to be invariant against potential non-stationarities in the data.

Another potential caveat arises when validating EEG data with block design, in which an experiment is divided into blocks of different experimental conditions and each block comprises several single trials of the same condition. Trials within one block are likely to be stochastically dependent, while stochastic independence can be assumed for data across blocks. In this case it is advised to employ the so-called *leave-one-block-out* cross-validation. As with generic cross-validation, one block is left out for testing, and the other blocks are used for training the model. However, for smaller numbers of blocks, the leave-one-block-out cross-validation tends to overestimate the generalization error because non-stationarities are not represented equally for both classes. In this case, it is advisable to employ a *leave-one-block-pair-out* cross-validation, where adjacent pairs of blocks are left out for testing in each fold.

3

ADVANCING THE ASSESSMENT OF OPERATOR WORKLOAD WITH BCIS

The development of BCIs capable of real-time assessment of the workload state of operators is an endeavor that has been followed for several decades now. The foundations of this idea were laid already two decades ago (Makeig et al., 1994; Gevins et al., 1995; Pope et al., 1995), showing that an EEG-based workload assessment can be used for adaptive purposes in operational environments. Numerous studies have since then successfully demonstrated this idea (Prinzel et al., 2000; Scerbo et al., 2003; Kohlmorgen et al., 2007; Wilson and Russell, 2007; Christensen et al., 2012). In this chapter, we aim to extend this line of experimental work and seek to advance the detection of operator workload with BCIs by exploring new possibilities rendered feasible by novel developments in machine learning techniques. We formulate several challenges in the development of BCI-based workload detection and suggest the means by which those challenges can be tackled. The proposed approach is evaluated on EEG data from an experiment in which participants executed a task with differing levels of workload. We present the results of the analysis, discuss their relevance and examine the degree to which the proposed challenges were accomplished.

Parts of the findings presented in this chapter were published in Schultze-Kraft et al. (2016b).

3.1 BACKGROUND AND MOTIVATION

In the following sections, we first of all present the background and motivation of this chapter and provide an overview of previous work on the detection of mental states from EEG.

3.1.1 *The Concept of Workload*

Humans are limited in the ability to process information, remember things and sustain a high level of attention over longer periods of time (Manzey, 1998). When challenged with arduous tasks, these limitations cause humans to become exhausted and to make errors. The study of *mental* or *operator workload* is closely related to these limitations. By means of assessing and examining the level of workload under different conditions, it aims to disclose the various factors that influence the level of workload and provides insights into the implications of excessive worklod on the performance, health and safety of the operator. Workload can be described by the "complex interaction between the characteristics of the person and the demands of the task to be accomplished" (Manzey, 1998, p. 800).

Different theoretical concepts of workload exist. Based on neurophysiological findings, the *activation model* proposes that several systems of activation and arousal are implemented as circuits in the brain and are directly associated with the accomplishment of complex tasks (Pribram and McGuinness, 1975). In the *resource model* workload is seen as the amount of capacity demanded by a task and identifies a direct correlation between mental workload and resource demands for information processing (Kahneman, 1973). Accounting for new findings from neurophysiology, this model was later refined by differentiating between resources corresponding to different processing stages, perception modalities and aspects of visual processing (Wickens, 2002). The workload state of humans is not directly observable but can be inferred indirectly through various variables, including task performance, subjective (Hart and Staveland, 1988) and peripheral physiological measures (Vogt et al., 2006; Karavidas et al., 2010; Reimer and Mehler, 2011).

3.1.2 *Motivation for Workload Assessment*

Our modern world has generated many fields of activity in which human operators are required to perform monotonous but attention-demanding tasks, such as in driving, air traffic control or in industrial contexts. Such environments are predestined to cause high levels of workload in individuals operating in them, having critical consequences for health, safety and efficiency aspects (Wilde, 1982; Sarter and Woods, 1995). It has thefore become important to study system performance and safety critical tasks under the scrutiny of potentially detrimental effects of excessive workload, with the ultimate goal to prevent this hazardous functional state by maintaining mental workload or task demand within an acceptable range (Hockey, 2003). A reliable and real-time assessment of the operator's workload would provide the possibility to mitigate the consequences of excessive workload, for instance by adapting the the task difficulty or instructing the operator to take a break (Prinzel et al., 2000).

One way to achieve a real-time assessment of workload is by measuring the operator's physiological markers such as heart rate, respiration rate or skin conductance and infer from them the level of workload. During the last decades, neurophysiology has proven to be a sensitive and informative modality for the measurement of workload (Gevins and Smith, 2003; Berka et al., 2007; Holm et al., 2009; Christensen et al., 2012). Neurophysiological markers of workload are not ascertainable via physiological measures and provide complementary, non-overlapping information (Hankins and Wilson, 1998; Matthews et al., 2015). This has led to concepts such as *neuroergonomics* (Parasuraman, 2003) and *augmented cognition* (Stanney et al., 2009), which suggest to use neurophysiologically assessed operator workload in order to enhance human-machine interaction. The level to which this approach is feasible depends on the sensitivity with

which such markers can be reliably obtained from neurophysiological measures like EEG.

3.1.3 *Assessment of Mental States from EEG*

Numerous studies have shown the suitability of using power modulations in particular frequency bands in the EEG for the decoding and prediction a variety of mental states, such as alertness, vigilance, fatigue and attention (Kecklund and Åkerstedt, 1993; Jung et al., 1997; Müller et al., 2008; Schubert et al., 2008; Schmidt et al., 2009; Stikic et al., 2011; Sonnleitner et al., 2012). In particular, EEG has been shown to provide reliable estimators of workload. EEG estimators of workload are based on the fact that changes in workload are associated with characteristic changes in the EEG. These typically amount to modulations in the power of oscillatory activity in particular frequency bands of the EEG (Buzsaki and Draguhn, 2004).

The most prominent frequency bands with power changes related to workload are theta (4-7 Hz) and alpha (8-13 Hz). Theta power has been shown to be positively correlated with workload, most notably over frontal regions, whereas alpha power is typically found to be negatively correlated with workload, in particular over parietal regions (Gevins and Smith, 2003; Holm et al., 2009) (although some studies have produced unclear or contradictory findings regarding the alpha band, see Section 3.5.3). An index for workload can be derived from the absolute power in the theta and alpha frequency bands in the EEG (Gevins and Smith, 2003; Berka et al., 2007) or from the ratio between them (Pope et al., 1995; Holm et al., 2009). Other studies have additionally made use of power changes in other frequency bands such as delta, beta and gamma (Brouwer et al., 2012; Christensen et al., 2012). EEG-based workload indices can be further obtained using not only spectral but also features from event-related potentials (ERPs) (Prinzel et al., 2003; Brouwer et al., 2012; Martel et al., 2014). Other studies have strived to make workload state detection robust against affective contexts (Mühl et al., 2014) and day-to-day variability (Christensen et al., 2012).

3.2 GOAL AND CHALLENGES

The ultimate goal to enhance human-machine interaction with brain-computer interfaces, as suggested by the neuroergonomic approach, requires fundamental research that provides the basis for the development of such systems. In this chapter we aim to contribute to that research by demonstrating the successful detection of different levels of operator workload from EEG on a single-trial level. Importantly, this endeavor is set under consideration of several challenges that we identify as being of particular importance for the development of modern workload detection with BCIs. We now elaborate on the motivation for those challenges and propose the means by which we seek to tackle them.

3.2.1 *Challenge 1: Assess Workload from Multiple Modalities*

Assessment of workload from EEG has so far been primarily focused on *mental* workload as induced by demands in mental effort such as working memory and attention, to a lesser extent by perceptual and motor demands. A widely used experimental protocol are n-back style tasks that demand sustained attention to a train of stimuli (Gevins et al., 1990; Gevins and Cutillo, 1993; Stikic et al., 2011; Brouwer et al., 2012; Hogervorst et al., 2014). The Multi-Attribute Task Battery (MATB), a personal computer-based multi-tasking environment (Comstock Jr and Arnegard, 1992), has been used as an experimental paradigm that provides a more naturalistic setting of human-computer interaction (Prinzel et al., 2000; Prinzel et al., 2003; Christensen et al., 2012). Even more tailored to everyday situations are efforts to assess operator workload from EEG in noisy environments, such as that experienced by aircraft pilots and car drivers (Kohlmorgen et al., 2007; Putze et al., 2010; Dijksterhuis et al., 2013; Borghini et al., 2014). Tasks in such environments typically involve increased requirements in multiple modalities, from attention and working memory to the executive control of visuomotor behavior.

Here, we aimed at assessing such a multimodally effected workload as it might be expected in an industrial setting. We envisioned an industrial workplace where an automated plant produces parts at a certain speed and a human operator assembles them into a final product as they are transported past them on a conveyor. Such a workplace offers the ideal scenario for employing the neuroergonomic approach because it involves several competing goals: While a high work speed is desired to maximize productivity, a too high workload of the operator may result both in an increased rate of defective goods and – most importantly – it may be detrimental to the operator's health. Here, a continuous assessment of workload would allow to dynamically adapt the work speed to a level that counterbalances the plant's productivity and the operator's performance and health.

Approach: We mimicked such a scenario by designing an experimental task on a touch screen that required continuous visuomotor demands by subjects. By changing task difficulty, the experiment induced two levels of operator workload on subjects.

3.2.2 *Challenge 2: Use Exclusively Brain Signals*

Such a task requires operators to constantly execute head and eye movements, which are both expected to be correlated with task difficulty. Unfortunately, the two main artifact sources in the EEG are electrooculogram (EOG) and electromyogram (EMG) activity. EMG activity that occurs near EEG channels, for instance due to head movements, leads to an increase of power in those channels in the beta and gamma frequency band. Similarly, EOG activity caused by eye movements like saccades or blinking is reflected as pronounced potentials in the EEG, which can result in an increase of EEG power in mul-

tiple frequency bands. This circumstance may become relevant for the detection of workload states when oscillatory signals in the EEG are used as markers, particularly when the experimental paradigm as the one outlined above involves movements of the head and eyes. If the task difficulty that modulates the workload is correlated with the amount of EMG and EOG activity, the spectral features extracted from the EEG are likely to be spurious. In rare cases, this issue is negligible because the workload inducing task is independent from the EMG and EOG activity (Kohlmorgen et al., 2007). However, in the typical case the task difficulty will be correlated with head and eye movements. Moreover, workload has been found to have an impact on eye blink frequency and duration (Brookings et al., 1996; Veltman and Gaillard, 1996).

Despite employing artifact rejection approaches, most studies that use oscillatory EEG signals for workload detection do so without further inspecting the sources of the signals eventually used for classification (e.g. Prinzel et al., 2000; Scerbo et al., 2003; Christensen et al., 2012). In such a practice the classifier can be considered a "black box" where the exact source of the used signals is unknown and irrelevat. While such an approach is technically legitimate, if relevant signals used for classification are not of cortical origin, the proper meaning of a BCI is reduced ad absurdum. If, for instance, the majority of signals used for classification are movement artifacts assossiated with the task (e.g. Dijksterhuis et al., 2013), one might as well use a classifier based on EMG activity, without the need for EEG electrodes. In this study, the emphasis was to ensure that non-cortical signals in the EEG were not use as markers for workload assessment, hence aiming for a "true" brain-computer interface in its proper meaning.

Approach: We tackled the outlined challenge by employing a threefold strategy. First, we limited the frequency range of the extracted spectral features to frequencies below 14 Hz. Because EMG activity has been found to be largely absent from frequencies below 20 Hz (Whitham et al., 2007), EMG contamination was negligible. Second, during preprocessing we estimated horizontal and vertical eye movements and removed them from the EEG data, thereby minimizing the impact of EOG activity. And finally, the use of state-of-the-art spatial filtering methods (Blankertz et al., 2008; Dähne et al., 2014a; Dähne et al., 2014b) allowed us to interpret the extracted signals neurophysiologically and therefore to inspect those signals for residual EOG activity.

3.2.3 *Challenge 3: Reduce Training Requirements*

We sought to explore the possibility to use progressively less label information from the experiment, eventually striving for an unsupervised approach, a hitherto unsought attempt. Let us start with the most common setting of supervised classification, where the exact condition labels of the examples used for training are known. The

classical practice here is to train a linear classifier on the extracted features using those exact labels.

In our industrial workplace scenario, however, a situation is very well conceivable in which the different workload conditions are neither externally induced nor known (but result e.g. from a self-regulation mechanism) but instead the performance of the operator (e.g. error rate) is known. This variable is expected to reflect the workload state and can be considered a noisy version of the true labels. The obvious approach in this case is to employ a linear regression on the EEG features, using the error rate as target variable.

In a third scenario we assume that also the error rate is unknown and no other information about the workload condition is available. This scenario is most intriguing, for two reasons. First, it requires an approach that combines EEG features using only the prior knowledge about the spectral changes in the EEG associated with workload and their spatial localization (Gevins and Smith, 2003; Holm et al., 2009). Because no label information is available, such an approach must be inherently unsupervised. And second, if feasible, it would open up the possibility to implement a workload detection system with minimal requirements for calibration, thus making it easy to deploy and to use in everyday situations.

Approach: We implemented several *predictive models* which fall into one out of three categories, depending on the amount of information required by the approach. These categories include (a) the use of binary class labels, (b) the use of a continuous error measure, and (c) no use of a supervision signal at all. Some of the models include the use of machine learning methods (described in Section 2.3.2) that account for the linear generative model of EEG in order to find spatial filters that are optimal for extracting oscillatory signals associated with changes of the workload level (Blankertz et al., 2008; Dähne et al., 2014a; Dähne et al., 2014b).

3.2.4 *Challenge 4: Explore the Added Value of Peripheral Physiology*

Previous studies have shown that workload is not only associated with changes in the EEG but also with peripheral physiological measures (PPMs) such as heart rate (Vogt et al., 2006), respiration frequency (Karavidas et al., 2010) and electrodermal response (Kohlisch and Schaefer, 1996; Reimer and Mehler, 2011). It was furthermore found that multiple measures for mental workload are only weakly correlated and provide non-overlapping information, calling into question whether they assess a common factor (Hankins and Wilson, 1998; Matthews et al., 2015). These findings suggest that physiological measures of workload may constitute an added value to the EEG in predicting different states of workload.

Approach: In addition to EEG, we recorded heart and respiration rate and electrodermal response. In the final analysis step we examined whether a fusion of EEG features with PPM features could improve the performance of workload state detection.

3.3 PROCEDURES

The following sections elaborate on the experimental procedures used in this study. First, the experimental task and setup are described. Subsequently, a general analysis pipeline is proposed that includes several preprocessing steps. And finally, the prediction models implemented with the goal to detect workload states from the recorded EEG are specified.

3.3.1 *The Experiment: Mimicking an Industrial Workplace*

Experimental Task

Ten healthy male subjects, aged 26 to 40, participated in the experiments. All participants gave their informed oral and written consent. Subjects were instructed to carry out a task on a 21-inch touch screen lying on a table in front of them (Figure 2). The task was designed as a computer game: Objects consisting of three vertically aligned screws (screw triplets) were falling vertically with equal velocity from random positions at top of the screen, approaching the bottom of the screen. Each screw in a triplet was randomly tagged and colored with one out of four predefined colors; multiple occurrences of one color were not allowed. At the bottom border of the screen was a bucket consisting of three vertical segments. Using their index fingers, subjects could tag (and untag) the bucket segments with colors by pressing colored buttons positioned both at the left and right borders of the screen. Furthermore they could move the bucket horizontally along the entire bottom screen border by sliding the bucket with one of the index fingers. The task was to catch each falling screw triplet with the bucket before it reached the bottom, ensuring that each time the bucket was tagged with the same colors and in the same order as the caught screw triplet. Catching with wrong colors was considered an error as well as letting a triplet hit the bottom of the screen. The falling speed of the triplets was constant throughout the experiment, however the interval between the occurrence of the triplets varied in two different conditions. In the low workload condition (L) the interval between each set was constant, whereas in the high workload condition (H) the intervals were shorter and varied randomly.

Experimental Setup

Before the experiment started the game's parameters were calibrated for each subject individually in three 5-minute runs. The first run was a free trial run during which subjects could familiarize themselves with the game. All participants quickly reached a fairly constant error rate. In the second run the falling velocity of the screw triplets and the intervals between them were adjusted such that subjects where able to accomplish the task with an error rate of approximately 10%. Participants consistently reported the task being moderately demanding but not stressful. This setting was then used during the experi-

Figure 2: Snapshot from one of the experiments showing a subject play the game on the touch screen.

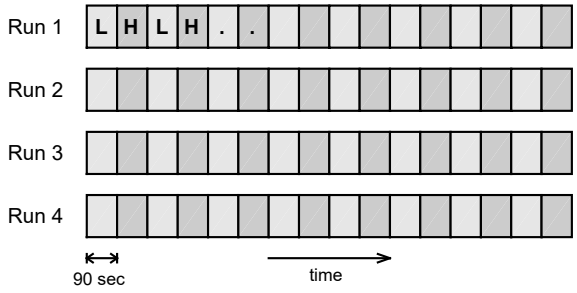

Figure 3: Block structure of the experiment. Participants performed four runs of 24 minutes, each consisting of 90 seconds blocks of alternating low (L) and high (H) workload condition.

ment for the low workload condition. In the third run the game parameters for the high workload condition were determined by adjusting the variance of the randomly occurring intervals between the screw triplets such that an increased sense of stress was reported and yielding error rates between 20 and 25%. Eventually, each subject performed four sessions of 24 minutes each during which EEG was recorded (Figure 3). Each session consisted of 16 blocks of 90 seconds each of alternating L and H conditions, starting with condition L. In order to mimic the conditions of an industrial workplace, during the whole experiment a closed loop recording of a real acoustic scenery of an industrial work environment was played through speakers at realistic volume. The touch screen task was implemented in the open source framework Pyff (Venthur et al., 2010b).

Data Acquisition

During the experiments, EEG data was recorded at 1000 Hz using BrainAmp amplifiers and 64 electrode actiCAP (Brain Products GmbH, Gilching, Germany), filtered by an analog bandpass filter between 0.1 and 250 Hz before being digitized and stored for offline analysis.

In addition to the EEG three peripheral physiological signals were recorded: Electrocardiogram (ECG) was recorded bipolarly with two surface Ag/AgCl electrodes positioned at breast height at the front and back of the body; respiration activity was recorded using a Sleepmate respiratory effort belt (Ambu, Ballerup, Denmark); skin conductance was recorded with a GSR module (Becker Meditec GmbH, Karlsruhe, Germany).

3.3.2 *Data Analysis*

The data analysis employed in this study is schematically described in Figure 4 and detailed in the following subsections. First, several preprocessing steps including artifact removal and bandpass filtering were performed on all data sets. Next, one of six prediction models was trained on part of the data and subsequently tested on data that were not used for training. The output of a prediction model was evaluated in two separate ways, namely by computing (i) the model's correct classification rate of workload conditions and (ii) the correlation of the model's output with the error rate. Some of the workload prediction models employ so-called spatial filtering methods which are in turn based on a linear generative model of EEG. For a detailed description of these methods, see Section 2.3.2. We now continue with a detailed account of the preprocessing steps and thereafter describe the workload prediction models.

Suppression of Eye Movement Artifacts

Due to the lack of electrodes that directly recorded this activity, we used the difference between electrodes *F9* and *F10* and the average of electrodes *Fp1* and *Fp2* to estimate horizontal and vertical EOG activity, respectively. Those four electrodes were excluded from all subsequent analyses. The estimated horizontal and vertical EOG activity was then removed from the EEG data by means of the regression approach described in Section 2.3.3.

Segmentation into Epochs

The bandpass filtered EEG data were then segmented into non-overlapping time windows of 90 seconds length. We refer to the data within such a time window as an *epoch*.

Extraction of Peripherial Physiological Signals

A subject-specific heart beat template was extracted from the raw ECG signal and subsequently correlated with the signal in a sliding window. The times of high correlation peaks detected by a threshold represented the times of heart beats, from which the time-resolved frequency was obtained. Similarly, the respiratory activity recorded by the respiratory effort belt was lowpass filtered and the peaks and troughs of each inhalation and exhalation threshold detected, yielding a time-resolved respiration frequency.

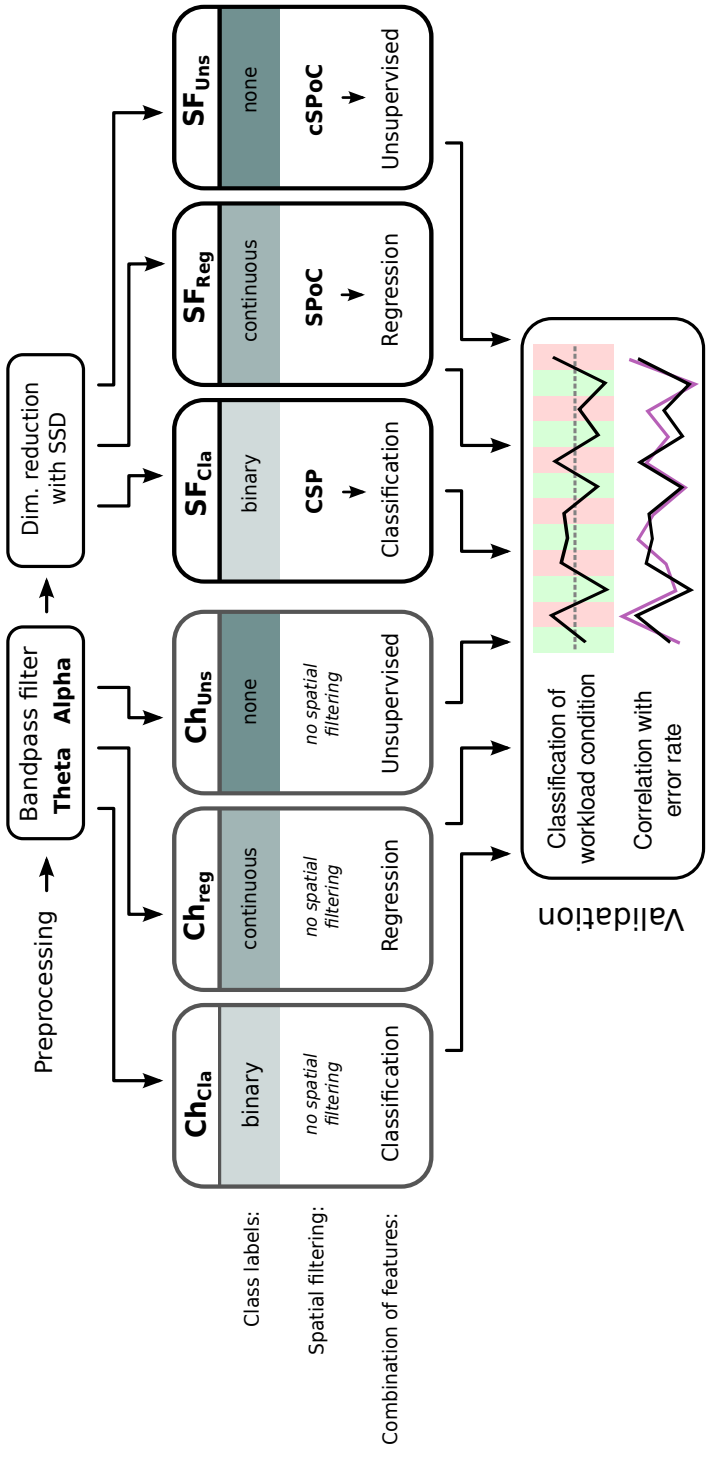

Figure 4: Schematic representation of the data analysis workflow. See text for details.

Bandpass Filtering and Dimensionality Reduction

The scalp EEG was bandpass filtered in two separate frequency bands, namely the theta range (4-7 Hz) and the alpha range (8-13 Hz). For each of the two frequency bands, a Butterworth filter of order 5 and non-causal IIR filtering was employed. This operation yielded two bandpass filtered datasets per subject, which served as input to the channel-based prediction models. For the spatial filtering methods (see next section) an additional preprocessing step consisting of dimensionality reduction was applied. We used Spatio-Spectral Decomposition (SSD) (Nikulin et al., 2011; Haufe et al., 2014a) (see also Section 2.3.2) in order to extract a maximally oscillatory subspace for the theta range and the alpha range. Thus, SSD was applied twice to the EEG data in order to optimize for theta and alpha separately. From both applications of SSD, the first 15 SSD components were retained while the remaining components were discarded, yielding two 15 dimensional datasets per subject, which served as input to the spatial-filter-based prediction models.

3.3.3 *Prediction Models*

We implemented six different predictive models, which fall into one out of two categories: (i) *channel-based* and (ii) *spatial-filter-based*. In the channel-based models, feature extraction is done for each recording channel separately. In the spatial-filter-based models the data are first projected onto a set of optimized spatial filters and features are then extracted from the output of the spatial filters. Furthermore, each of the channel-based and spatial-filter-based models fall into one out of three sub-categories, as outlined above: (a) the use of binary class labels, (b) the use of a continuous error measure, and (c) no use of a supervision signal at all. In all models, we used log-variance of bandpass filtered data, computed within 90s epochs, as features that represent spectral modulations.

For the *channel-based* models, log-var features are computed according to

$$P_{i,f}(e) \quad = \quad \log\left(\mathrm{Var}(\mathbf{x}_{i,f}(e))\right) \ , \tag{15}$$

where $\mathbf{x}_{i,f}(e)$ denotes the signal in of a single EEG channel indexed by $i \in \{1, ..., N_{\text{channels}}\}$, bandpassed filtered for frequency band $f \in \{\theta, \alpha\}$, within the epoch indexed by $e \in \{1, ..., N_{\text{epochs}}\}$.

For the *spatial-filter-based* models, log-var features are computed according to

$$P_{i,f}(e) \quad = \quad \log\left(\mathrm{Var}(\mathbf{w}_{i,f}^{\top}\mathbf{X}_f(e))\right) \ , \tag{16}$$

where $\mathbf{X}_f(e)$ denotes the signal of all bandpass-filtered EEG channels within the epoch e, while $\mathbf{w}_{i,f}$ denotes the frequency-band-specific spatial filter indexed by $i \in \{1, ..., K\}$ with K being the number of filters to be used per frequency band.

In order to suppress drifts and fluctuations that are outside of the relevant time-scale, the log-var features were high-pass filtered at

1/600 Hz (thereby removing changes slower than 10 minutes). Once the log-var features have been computed and filtered, they are combined according to

$$\hat{y}(e) = \sum_{f=\{\alpha,\theta\}} \sum_{i=1} b_{i,f} \cdot P_{i,f}(e) \,, \tag{17}$$

where $\hat{y}(e)$ denotes the scalar output of the model for the eth epoch.

The parameters that all prediction models have to estimate using training data are the weighting coefficients $b_{i,f}$. Additionally, spatial-filter-based models have to estimate the spatial filters $\mathbf{w}_{i,f}$. The prediction models differ in the algorithms that are used to optimize the spatial filters and weighting coefficients. In the following we describe the properties of each prediction model in detail.

Classification Models

If the true exact labels from the experiment are available, it is possible to employ a classification-based approach.

Ch$_{Cla}$ (classification on channels): This model uses regularized Linear Discriminant Analysis (LDA) to train the weighting coefficients based on labels. The regularization is based on shrinkage of the feature covariance matrix, as described in Section 2.3.1.

SF$_{Cla}$ (spatial filtering & classification): The corresponding spatial-filter-based model uses the Common Spatial Patterns (CSP) algorithm (see Section 2.3.2) to train the spatial filters and LDA to combine the resulting log-var features. CSP finds filters that increase the power contrast between two experimental conditions and is an established method in BCI research. The spatial filters were optimized using the CSP algorithm separately for each frequency band, such that the resulting CSP signals have maximal variance difference between the two workload classes. From each of the two resulting set of filters, the $K = 3$ filters with the largest absolute Eigenvalue were selected, yielding six filters in total.

Regression Models

Whenever a continuous measure, such as the the error rate, is available a regression-based approach can be used.

Ch$_{Reg}$ (regression on channels): In this model the error rate is used as a supervision signal to optimize the weighting coefficients using ridge regression, which is a regularized version of ordinary regression. The regularization is based on shrinkage of the feature covariance matrix.

SF$_{Reg}$ (spatial filtering & regression): In order to train the spatial filters for the corresponding spatial-filter-based model, we employ a novel method called the Source Power Co-Modulation (SPoC) analysis, which optimizes the correlation of band power to a given target function, in this case the error rate (Dähne et al., 2014a). The spatial filters were optimized using the SPoC algorithm separately for each frequency band. From each of the two resulting sets of filters,

the $K = 3$ filters with the largest absolute Eigenvalue were selected, yielding six filters in total. The resulting log-var features were then combined using ridge regression.

Unsupervised Models

In this setting no supervision signal is present; thus the employed methods must be unsupervised. The well-known workload modulated interaction between frontal theta and parietal alpha power (Gevins and Smith, 2003; Holm et al., 2009) forms the basis of both models.

Ch_{Uns} (unsupervised on channels): Because this model operates on single channels, it must be fundamentally simple in order to be unsupervised. The model output is constructed by subtraction of theta log-var features at channel *Fz* from alpha log-var features at channel *Pz*.

SF_{Uns} (spatial filtering & unsupervised): The filters for for this model were optimized using the cSPoC algorithm (Dähne et al., 2014b). Given two datasets, cSPoC maximizes pairs of filters such that the bandpower dynamics between pairs are highly (anti-)correlated. In this setting, cSPoC was employed to maximize anti-correlation between theta and alpha bandpower dynamics. Three filter pairs (i.e. $K = 3$ filters per frequency band) were optimized and the resulting log-var features are combined by averaging them within bands and then subtracting the resulting averaged theta cSPoC features from the averaged alpha cSPoC features.

Prediction Model Based on Peripherial Physiological Signals

In addition to the six prediction models outlined above, we tested whether features derived from the peripheral physiological measures (PPM) constitute an added value. This model is comprised of the PPMs recorded during the experiment. An inspection of their change over time confirmed that they were modulated by the induced workload state with equal direction (see Figure 5 and Section 3.4.1). The mean heart rate, respiration rate and skin conductance in each data epoch were computed, high-pass filtered at 1/600 Hz (thereby removing changes slower than 10 minutes), z-scored, and finally summed up in order to generate the model output. Note that this model is unsupervised as well, since it comprises a simple summation of features that does not require label information.

Overview of Prediction Models

The six models are summarized in Table 1. In this table, the models are categorized according to the level at which features are extracted and to how much information is required during training.

What all models have in common is that they yield a one dimensional output with one value for each data epoch. This model output was then used two-fold for validation: One validation approach consisted in treating the sign of the output as the classification of

workload into either the low (positive sign) or high (negative sign) state and computing the average classification accuracy. The other approach consisted in computing the correlation of the model output with the error rate of the subject. In order to test for generalization, the validation was done in a chronological 4-fold cross-validation. In this cross-validation scheme, each of the four sessions became the test set once, while the remaing three were used for training. The classification accuracy and correlation value were then computed from the average across test folds.

3.4 RESULTS

3.4.1 *Impact of Task on Error Metrics and Physiology*

Before analyzing the recorded EEG data, we first examined the impact of the experimental task on task performance and on the physiological data. Participants consistently reported the difference between the low and high workload condition as clearly distinguishable. These two conditions were calibrated before the experiment for each participant individually, such that the error rate in each condition was approximatly 10% and 20%, respectively.

Error Metrics

Figure 5a confirms the strong effect that the task had on subjects' error rate. The error rate was modulated by the condition in a step function manner. During the low workload condition the rate was approximately 10%. When the condition was changed from low to high workload (at $t = 90$ sec) the error rate rapidly increased to about 20 to 25% after which it remained approximately constant throughout the high workload condition. Accordingly, the opposite occurred when switching from high to low workload.

	channel-based	spatial-filter-based
classification	Ch_{Cla} (LDA)	SF_{Cla} (CSP + LDA)
regression	Ch_{Reg} (Regression)	SF_{Reg} (SPoC + Regression)
unsupervised	Ch_{Uns} (Power diff.)	SF_{Uns} (cSPoC + Power diff.)

Table 1: The six models used to predict workload and which algorithms they use. The models are categorized with respect to the level at which log-var features are extracted (channel-based vs spatial-filter-based) and the amount of information required during training (binary labels for classification, continuous measure for regression, no supervision signal for unsupervised).

Peripheral Physiological Measures

In a next step, we also analyzed the task's impact on the three peripheral physiological measures (PPMs) respiration, heart beat and electrodermal response. We found that also these were clearly modulated by the task (Figure 5b-d). Similar to the error rate, the respiratory and cardiac frequency were modulated by the condition in a step function manner, with lower rates during the low workload condition. Electrodermal response, on the other hand, constantly decreased during low workload and increased during high workload condition.

The impact of condition switch had delay of 10 to 20 seconds both with the three PPMs and the error rate. This effect is partly a result of the way the touch screen task was implemented: In order to avoid undesirable behavioral effects by sudden changes in the game, the switch of task difficulty occured slowly, taking full effect only after roughly 10 seconds.

3.4.2 *Performance of Predictive Models*

Spatial-Filtering Models

We assessed the ability of each of the three predictive models based on spatial filtering to classify between both workload conditions and to predict the error rate. Therefore, according to the analysis pipeline described above, the models were trained and validated individually. Figure 6a shows the mean classification accuracies for the three models. As the average across subjects shows, SF_{Cla} performs best (94.1%), followed by SF_{Reg} (91.8%) and SF_{Uns} (82.3%). The correlations of model outputs with the error rate show a very similar picture (Figure 6b), with mean correlations of 0.68, 0.67 and 0.60, respectively.

Impact of Label Degradation

Across validation type (i.e. classification accuracy or correlation with error rate) we find a successive decrease of performance with respect to the type of labels used by the model: $Cla > Reg > Uns$. A statistical test shows that this difference is significant for models SF_{Cla} and SF_{Uns} across both validation types (classification accuracy: two-sided, paired $t(9) = 3.71$, $p = 0.005$; correlation: two-sided paired $t(9) = 3.45$, $p = 0.007$), as well as for models SF_{Reg} and SF_{Uns} (classification accuracy: two-sided, paired $t(9) = 3.32$, $p = 0.009$; correlation: two-sided paired $t(9) = 3.13$, $p = 0.012$).

Single Subjects

An inspection of results from single subjects (Figure 7) shows that this performance gradient is most evident for subjects with lowest classification accuracies or correlations (subjects *ed-ik*) but is otherwise less pronounced or absent. Considering that a classification accuracy of 70% has been suggested as a minimum criterion for BCIs (Kübler et al., 2001), Figure 7a shows that this value is achieved in 10 out of

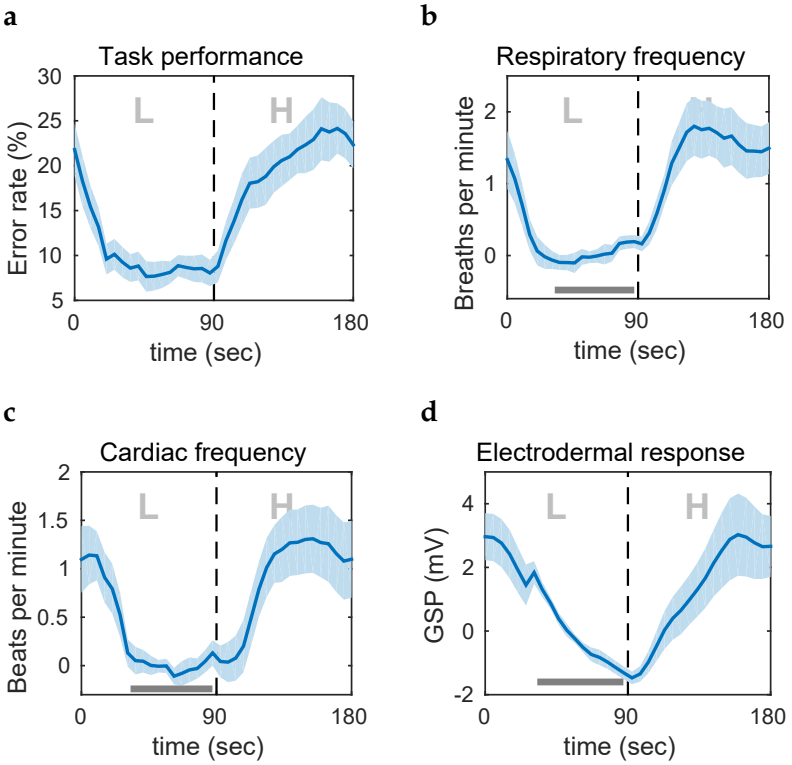

Figure 5: Impact of the experimental paradigm on task performance and peripheral physiological measures (PPMs). Shown are the grand averages of the mean over all L-H block pairs of the error rate (**a**), respiratory frequency in breaths per minute (**b**), cardiac frequency in beats per minute (**c**) and electrodermal response in Galvanic skin potential (**d**). Light blue shadings indicate the standard error of the mean. Single subject data were computed over 5-second segments and subsequently smoothed with a 20-second sliding zero-phase boxcar window and averaged over all 32 pairs of consecutive L-H blocks. Due to large inter-subject differences in the average of the PPMs, the grand average and standard error were computed after subtracting the mean in the indicated bar. Thus, the plotted values represent changes from this baseline.

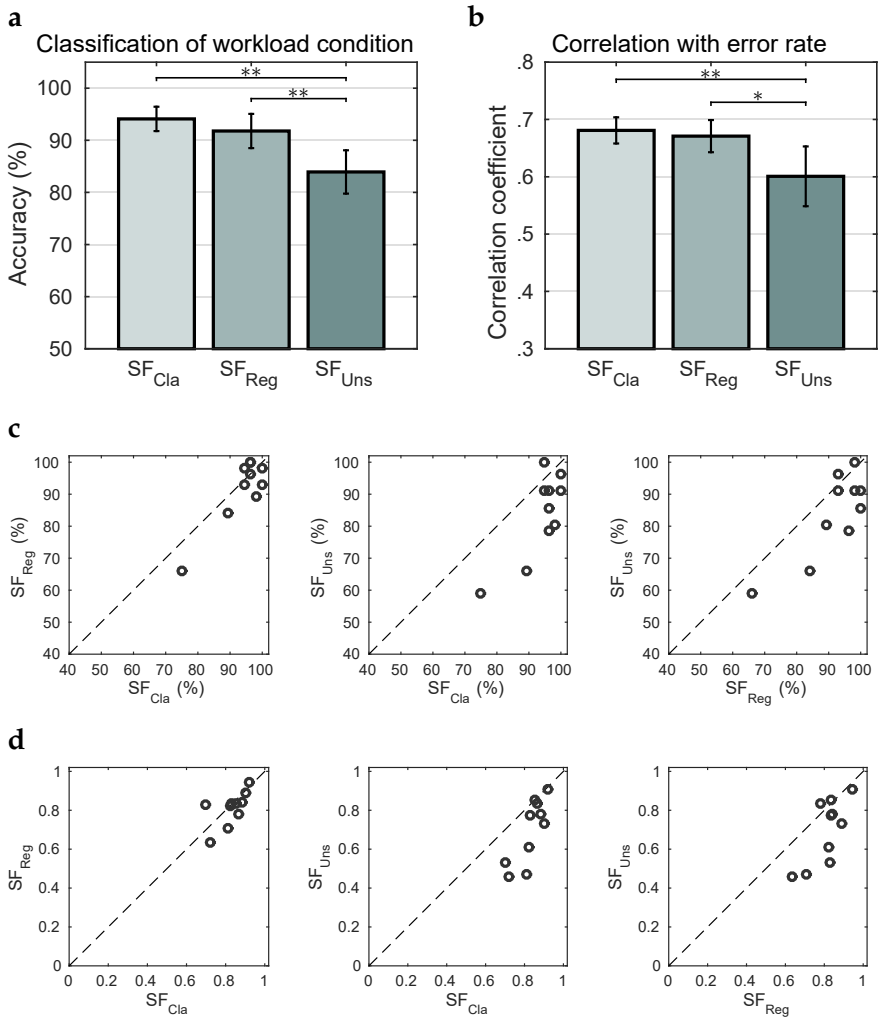

Figure 6: Performance of spatial-filtering-based models SF_{Cla}, SF_{Reg} and SF_{Uns}, assessed by the mean classification accuracy (**a**) and the correlation of the models' output with error rate (**b**). Error bars indicate the standard error of the mean and asteriscs indicate statistically significant difference of means ($* : p < .05$, $** : p < .01$). Scatter plots in **c** and **d** show between-model comparisons of single subject classification accuracies and correlations, respectively.

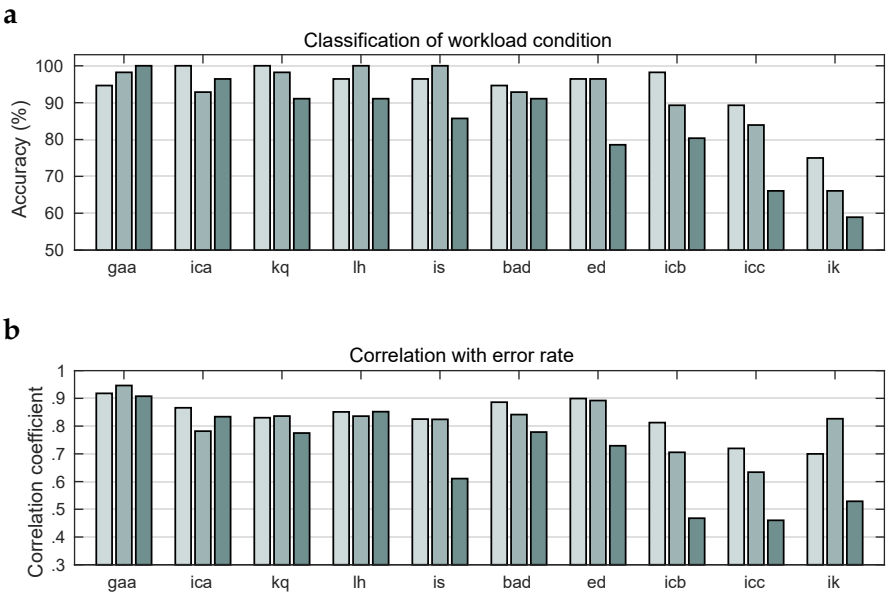

Figure 7: Single subject classification accuracies (**a**) and correlations with error rate (**b**) of models SF_{Cla}, SF_{Reg} and SF_{Uns}, color coded as in Figure 6. Each bar group corresponds to one subject. Subjects are ordered by the mean classification accuracy across models.

10 subjects with the SF_{Cla} model, followed by SF_{Reg} (9/10) and SF_{Uns} (8/10).

Comparison with Channel Models

We next compared the performance of these models with that of the three analogous models that did not use spatial filtering, namely Ch_{Cla}, Ch_{Reg} and Ch_{Uns}. This comparison shows that the lack of a spatial filtering method in the models consistently results in a decrease of performance, both in the classification accuracy and in the correlation with the error rate (Figure 8). When considering the classification accuracy, there is a descrease of 3.75%, 4.29% and 8.21% within the classification, regression and unsupervised models, respectively. Similarly, when considering the correlation with error rate, there is a respective descrease in correlation of 0.025, 0.039 and 0.133. A statistical test reveals that this decrease is significant across validation types, but only among the regression models (classification accuracy: one-sided, paired $t(9) = 2.27$, $p = 0.025$; correlation: one-sided paired $t(9) = 2.16$, $p = 0.020$), but not among the classification models (classification accuracy: one-sided, paired $t(9) = 1.60$, $p = 0.072$; correlation: one-sided, paired $t(9) = 1.80$, $p = 0.053$) or unsupervised models (classification accuracy: one-sided, paired $t(9) = 1.32$, $p = 0.110$; correlation: one-sided, paired $t(9) = 1.66$, $p = 0.066$).

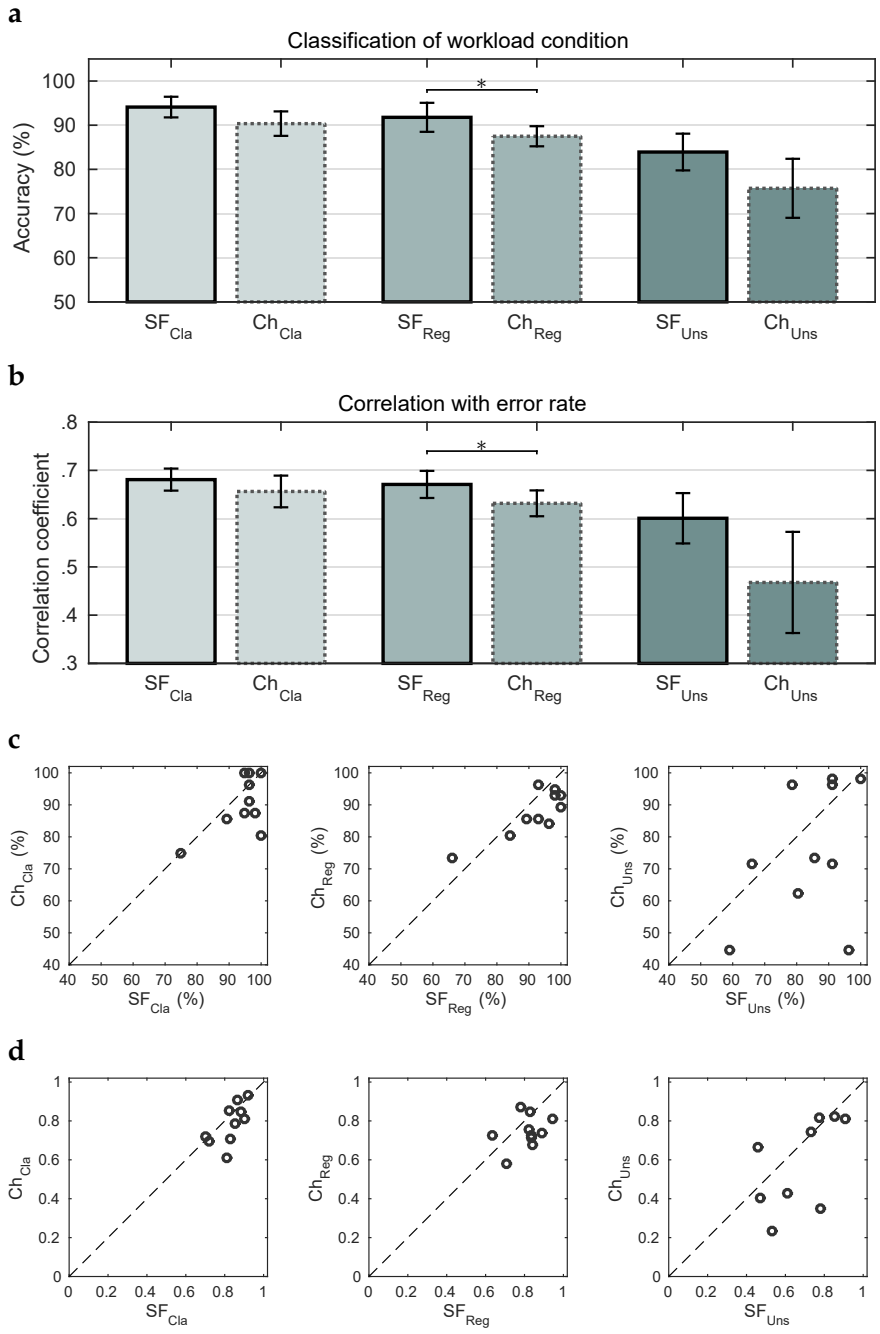

Figure 8: Performance comparison of spatial-filtering-based models with the channel-based models Ch_{Cla}, Ch_{Reg} and Ch_{Uns}, assessed by the mean classification accuracy (**a**) and the correlation of the models' output with error rate (**b**). Scatter plots in **c** and **d** show between-model comparisons of single subject classification accuracies and correlations, respectively. Note that in the most right scatter plot in **d** one data point is not shown, because model Ch_{Uns} achieved a correlation of -0.2.

3.4.3 *Inspection of Model Components*

We further aimed to investigate whether the EEG features used to train the CSP, SPoC and cSPoC filters were of cortical origin or whether they might stem from ocular or other artifact sources. For this purpose we examined the spatial activation patterns that correspond to the components found by the three methods as well as the corresponding power envelopes of the components' time series. In contrast to spatial filters, the spatial activation patterns of components can be interpreted physiologically, as they allow to draw conclusions about the spatial location of the cerebral source that generated the component's activity (Haufe et al., 2014c). Figure 9 shows the patterns and power envelopes of the three spatial filtering methods. The components were computed on the whole data set and then projected on the band-pass filtered data that had been segmented into epochs of 10 seconds length. The resulting power envelope was then smoothed with a 50-second, sliding, zero-phase boxcar window and averaged over all 32 pairs of consecutive *L-H* blocks.

In the following, we show results exemplarily for four different subjects. Subjects were selected such that they roughly represent the spectrum of classification performance in our study, from best (subject *gaa*), over moderate (subject *lh*) to lowest (subjects *icc* and *ik*). Furthermore, we show the component pairs that correspond to the *highest* value of the corresponding optimization criterion, that is, for example, the component with largest absolute-value Eigenvalue in the case of CSP.

The results for the remaining six subjects are shown in Appendix A in Figures 23 and 24. Likewise, in Appendix A the results of *all* subjects that correspond to the *second highest* and *third highest* values of the corresponding optimization criterion are shown in Figures 25 to 28, respectively.

Spatial Activation Patterns

The form of the CSP, SPoC and cSPoC components' activation patterns shown in Figure 9 – but also the patterns of the components of the second and third highest optimization criterion values, as well as all those of the other subjects (see Figures 23 to 28) – shows none of the characteristics of patterns related to EOG (see e.g. Figure 1a) or EMG (see e.g. Figure 10) activity, hence suggesting that the components found by the three methods are of cortical origin. An examination of the patterns in the theta frequency band shows that all three methods consistently found a characteristic theta mid-frontal component, either among the component with the highest value of the corresponding optimization criterion (Figure 9: cSPoC for subject *gaa*, all methods for subject *lh*, CSP and SPoC for subjects *icc* and *ik*), or among the components with lower values of the optimization criterion. Regarding the patterns of the alpha band components, although no particular consistency is observable across subjects, the spatial dis-

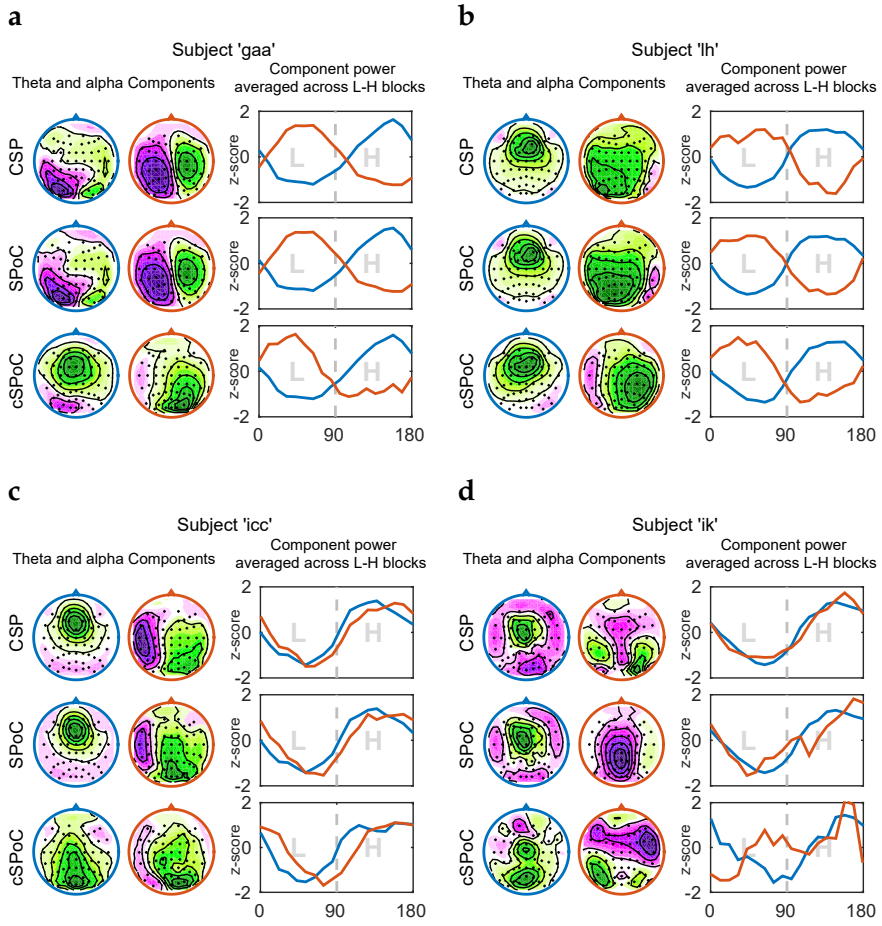

Figure 9: Spatial activation patterns and power envelopes of components extracted by the three EEG spatial filtering methods. Shown are four exemplary results from subjects *gaa* (**a**), *lh* (**b**), *icc* (**c**) and *ik* (**d**). The shown activation patterns (scalp maps) and power envelopes correspond to the components with the highest value of the optimization criterion of the respective method. The left and middle column show the activation patterns of components obtained from the theta (blue) and alpha (red) bandpassed data, respectively. The color coding and sign of the activation patterns were adjusted to be consistent across methods and subjects but are arbitrary otherwise. The power envelopes (right column) are color coded accordingly (theta: blue, alpha: red), the x-axis shows time in seconds. Due to standardizing to z-scores, the amplitudes of the curves do not relate to discriminative power.

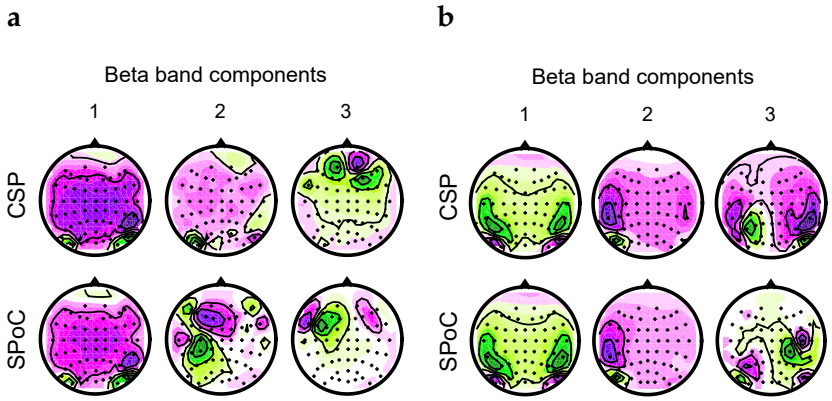

Figure 10: The first three spatial activation patterns found by CSP and SPoC for the beta band (14–29 Hz), exemplarily for subjects *lh* (**a**) and *icc* (**b**).

tribution of these patterns suggest that the sources that generated them are of cortical origin as well.

Inspection of Beta Band Patterns

Independent of the analysis pipeline of the predictive models, we furthermore examined the spatial activation patterns found by CSP and SPoC when applied to EEG data filtered in the beta frequency range (14–29 Hz). In contrast to those in the theta and alpha band, they all display the characteristics of patterns related to EMG activity (Figure 10). In this frequency range, the EMG activity caused by head movements has a strong impact on the outermost channels, resulting in patterns with either a clear ring shape (e.g. first components for subject *lh*), or with very focal contributions from only a few channels (e.g. third components for subject *lh*).

Power Envelopes

The right column in the four panels of Figure 9 shows the power envelopes of the theta and alpha components' time series, averaged over all L-H block pairs. The envelopes of theta components (blue) depicted in Figure 9 all show a positive correlation between band power and the task difficulty, i.e. low power during the L, high power during the H condition. Also a majority amongst all other theta components used for classification shows this positive correlation. This finding is consistent with workload literature (Gevins and Smith, 2003; Holm et al., 2009) and substantiates the assumption that the theta components found by the three models are sound. The power envelopes of alpha components (red), on the other hand, don't show a consistent tendency towards a negative correlation of alpha power against induced workload state, as is often reported in workload literature. For instance, while for subjects *gaa* and *lh* the expected negative correlation is indeed observed in all models, for subjects *icc* and *ik* the correlation

has the same sign as that of the its theta counterpart. Interestingly, the correlation of alpha power with workload level is directly related to the performance of the predictive models.

3.4.4 *Added Value of Physiological Measures*

Given the modulation of PPMs by the workload condition (Figure 5b-d) and given that PPM features can be extracted from the data as an unsupervised signal, we assessed whether PPM features consitute an added value to the features extracted in the unsupervised models Ch_{Uns} and SF_{Uns}. We first of all found that the mean classification accuracy using only PPM features was 81.8% (Figure 11, white bar). We then repeated the cross-validation with models Ch_{Uns} and SF_{Uns}, this time however augmenting the EEG features with PPM features, resulting in classification accuracies of 79.3% for model Ch_{Uns} (3.6% increase) and 88.2% for model SF_{Uns} (4.3% increase). While the increase for model Ch_{Uns} is not significant (paired, one-sided $t(9) = -0.90$, $p = 0.19$), the increase for model SF_{Uns} is significant (paired, one-sided $t(9) = -3.03$, $p = 0.007$). These results support the assumption that peripheral physiology can indeed provide an added value to the unsupervised model SF_{Uns} for the classification of workload.

3.5 DISCUSSION

3.5.1 *Performance Loss Due to Label Degradation*

We investigated the limits of classifying workload states by progressively confining the information about the experiment available to the BCI, ultimately striving for a fully unsupervised approach. We therefore employed six predictive models, three of which use state-of-the-art spatial filtering methods. In order to classify both workload conditions, all models exploit the known relationship between workload and power modulations in the theta and alpha frequency bands in the EEG. However, they differ in the type and amount of information they require about the experiment. While the classification and the regression models required either direct or indirect label information from the experiment, the unsupervised models do not require any information at all, thus constituting virtually unsupervised approaches.

The progressive restriction of information is reflected in a decrease of classification performance. The predictive models SF_{Cla} and SF_{Reg} (and the spatial filtering methods used therein, CSP and SPoC) both represent typical examples of supervised approaches. However, while CSP and LDA need to be trained using binary labels of induced workload states, SPoC in combination with regression may use any continuous variable or measurement that reflects the induced state. In our study the error rate of subjects is an obvious candidate for a target variable for SPoC, since it was found to be clearly modulated by the workload state (Figure 5a). However, it is likely that changes in the er-

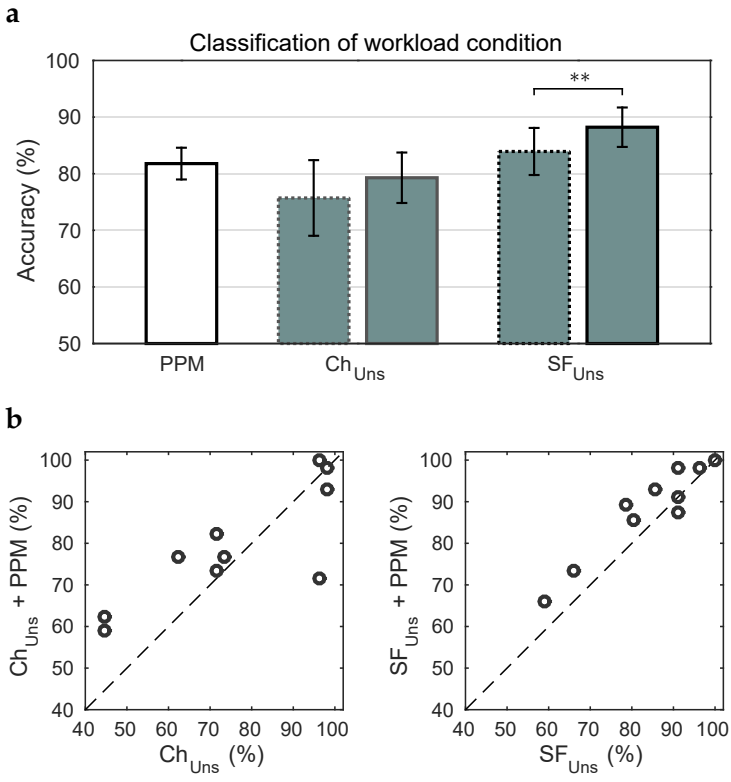

Figure 11: Added value of peripheral physiological measures. **a**. Mean classification accuracy and standard error across subjects when using only PPM features (white) and comparison to the two unsupervised predictive models Ch_{Uns} and SF_{Uns} before (dotted, same as in Figure 6a) and after (solid) augmenting with PPM features. Scatter plots in **b** show the comparison on single subject results.

ror rate are additionally influenced by other, perhaps more stochastic, aspects of brain activity, or that they are inluenced by the structure of the experiment (Porbadnigk et al., 2015). The error rate can thus be regarded as a noisy version of the workload condition labels. Therefore, a decline in classification accuracy as well as error rate prediction performance is to be expected when going from the SF_{Cla} model (trained with noise-free workload condition labels) to the SF_{Reg} model (trained with the error rate).

The mean classification accuracy of the SF_{Uns} model showed a further decline in performance relative to that of the SF_{Reg} model. This decrease was expected as well, since – as opposed to models SF_{Cla} and SF_{Reg} – the optimization procedure in cSPoC (the spatial filtering method used in model SF_{Uns}) is agnostic of the precise experiment structure and relies solely on the known workload induced modulations of cross-frequency couplings in the EEG. To some degree this method may suffer from the fact that the sign of workload induced power modulations in the alpha band is not so clear (see Section 3.5.3). This assumption is supported when inspecting the power envelopes of the cSPoC components of subjects *icc* and *ik* (Figure 9c,d). Although it is intrinsic to the optimization procedure of cSPoC to find component pairs whose power envelopes are maximally negatively correlated, the power envelopes of the cSPoC alpha components of these subjects show a rather positive correlation with the envelopes of the theta components and therefore with the workload condition. Correspondingly, those two subjects have the lowest classification accuracies with the predictive model SF_{Uns}.

3.5.2 *The Advantage of Spatial Filtering*

For similar reasons as stated above, the three channel-based models Ch_{Cla}, Ch_{Reg} and Ch_{Uns} show the same decline of performance when going from using class labels to the unsupervised case. While model Ch_{Cla} uses precise binary labels to combine the extracted features, model Ch_{Reg} performs a regression on the error rate, a noisy version of the class labels. Finally, model Ch_{Uns} comprises a fundamentally simple unsupervised approach that makes use solely of the known workload-induced, localized anticorrelation of theta and alpha power. The more interesting finding, however, is that for the classification-based, regression-based and unsupervised models, the use of spatial filtering leads to performance increases of roughly 4%, 4% and 8%, respectively. Due to the small number of subjects and – particularly for the unsupervised models – due to the large spread of accuracies across subjects, this increase is not statistically significant for all models. Nevertheless, this finding substantiates the argument that the use of spatial filtering is essential for extracting meaningful features from oscillatory EEG signals and can result in considerable performance increases in the classification of workload states from EEG.

3.5.3 *Interpretation of Model Components*

An inspection of the patterns corresponding to the filters found by the methods CSP, SPoC and cSPoC shows that they all lack the characteristics of components associated with EOG or EMG activity (Figure 9). This finding suggests that the signals used by the four EEG models were indeed generated by cortical sources and were not confounded by other (non-EEG) variables related to workload or to the task.

Findings from neurophysiology indicate a relationship between theta and alpha oscillations in the EEG on the one hand and cognitive effort, task engagement and workload on the other hand (Klimesch, 1999). Furthermore, time pressure effects on visuomotor task performance are reflected in power changes in midline theta and parietal alpha (Slobounov et al., 2000). An increase of theta power has been shown to be associated with working memory and cognitive control, predominantly over frontal regions (Jensen and Tesche, 2002; Onton et al., 2005; Cavanagh and Frank, 2014). Our results confirm the positive correlation with workload (Figure 9). Not only did all three spatial filtering methods find at least one component that shows the characteristic frontal midline theta activation pattern, but also the power envelope corresponding to those patterns was positively correlated with the workload condition.

The exact role of the alpha rhythm with respect to workload, on the other hand, is still not very clear. Findings from numerous studies have lead to the prevailing idea of alpha band synchronization as a cortical 'idling' mechanism. Accordingly, a decrease in alpha power has been shown to be associated with an increase in resource allocation or workload (Klimesch, 1999; Keil et al., 2006), thus representing a marker for workload that is opposite to that of the theta band. However, several studies have questioned a clear negative relationship between alpha power and workload, showing that alpha power can indeed increase with memory load (Jensen et al., 2002) and that the exact direction depends on the specific task and the strategy of subjects (Klimesch et al., 1999; Cooper et al., 2003) and even depends on the precise frequency sub-range (Fink et al., 2005). Findings from some studies using non-visual tasks even contradict the negative relationship between alpha power and workload, showing that the parietal alpha power increases with workload (Galin et al., 1978; Markand, 1990), while other findings suggest that in tasks with constant high visual flow the alpha rhythm might be completely blocked already, showing little to no changes related to workload (Kohlmorgen et al., 2007).

This unclear role of the alpha band is a likely explanation for the fact that our data show neither an apparent consistency across subjects in the shape of the activation patterns, nor in the sign of the correlation between the envelopes and the workload condition. Since the spectral features resulting from the spatial filters in the predictive models SF_{Cla} and SF_{Reg} are subsequently optimized via LDA and regression, respectively, the inconsistency in the sign of the relationship between alpha power and workload is irrelevant for these mod-

els. For the unsupervised model SF_{Uns}, however, the unsupervised subtraction of cSPoC features may have a detrimental effect on its performance.

3.5.4 *Added Value of Peripheral Physiology*

Previous studies have shown that workload is not only associated with changes in the EEG but also with peripheral physiological measures (PPMs) such as heart rate (Vogt et al., 2006), respiration frequency (Karavidas et al., 2010) and electrodermal response (Kohlisch and Schaefer, 1996; Reimer and Mehler, 2011). We recorded these three PPMs in addition to the EEG and investigated their ability to classify the induced workload states. We found that the three PPMs were modulated by task difficulty (Figure 5) and that features extracted from them can be combined in an unsupervised manner to classify the workload conditions with an accuracy of 81% (Figure 11). Previous studies have reported only small and non-significant classification increases when fusing EEG features with features from physiological measures, as compared to using only EEG (Christensen et al., 2012; Hogervorst et al., 2014).

In contrast, we found that even an unsupervised fusion of PPM features with the cSPoC features in model SF_{Uns} resulted in a significant increase of classification performance of 4.3%. A possible explanation for this disagreement is that the type of workload induced in this study, which involved constant motor engagement, has a stronger effect on the vegetative system than the mental workload as induced by an n-back task (Hogervorst et al., 2014). Hence, physiological measures can indeed constitute an added value to EEG-derived signals for the classification of workload states, even with an unsupervised approach.

3.6 CRITICAL ASSESSMENT OF CHALLENGES

At the beginning of this chapter we formulated several challenges that were of major interest. In the following, we assess to what extent those challenges were met and how they contribute to the goal of developing brain-computer interfaces capable of online detection of workload states.

3.6.1 *Assessment of Challenge 1*

The first challenge was to go beyond the hitherto prevailing efforts to assess workload as induced by purely mental effort (Gevins et al., 1990; Stikic et al., 2011; Brouwer et al., 2012; Hogervorst et al., 2014). With the experimental design presented here, participants faced several challenges: (i) They were required to be constantly attentive of the falling screw triplets, (ii) to memorize the color code of (multiple) triplets when tagging the catching bucket and (iii) to coordinate the execution of hand movements with the visual perception of the

game. The task is thus likely to increase requirements in attention, working memory and in visuomotor coordination. Our findings confirm the expected effects of working memory and attention demands on the theta and alpha frequency bands (Section 3.5.3). However, the integration of sensory information into executive control components of complex visuomotor tasks has been found to be associated with modulation of long-range coupling (Von Stein and Sarnthein, 2000; Sauseng et al., 2007), coherence (Classen et al., 1998; Aoki et al., 2001) and power (Chen et al., 2003) in the theta and alpha frequency bands. It is therefore not trivial to find the same effects of a multimodally effected workload on those frequency bands as for purely mental effort (Gevins and Smith, 2003; Holm et al., 2009). Nonetheless, the interpretation of the found model components (Section 3.5.3), in combination with the clear success of the predictive models (Section 3.4.2), supports the validity of our approach.

3.6.2 *Assessment of Challenge 2*

The second challenge was to develop a "true" brain-computer interface in its proper meaning, and is closely related to the first one. This is becasue the task required participants to continuously move their head and eyes and the intensity and frequency of those movements was likely to be correlated with the task difficulty. An inspection of the components found by the three spatial filtering methods (Section 3.4.3) reveals that none of them displays the characteristics of components associated with EOG or EMG activity (Figures 1 and 10). The introduction of EMG activity into the signals used for classification was averted by simply restricting the used frequencies to bands clearly below 20 Hz (Whitham et al., 2007). The influence of EOG activity was minimized by removing the estimated eye movements from the EEG data via a regression approach (Parra et al., 2005).

Most importantly, however, the very ability to assess the origin of the signals used by the models via inspection of the spatial activation patterns is only rendered possible by the use of the spatial filtering methods. While one can obtain spatial activation patterns from the weighting coefficients in models Ch_{Cla} and Ch_{Reg}, they cannot be interpreted physiologically because the bandpower is computed at the level of channels, which corresponds to a non-linear transformation of linearly mixed signals. Only by accounting for the generative model, i.e. by first applying a linear unmixing and then applying the non-linearity (computing the bandpower), a phyiological interpretation becomes possible (Dähne et al., 2014a; Dähne et al., 2014b; Haufe et al., 2014c). Thus, only the use of the spatial filtering methods CSP, SPoC and cSPoC allows for a thorough scrutiny of the origin of signals in verifying that this origin is cortical.

3.6.3 *Assessment of Challenge 3*

These spatial filtering methods are also the essential ingredient for tackling the third challenge. The CSP analysis (Blankertz et al., 2008) is widely used among the BCI community and has become one of the corner stones of sensorimotor rhythm based BCIs (Fazli et al., 2015). Given a binary classification setting it is well suited for maximizing the signal-to-noise ratio of power modulations in a frequency band. The SPoC algorithm (Dähne et al., 2014a) can be considered a generalization of CSP where the two-class labels become a continuous target variable and thus can be applied in a regression setting. The finding that the roughly 2% decrease in performance between models SF_{Cla} and SF_{Reg} (which use CSP and SPoC, respectively) is almost negligible suggests that the strict requirement for binary labels can be abandoned if a continuous variable closely related to the workload state is available.

The use of the canonical SPoC algorithm (Dähne et al., 2014b) in model SF_{Uns} demonstrates that we can go even one step further and completely eliminate the need for a supervision signal. A mean performance of roughly 82% and 8 out of 10 subjects achieving more than 70% accuracy are substantial results considering the completely unsupervised approach in this model. They furthermore demonstrate that the effect of workload level on the well-known anti-correlation of theta and alpha power is robust enough to be used in an unsupervised setting where no label information is available. This finding shows that it is in principle possible to develop a BCI for workload detection with minimal requirements for calibration.

3.6.4 *Assessment of Challenge 4*

The fourth challenge aimed at exploring the fusion of brain and peripheral physiological measures for detecting workload levels. The convenience in this approach comes from the unsupervised nature of the extracted PPM features. This allows to combine them with the EEG features extracted in the unsupervised predictive models Ch_{Uns} and SF_{Uns}. Our findings show that in the case of model SF_{Uns} a significant increase of more than 4% is achieved, resulting in a mean performance of 88% and achieving more than 70% accuracy in all but one subject. Hence, the fusion of neuro- with peripheral physiological signals yields a substantial improvement of performance for the unsupervised approach. At first sight, the idea to fuse the features of several modalities might seem contradictory given that challenge 2 aimed at excluding any non-cortical signals for workload detection. However, our proposed procedure allows for a fully controlled fusion, where the contribution of each modality is known. Thus, depending on the precise specifications of the ultimate BCI application and on the availability of such physiological signals, the augmentation of the feature space can be turned on and off as needed.

4

INVESTIGATING THE ROLE OF THE READINESS POTENTIAL

It has been repeatedly shown that many voluntary decisions are preceded by specific brain signals. The most well-studied instance is the so called readiness potential (RP), which starts more than one second before spontaneous, voluntary movements (Kornhuber and Deecke, 1965). Similar signals have also been demonstrated using other imaging techniques including functional magnetic resonance imaging (fMRI) (Soon et al., 2008), invasive measures such as single neuron recordings (Fried et al., 2011) and local field potentials (Maoz et al., 2012). Such preceding signals are not only found for movement decisions but also for free choices between high-level cognitive tasks (Soon et al., 2013), for perceptual choices (Bode et al., 2012) and for value-based decisions (Maoz et al., 2013). These findings suggest that such signals may constitute a part of a general mechanism of decision preparation.

To date, the exact nature and causal role of the RP in voluntary movements – but also of other choice-preceding brain activity – is debated controversially. On the one hand, it is evident that the very last part of the RP close to the movement is directly linked to movement preparation and execution (Shibasaki and Hallett, 2006). And yet the finding that the RP starts more than one second before the movement is remarkable, even more so considering the famous experiment by Libet et al. (1983). They reported that the onset of the RP preceded not only the movement but also the perceived time of the intention to move. Libet's findings and subsequent variants of his experiment (Haggard and Eimer, 1999; Soon et al., 2008; Fried et al., 2011) seem to demonstrate that the decision to move is generated unconsciously by preconscious neural processes and only enters awareness later. In contrast, recent studies have put forward a reinterpretation of the RP, suggesting that its early onset is the result of averaging stochastic, autocorrelated background fluctuations (Schurger et al., 2012; Jo et al., 2013) and that the neural commitment to move occurs indeed later, shortly before the movement (Schurger et al., 2016).

In this chapter, we sought to contribute to this line of research by employing a brain-computer interface as a research tool. We thus exploit the ability of a real-time BCI to detect covert movement intentions from the ongoing EEG and therefore to interact with the person, even before any overt movement occurs. This allows us to investigate the role of the RP and study the degree of control that a person exerts in the generation of voluntary movements. In the following sections, we first describe the existing research on the RP and on inhibitory control and subsequently formulate questions that result from the connection of these two research directions. We then continue to propose an experiment in which a brain-computer interface is employed

in order to test the underlying hypotheses and finally present our findings and discuss how they relate to the ongoing controversy on movement preceding brain signals.

Parts of the findings presented in this chapter were published in Schultze-Kraft et al. (2016a).

4.1 THE OBJECTIVE OF INVESTIGATION

4.1.1 *The Readiness Potential*

The readiness potential (RP) was first described by Kornhuber and Deecke (1965). They found that a slow negative EEG potential is observed preceding voluntary, self-initiated movements (Figure 12). They termed this activity "Bereitschaftspotential", which was then appropriated in English to readiness potential. The RP starts more than one second before the onset of self-initiated movements and is observed over central EEG channels. Ever since, numerous studies have examined the individual components and neural mechanisms of the RP. From its onset and up until about 400 ms before movement onset, the RP shows a slow negativation that is maximal at the midline centro-parietal area and is symmetrically distributed over the scalp, independent of the body part that is moved (Deecke et al., 1969; Cui et al., 1999). About 400 ms before movement onset, the RP suddenly increases its slope and becomes asymmetrically distributed on the scalp, with a stronger negativity over the hemisphere contralateral to the moved body part (Coles et al., 1988; Eimer, 1998). Hence, this late component of the RP has been coined the lateralized readiness potential (LRP).

The early RP is generated in the pre-supplementary motor area (preSMA) and the SMA proper, while the late component is generated by the contralateral primary motor cortex (M1) (Lang et al., 1991; Cui et al., 1999; Yazawa et al., 2000; Shibasaki and Hallett, 2006). Furthermore, while RPs are mostly reported for self-initiated movements of body limbs or fingers, they have been also observed before eye saccades (Papadopoulou et al., 2010), speech (Galgano and Froud, 2008) and imagined movements (Cunnington et al., 1996). Recently, Alexander et al. (2016) also reported readiness potentials driven by non-motoric processes.

4.1.2 *Is there a Point of no Return?*

Given the early onset of the RP before a voluntary movement, the question arises how much its presence undermines a person's *degree of control* over their behavior. Let us consider the following analogy: One possibility is that the onset of the readiness potential triggers a chain of events that unfolds in time and cannot be cancelled. The onset of the readiness potential in this case would be akin to tipping the first stone in a row of dominoes. If there is no chance of intervening, the dominoes will gradually fall one by one until the last one is

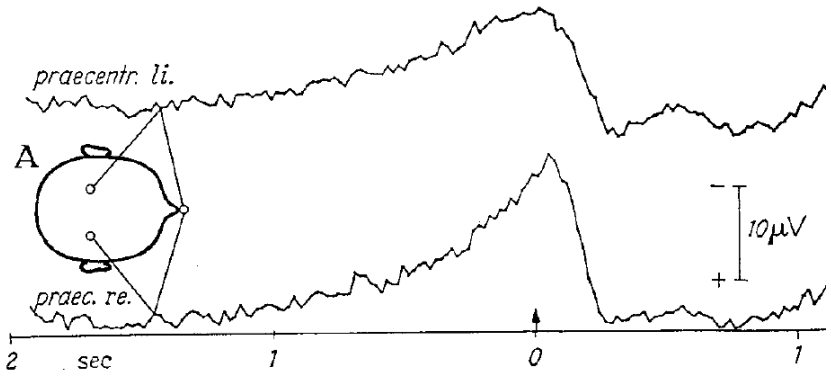

Figure 12: The first depiction of a readiness potential (figure taken from Kornhuber and Deecke (1965)). The shown potentials are the average of 512 movements of the left hand, unipolarly recorded with two electrodes over the left (*praecentr. li.*) and right (*praec. re.*) motor areas and referenced against an electrode on the nose. The arrow (at $t = 0$ sec) indicates movement onset. The onset of the RP was reported to be between 1 and 1.5 seconds before movement onset. The stronger negativation of the potential close to the movement at the right electrode (contralateral to the moved hand) already indicated what was later termed the lateralized readiness potential (LRP) (Coles et al., 1988).

reached. A different possibility is that a person can still terminate the process, akin to taking out a domino at some later stage in the chain and thus preventing the process from completing. In other words, is there, along the time course of the RP, a *point of no return* after which the process of movement preparation becomes "ballistic" and the intended movement can no longer be aborted?

The question whether there is a point of no return in movement (preparation) has so far been investigated in the context of the stop-signal paradigm (Logan and Cowan, 1984). In this paradigm, subjects are given a primary task to perform and, on occasion, a stop signal is presented that tells them not to respond on that trial. Findings from such studies have led to a model for response inhibition called the race model: It proposes that a go process (triggered by the go stimulus) and a stop process (triggered by the stop signal) race against each other until a point of no return is reached (Osman et al., 1986). If the go process wins, then there is a response despite the stop signal. If the stop process wins, then no response occurs. The point of no return is said to separate the initially *controlled* stage from the subsequent *ballistic* stage of the race. Previous work on event-related potentials has indicated that planned movements can be interrupted by stop signals until very late stages, even beyond central planning and all of the way into motor execution. This has been taken to indicate that there is no final ballistic stage in the brain where a movement will necessarily unfold fully once triggered (De Jong et al., 1990).

In contrast to stop signal studies, in the case of spontaneous, voluntary movements the initial decision to move is not externally but internally triggered. It has as yet remained unclear whether a person is able to cancel self-initiated movements after the onset of a RP, and if so, whether there is a point of no return after which the process becomes ballistic and a cancellation impossible.

4.1.3 *Can a Person Override the RP?*

Another related question that departs from the concept of inhibitory control is whether subjects can intentionally override or manipulate the RP. Answering this question would allow to reveal whether the readiness potential is a uniform and inalterable – and thus, ultimately, a *necessary* – feature of movement preparation (Pockett and Purdy, 2010). Although no direct evidence for the ability to intentionally override the RP exists, previous findings suggest that such a mechanism could hypothetically exist. For instance, conscious attention to the intention in voluntary movements results in an increased activity in the pre-SMA (Lau et al., 2004), the brain area where the early RP is believed to be generated. Furthermore, the amplitude of the RP has been shown to be influenced by several factors, such as effort, precision and complexity of the movement (Kitamura et al., 1993; Masaki et al., 1998; Slobounov et al., 2004). And finally, the amplitude of the RP has also been found to differ substantially depending on whether a spontaneous movement is performed consciously or unconsciously (Keller and Heckhausen, 1990). These findings support the idea that the readiness potential might indeed be under the conscious control of an individual, possibly enabling them to behave in an unpredictable fashion.

4.1.4 *A Man–Machine Duel*

We directly tested these two hypotheses in an experiment in which participants played a game against a "decision prediction machine" (Chiang, 2005; Haynes, 2011) that is able to detect the readiness potential from the EEG and feed back its occurrence to a person instantaneously and in real-time. In this game, participants made spontaneous, voluntary movements, but were instructed to terminate their decision and withhold any movement whenever a stop signal was elicited by the prediction machine. If they moved without being predicted they would win points; if they moved despite the elicitation of the stop signal they would lose points. Hence, subjects were challenged to avoid having their decision to move predicted from previous brain activity, either by stopping the intended movement or – alternatively – by modifying or overriding their RP. Because of the similarity with a shootout scenario in a western, where a gunman has to draw unpredictably, we coined our experiment the "duel game".

Evidently, the basic requirement for the machine in this duel is to be able to elicit the stop signal after the onset of the RP but be-

fore the onset of the movement. This machine was implemented by means of a brain-computer interface that had been trained to detect the occurrence of a RP in the EEG. Detection of movement intention from preceding brain signals has been typically studied offline (Lew et al., 2012; Salvaris and Haggard, 2014), whereas to date only few have undertaken the approach in real-time (Bai et al., 2011; Maoz et al., 2012). Here, we used features from EEG segments preceding voluntary movements in order to train a BCI to detect RPs from the ongoing EEG. During the experiment, such a detection immediately elicited a stop signal that instructed participants to withhold any intended movement.

4.2 PROCEDURES

In the following sections, the experimental procedures employed in this chapter are described. We start with presenting the "duel game" task that participants performed during the experiment and conclude with the description of the BCI predictor and several offline analyses that were conducted after the experiment.

4.2.1 *The "Duel Game"*

Subjects

We investigated twelve healthy, right-handed, naive subjects (7 female, mean age 24.9, SD 2.3 years). Two subjects (one male, one female) were removed directly after stage I because their low RP amplitudes yielded classifier accuracies near chance level. The experiment was approved by the local ethics board and was conducted in accordance with the Declaration of Helsinki. All subjects gave their informed oral and written consent.

The Task

Subjects were seated in a chair facing a computer screen at a distance of approximately 1 m. They were asked to place their hands in their lap and their right foot 1-2 cm in front of a 10 cm x 20 cm switch pedal (Marquardt Mechatronik GmbH, Rietheim-Weilheim, Germany) attached to the floor. The delay times between motor cortex and onset of EMG in the peripheral muscle (soleus) are well described and amount to around 25 ms (Morita et al., 2000), which is slightly slower than delay times for hand movements of 15 ms (Calancie et al., 1987). However, depressing a pedal/button with the foot is a very standard effector. Especially to everyone driving a car this foot movement is well learned due to its similarity to pressing the brake pedal in a motorized vehicle. It has also been studied in several BCI settings, e.g. in the context of emergency braking (Haufe et al., 2011). The precise movement task consisted in lifting the foot from the floor and pressing the button as fast as possible and in a consistent way. Foot

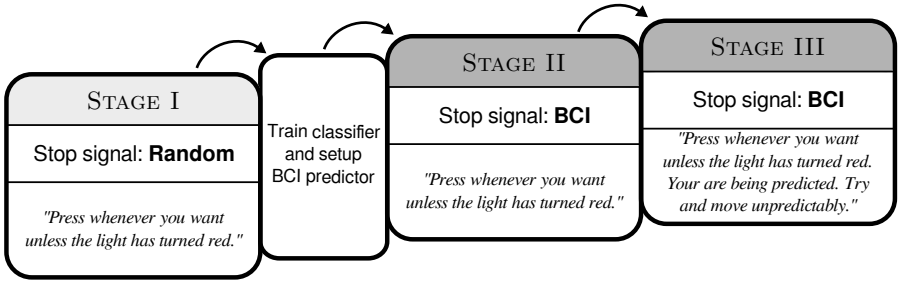

Figure 13: Experimental design. The experiment consisted of three consecutive stages. In all three stages, after seeing the green trial start cue subjects were instructed to press the floor mounted foot button at any time, unless the light turned red (stop signal). During stage I the stop signals were random. After stage I a classifier was trained on button presses from stage I and the BCI predictor was activated. In the subsequent stages II and III stop signals were elicited in real-time by the BCI predictor. After stage II subjects were informed about the predictor and instructed to try and move unpredictably.

movements were chosen after piloting instead of hand movements because they yield larger readiness potentials (Brunia et al., 1985).

In the experiment subjects played a novel "duel game" based on the Libet experiment (Libet et al., 1983) using aspects of interruption and stop signal tasks. The duel game consisted of individual trials of which each subject performed an average of 326 during the whole experiment. The start of a trial was signaled by the circle in the middle of the screen turning green. Subjects were instructed to wait for 2 seconds after the start cue, after which they could press the button at any time, unless the stop signal – indicated by the circle turning red – was shown. In that case they were told to withhold any movements. The framing of a game was chosen so that subjects would feel encouraged to execute button presses as late as possible. In order to achieve this, at the end of the experiment subjects were paid 10€ per hour but could earn an additional bonus. This bonus was based both on the number of trials in which they pressed the button without being interrupted by the stop signal and on the duration between trial start and the time of button press.

The task was organized into three stages (each organized into two 10-minute blocks) (Figure 13). During stage I stop signal times were randomly drawn from a uniform distribution in the interval 2 to 18.5 seconds after the trial start cue. During stages II and III stop signals were triggered in real-time by the beforehand trained BCI predictor. Furthermore, in these two stages 40% of trials were randomly assigned as "silent". In these trials the BCI predictions were recorded but the stop signal was turned off; thus these trials were always ended by the subject pressing the button. Before stage I subjects were informed that the computer generated the stop signals "randomly" and that there was "no particular pattern". No new information was pro-

vided to subjects before stage II, i.e. they were unaware of the change of the origin of stop signals. Before stage III, subjects were told that the computer was trying to predict them: "The computer will try to guess when you are about to move and interrupt you, the interruptions are based on your history of previous actions." Subjects were asked not to test the system by making false or bizarre movements – with the new instruction that they should "try to be unpredictable."

Questionnaire

A questionnaire was used to collect information about each subject's subjective experience. After each stage subjects were asked two questions: "Did you use a particular strategy during the last round?" and "Did you feel there was a connection between your actions and the appearance of an interruption?" After stage III subjects were asked three further questions: Whether or not they felt predicted; how good the computer's predictions were; and if predictions had improved or worsened since the last stage.

4.2.2 *Data Acquisition*

EEG was recorded at 1 kHz with a 64-electrode Ag/AgCl cap (64Ch-EasyCap, Brain Products GmbH, Gilching, Germany) mounted according to the 10-20 system, referenced to FCz and re-referenced offline to a common reference. The amplified (analog filters: 0.1, 250 Hz) signal was converted to digital (BrainAmp MR Plus and BrainAmp ExG), saved for offline analysis, and simultaneously processed in real-time by the Berlin Brain-Computer Interface (BBCI[1]) toolbox (Blankertz et al., 2007a). The "duel game" task was implemented using the Pythonic Feedback Framework (PyFF) (Venthur et al., 2010b).

In addition to EEG, electromyogram (EMG) was recorded from the right calf using surface Ag/AgCl electrodes in order to obtain the earliest measure of movement onset. EMG onset was determined by first computing the square of the EMG signal and then detecting the time points of crossing of a subject-specific threshold of 99.9% above baseline.

4.2.3 *Online BCI Predictor*

At the end of stage I, a linear classifier was trained using segments of EEG data from all stage I trials which were not ended by a random stop signal but by a button press. From each of these trials, two periods were defined as "movement" and "no movement": The former were 1200 ms long segments immediately preceding EMG onset, while the latter were 1200 ms long segments immediately preceding the trial start cue. EEG data from those segments were averaged over 100 ms windows, resulting in 12 samples per window and channel.

1 github.com/bbci/bbci_public

The samples from a subset of channels were concatenated and used as features to train a regularized Linear Discriminant Analysis (LDA) classifier with automatic shrinkage (Blankertz et al., 2011). Channels in which the RP peak amplitude was above the mean RP amplitude across all channels were chosen as the subset, the number varied between 8 and 12 across subjects. The so-trained classifier was eventually used to make predictions of movements in real-time during stages II and III. Every 10 ms a feature vector was constructed from the immediately preceding 1200 ms of EEG data and used as input to the classifier, generating a classifier output value every 10 ms. Whenever this value crossed a threshold this was considered a prediction, the event time was recorded and a stop signal issued (except for silent trials).

The classifier output threshold was determined individually for each subject after the training of the classifier. For this we performed a 10-fold cross-validation where – mimicking the real-time predictor with a sliding window – we computed the time of first threshold crossing of the classifier output for different threshold values. We assumed that predictions earlier than the onset of the readiness potential at 1000 ms before movement onset likely represented false positives. Since we sought to predict subjects as early as possible, the threshold was chosen such that the number of predictions in the interval -1000 to 0 ms with respect to movement onset was maximal.

4.2.4 *Offline Analyses*

Three offline analyses were performed on the EEG data after recording. A detailed overview of each analysis is provided in Appendix A in Table 2. Analysis 1 was used as a qualitative assessment of the amplitude of the RP at the time of EMG onset in Section 4.3.2, analyses 2 and 3 were used to search the EEG for markers of movement preparation prior to stop signals in Section 4.3.5.

4.3 RESULTS

4.3.1 *Behavioral Results*

We first examined the participants' behavior in pressing the button. Since a certain variability in the velocity of movements was expected, the EMG onset was used as a reference point throughout all analyses. The mean waiting time between trial start and EMG onset across subjects and stages was 5441 ms and the mean movement duration from EMG onset to button press across subjects and stages was 316 ms. Figure 14 shows the waiting times and movement durations for single stages. Although the distributions pooled across all subjects in Figure 14a suggest that participants waited less to press the button after the trial start cue, a one-way three-level repeated measures ANOVA revealed that the effect of stage on waiting time is not significant ($F(2, 18) = 3.36$, $p = 0.06$). The same analysis on movement ve-

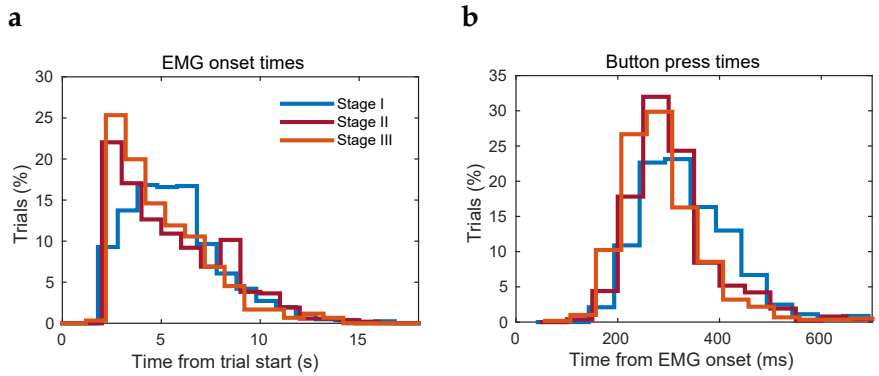

Figure 14: Behavioral results. **a.** Distribution of waiting times (time from trial start to EMG onset) for the three stages, pooled across all subjects. Waiting times shorter than 2 seconds were discarded from all analyses. The mean waiting time across subjects was 5995 ms, 5462 ms and 4907 ms in successive stages I, II and III, respectively. **b.** Distribution of movement duration (time from EMG onset to button press) for all three stages (as in a). The mean duration of movements from EMG onset to button press was 345 ms, 305 ms and 303 ms in stages I, II and III, respectively.

locity, however, revealed a significant effect of stages ($F(2, 18) = 9.86$, $p = 0.0013$), such that movements were made faster in stages II and III.

4.3.2 *Readiness Potential*

Next we examined the readiness potential of foot movements as recorded by the EEG. Figure 15 shows the mean EMG activity (top), the distribution of button press times (inset) and the average readiness potentials (RPs, main panel) for the three experimental stages, time-locked to EMG onset. During all experimental stages the event-related potential time-locked to EMG onset showed the typical exponential-looking readiness potential at channel *Cz* (Deecke et al., 1969). As the scalp topographies of the three shaded intervals show, the RP has the highest amplitude over channel *Cz*. Furthermore, the RP did not manifest a lateralization at any time. This is to be expected for foot movements because in contrast to hand movements the motor representation of the leg and foot are not on the lateral surface but on the medial wall (Brunia et al., 1985). Despite the differences in experimental conditions, there was no significant difference between RPs in the three stages. Thus, the instruction given to subjects between stages II and III to use strategies to avoid prediction did not alter the shape of the readiness potential. There was no significant main effect of stage at either interval ($F(2, 18) = 0.02$, $p = 0.97$; $F(2, 18) = 0.12$, $p = 0.89$; and $F(2, 18) = 0.20$, $p = 0.82$, respectively), suggesting that

the subjects' strategies to avoid prediction did not alter these preceding brain signals.

We further investigated the relationship between RP amplitude on the one hand and waiting time and movement duration on the other. Therefore, we first performed a qualitative assessment of the amplitude of the RP at the time of EMG onset. For this, we performed the offline analysis 1, as defined in Section 4.2.4. We used the cross-validated classifier output at EMG onset as an estimate for RP amplitude, since both quantities are directly related. As depicted in Figure 16, the amplitude of the RP at EMG onset showed a significant negative correlation both with waiting time ($r = -0.12$; $p < 0.001$) and with movement duration ($r = -0.22$; $p < 0.001$). Thus, the stronger the RP, the shorter the waiting time and the faster the movement.

4.3.3 *Possible Trial Outcomes*

Each trial could end in one of four possible ways (Figure 17): In the first case the subject pressed the button while the light was green, thus without being detected. We refer to these as *missed button press* trials. In this case the participant wins. A second case was that the computer predicted a movement, turned on the stop signal and the subject subsequently pressed the button within the next 1000 ms. We term this a *predicted button press* trial. In this case the computer has won the trial. Another possibility is that the BCI indicated a readiness potential and elicited a stop signal but the subject didn't press the button within a period of 1000 ms. In these cases neither the participant won (because they didn't manage to press the button without being detected) nor the computer won (because the participant did not move as was required by the task).

At first sight one might consider all such trials as false alarms, with the classifier indicating a movement without any decision or preparation on the side of the participant. However, it is also possible that the classifier detected a button press that was being prepared but that the participant was able to cancel the process in time. One such case would be if the participant indeed started to move – as indicated by an EMG onset – but then didn't complete the button press. We term these trials *aborted button press* trials because the movement starts but is then cancelled at a late stage after EMG onset.

A second possibility is that the stop signal was elicited and the participant showed no overt sign of movement. These cases might either result from a movement preparation being terminated at an early stage of preparation, which we would term *early cancellation* trials. Alternatively such cases might reflect spurious or false positive detections by the classifier, which we term proper *false alarm* trials. Please note that there is no overt difference in behavior between these latter two cases and thus we jointly refer to trials with stop signals but without overt movement as *ambiguous* or *early cancellation / false*

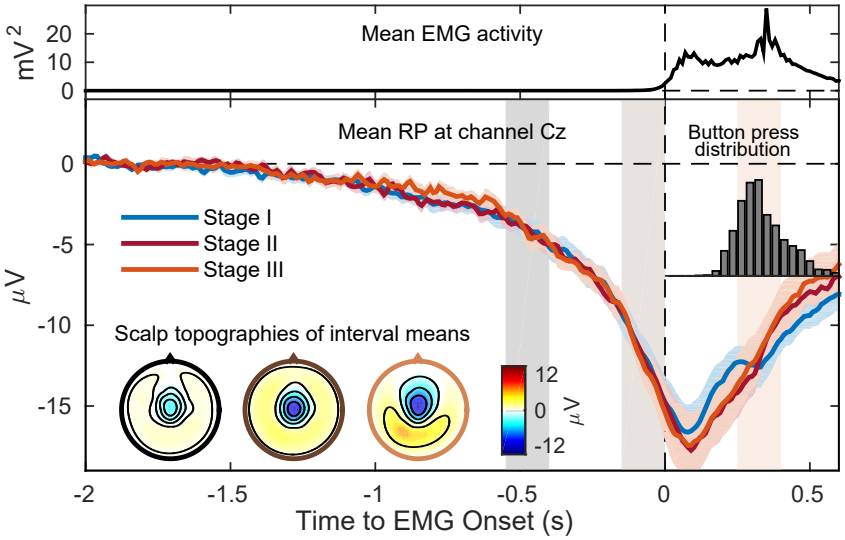

Figure 15: Mean readiness potential (RP), EMG activity and button press distribution. The top panel shows the squared EMG potential recorded at the right calf, averaged over all stages and subjects. The 99.9% quantile of the baseline signal was used as a threshold for EMG onset detection. The three colored lines in the bottom panel show the grand average RP at channel *Cz*, during individual stages of the experiment. RPs were computed by averaging EEG segments time-locked to the time of EMG onset and baseline corrected to the mean between -2000 and -1800 ms. For stage I, trials with uninterrupted button presses were used, for stages II and III, silent trials were used because these provide an unbiased selection of trials which were not actively interrupted by the BCI. Individual RPs were then averaged across subjects, the squared error of the mean is shown in the corresponding colored shadings. The scalp topographies show the EEG potential of all recorded channels, averaged over the three time intervals indicated by the shaded regions: [-550 -400] ms, [-150 0] ms and [250 400] ms. The inset panel on the right shows the button press distribution relative to EMG onset, pooled across all stages and subjects.

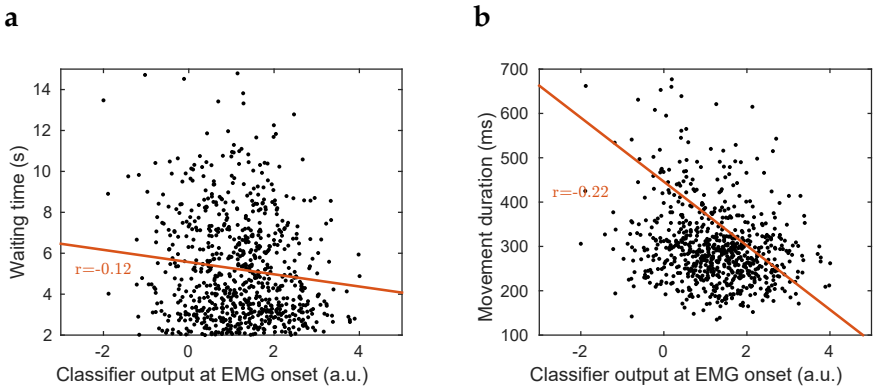

Figure 16: Waiting time (**a**) and movement duration (**b**) as a function of classifier output at time of EMG onset. Classifier output was obtained via cross-validation from all silent trials in stages II and III. Correlation of waiting time and movement duration with classifier output and the linear fit are indicated in red.

alarm trials. Figure 18 shows the proportion of trials that had these four outcomes, separately for stages I, II and III:

Missed button presses: In stage I (black bars in Figure 18) when stop signals were random, most trials (66.5%) end with an undetected button press, i.e. the subject wins by pressing the button without being predicted. The proportion of these trials is substantially reduced in stages II and III (31.9% and 30.8% respectively; paired $t_9 = 6.49$, $p < 0.001$ and paired $t_9 = 9.99$, $p < 0.001$) when the classifier is active. Please note that between stages II and III subjects were informed that a prediction algorithm was being used and that they should act unpredictably. Nonetheless, there is no difference in the number of undetected button press trials between stages II and III (paired $t_9 = 0.33$, $p = 0.75$).

Predicted button presses: In stage I a very small number of trials (1.2%) ends with a detected button press, i.e. a case where the random "classifier" has won. In contrast, during stages II and III the proportion of such trials is strongly increased by a factor of around 18 (19.5% and 22.8%; paired $t_9 = 5.52$, $p < 0.001$ and paired $t_9 = 7.19$, $p < 0.001$).

Aborted button presses: In stage I also aborted button presses occur very rarely (2.2%), a rate that substantially increased in stages II and III (15.2% and 16.3%; paired $t_9 = 2.67$, $p = 0.025$ and paired $t_9 = 2.81$, $p = 0.020$).

Ambiguous (early cancellations or false alarms): These types of trial occurred with similar rates in stages I, II and III (30.1%, 33.5% and 30.0%) with no significant difference between stage I and stages II and III (paired $t_9 = 0.77$, $p = 0.46$ and paired $t_9 = 0.023$, $p = 0.98$).

If one were to count any movement after a stop signal (whether completed or aborted) as a win for the BCI predictor then the proportion of trials on which the BCI "wins" is considerably increased.

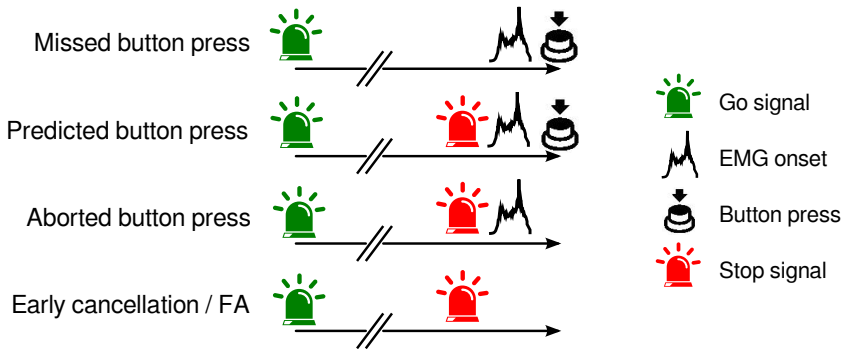

Figure 17: Possible trial outcomes. If the button was pressed without a preceding stop signal this ended the current trial. We refer to this as a missed button press trial. If a stop signal was issued and the subject pressed the button during the subsequent second, we term the trial predicted button press. If no button press but an EMG onset occurred after the stop signal we term the trial aborted button press. Otherwise if no observable movement followed a stop signal we refer to this as an ambiguous trial that reflected either an early cancellation or a false alarm. Furthermore, during stages II and III 40% of trials were silent (not shown here). In these trials the time of a planned stop signal was recorded but the red stop signal itself was not presented. These trials always ended when the participant eventually pressed the button.

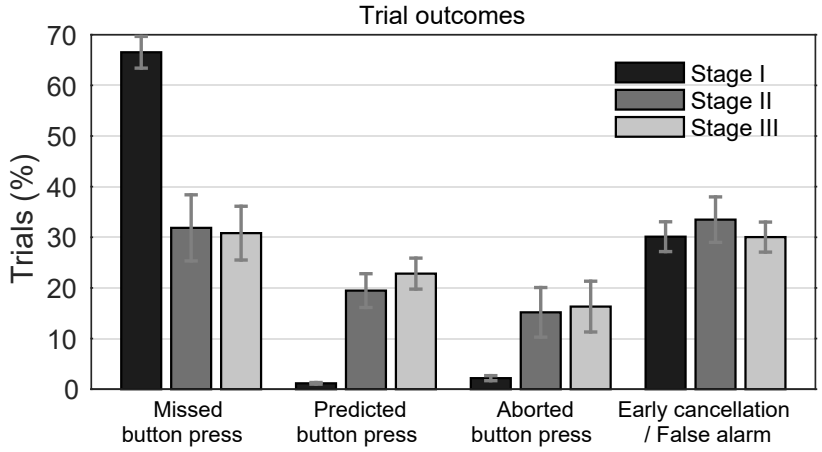

Figure 18: Percentage of trial outcomes across stages for the four trial categories described in Figure 17. All trial categories in one stage (bars of same color) add up to 100%. Shown is the average across subjects (error bars = SEM). In missed button press trials the participant wins. In predicted button press trials the BCI wins. Aborted button press trials and the ambiguous early cancellation / false alarm trials constitute draws because the participant's task was to press a button without being detected.

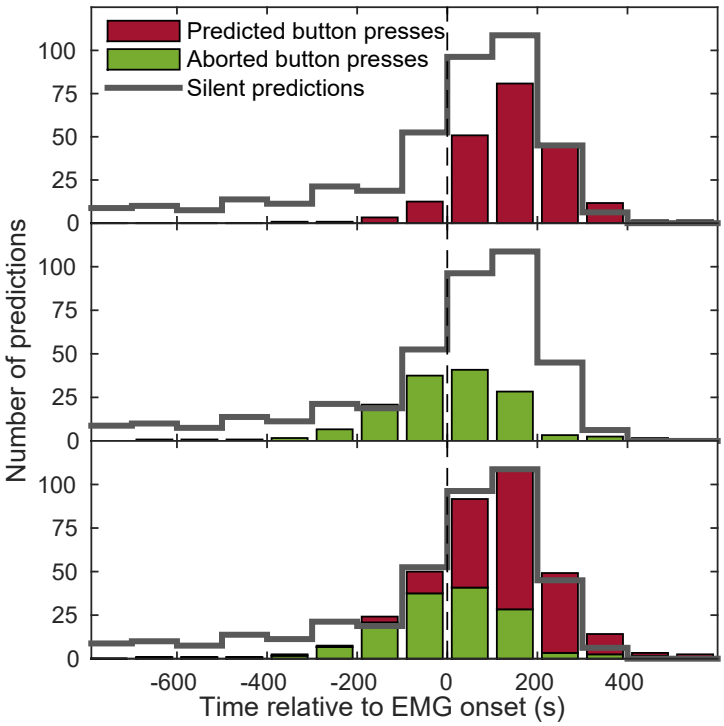

Figure 19: Distribution of BCI predictions time-locked to EMG onset. The three panels show the distribution of stop signals timings in predicted button press trials (a, red) and in aborted button press trials (b, green). Panel (c, red and green) shows their joint distribution. The black distribution superimposed as outline in all three panels shows the stop signal distribution in silent trials adjusted to account for the imbalanced probability of a trial being silent (40%) or not (60%). All bins comprised intervals of 100 ms and counts were pooled across stages II and III of all subjects. Please note that in silent trials the distributions refer to the first stop signals that would have been emitted.

In that case there is no significant difference between the percentage rate of missed button press trials and correct detections (combined predicted button presses + aborted button presses) in stages II and III (34.6% and 39.1%; $t_9 = -0.27$, $p = 0.79$ and paired $t_9 = -0.88$, $p = 0.39$).

4.3.4 *Timing of Predictions*

We also assessed how the timing of stop signals was related to movement onsets (as assessed by the onset of the peripheral EMG signal). Figure 19a (red) shows the distribution of stop signals in *predicted button press* trials, i.e. trials where subjects pressed the button despite an immediately preceding red light. The vast majority of stop signals occurred after EMG onset, thus when subjects had already begun to move but before the button was pressed. Here the stop signal pre-

sumably came too late to prevent the subjects from finishing their movement and pressing the button.

Figure 19b (green) shows the distribution of stop signal times for aborted button press trials, i.e. where subjects began to move but cancelled the movement before the button was completed. Here, the stop signals occurred earlier (starting around 200 ms before EMG onset). Thus, when stop signals were presented at late stages of movement preparation subjects could not prevent *beginning* to move, even though they could abort the movement. There was a gradual transition between stop signal times where movements could be aborted and those where they could not be aborted (Figure 19c), presumably reflecting a variability of stop signal reaction times (Logan and Cowan, 1984).

There were hardly any cases where subjects moved despite being presented with stop signals earlier than 200 ms before EMG. This is interesting given that the readiness potential begins to deviate from baseline more than 1000 ms before EMG onset (Figure 15). One possibility is that some detections were made at this early stage but that participants were almost always able to cancel the movement completely. In order to assess how early predictions could be made in principle, independent of the presentation of a stop signal, we studied the behavior of the predictor in silent trials. Please recall that here, when the BCI predicted a movement, the prediction time was silently recorded but the stop signal was not turned on and the trial continued until the button was pressed. As Figure 19a-c (black distribution) shows, a majority of predictions also in *silent* trials occurred around movement onset.

However, many silent predictions occurred more than 200 ms before movement onset, compatible with the early RP onset. These early detections are not found for *predicted button press* trials (Figure 19a, red) or *aborted button press* trials (Figure 19b, green) when stop signals are active. Thus, had the stop signal been active for these early predictions, subjects might have been caught preparing a movement but been able to cancel preparation early enough to prevent any observable movement. Resolving this issue would directly address the question whether trials with stop signals but no overt movements constitute early cancellations or false alarms, and thus help interpret this ambiguous trial category.

4.3.5 *In Search of Early Cancellations*

If a proportion of these trials indeed reflected early cancellations instead of false alarms, one might observe some signs of movement preparation given that movement-preceding signals have been proposed to start before a decision (Schurger et al., 2012). We therefore hypothesized one prediction: If the stop signals that occur without any sign of subsequent movement are due to cancellations at an early stage of motor preparation, neural signatures of such motor preparation should be observable in the EEG at the time of BCI stop signals.

We tested this prediction with the offline analyses 2 and 3 described in Appendix A, Table 2. In both analyses, a classifier was trained on EEG features preceding uninterrupted movements (*missed button press* and *silent* trials) and applied to EEG features preceding stop signals from several trial types: trials from stages II and III without any sign of movement (*early cancellation/false alarm* trials, *aborted button press* trials, *predicted button press* trials) and all trials with stop signals from stage I.

Probing the Presence of RPs

In the first test, the classifier was trained in analogy to the BCI predictor, i.e. on the RP that precedes movements, and applied with a sliding window on the tested trials (Figure 20). In stage I the computer predictions were generated randomly. As expected, the classifier did not detect a readiness potential (Figure 20, blue line), which is easily explained by the fact that the random stop signals were unlikely to catch subjects by chance just while they were preparing a movement. In the *early cancellation/false alarm* trials (trials without any overt movement), however, the classifier output shows a positive deflection (indicating the detection of a RP) that starts roughly 1 second before prediction time and reaches the threshold at the time of prediction (Figure 20, yellow line). The shape and time course before the time of prediction were undistinguishable from trials which containted actual movements (*aborted button press* and *predicted button press* trials, orange and red lines in Figure 20).

On the one hand, the similarity of the running classifier outputs between *early cancellation/false alarm* trials and trials containing overt movements confirms that the BCI elicited a stop signal in the former trial types because the EEG at that moment manifested the topology of a readiness potential. However, from this it doesn't follow that participants were indeed preparing a movement and then cancelled it. This is because the classifier that initiated the stop signal was trained on the RP. Thus a false alarm should exhibit an RP-like topography as well.

Probing the Presence of ERD

Hence, we searched for an independent indicator of movement preparation in ambiguous trials that was not based on the RP. For this we chose the event-related desynchronization (ERD) that occurs before and during movements in particular frequency bands in the EEG (Pfurtscheller and Aranibar, 1979). ERD and RPs have been shown to have different generators in the brain and thus provide different information (Nagamine et al., 1996; Babiloni et al., 1999; Bai et al., 2006; Sochůrková et al., 2006), therefore making ERD an index for motor preparation that is independent of the RP. If the stop signals that occur without any sign of subsequent movement are due to cancellations at an early stage of motor preparation, ERD might have been present at the time of prediction, even if subjects didn't move. To test this, according to the offline analysis 3 described in Appendix A,

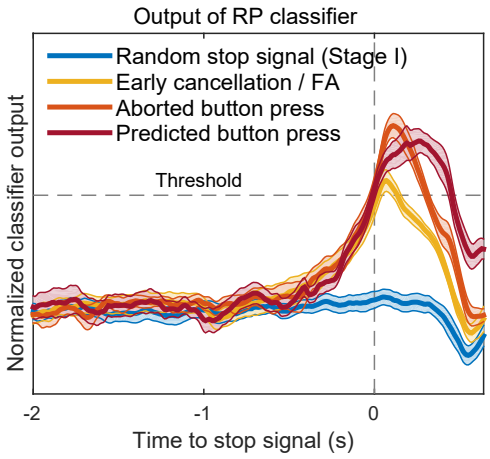

Figure 20: Time-resolved output of a classifier trained to detect RPs, time-locked to the onset of stop signals. Shown is the grand average for all random stop signals in stage I (blue) and for stages II and III from the three trial categories that involved stop signals: yellow = early cancellation/false alarm (FA); orange = aborted button press; red = predicted button press. The classifier output at time T is an index of the presence of a RP in a backward-looking time window ranging from T-1200ms to T. Classifier outputs below the threshold correspond to a "no RP detected" and otherwise to an "RP detected" decision of the classifier (absolute values are arbitrarily scaled).

Table 2, we trained a classifier on the ERD preceding uninterrupted movements and eventually applied it to the four trial types shown in Figure 21.

In stage I the computer predictions were generated randomly. As expected, classification performance was at chance level for the random predictions in stage I (mean $50.5\% \pm 2.0\%$ SEM, $t_9 = 0.26$, $p = 0.79$). BCI predictions in ambiguous trials of stages II and III, however, could be classified with accuracies that were significantly above chance level (mean $58.9\% \pm 2.6\%$ SEM, $t_9 = 3.38$, $p = 0.008$). Classification accuracies of predictions in trials which contained actual movements were better (mean $64.6\% \pm 2.0\%$ SEM, $t_9 = 6.99$, $p = 0.0001$ and mean $66.3\% \pm 3.2\%$ SEM, $t_9 = 5.08$, $p = 0.0007$). This is to be expected for two reasons. First, in *aborted button press* and *predicted button press* trials at the time of prediction a movement had already begun, whereas in hypothetical *early cancellation* trials no movement would have occurred at all. Second, we can expect that a certain fraction of stop signals in the grouped *early cancellation/false alarm* trials were actually false alarms of the BCI predictor caused by random fluctuations in background activity or artifacts in the EEG, whereas in movement trials every stop signal involved a movement. Using the ERD as an independent physiological signal (Pfurtscheller and Aranibar, 1979) confirmed that at least a subset of ambiguous trials

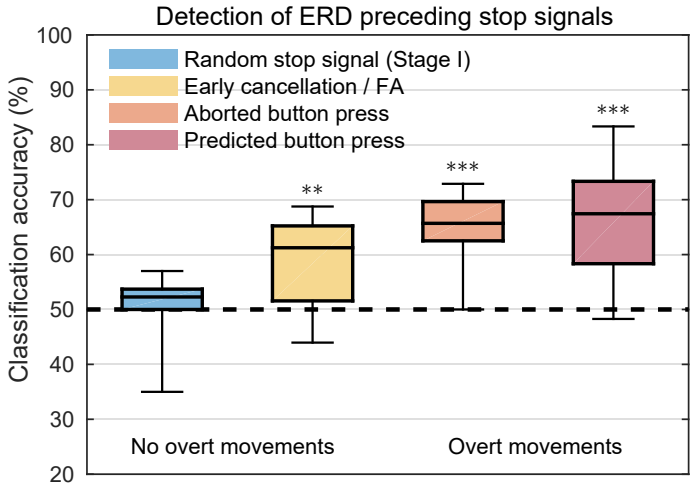

Figure 21: Detection of event-related desynchronization (ERD) preceding stop signals. A classifier was trained to detect event-related desynchronization (ERD) and applied to 500 ms windows immediately preceding stop signals. The box plots show the median and lower and upper quartile accuracies over subjects for the same four trial categories as in Figure 20, the whiskers show the range (i.e. the largest and smallest values). Asterisks indicate statistically significant accuracy mean above chance level (50%) with $** : p < .01$ and $*** : p < .001$.

had possibly already reached a movement preparation stage and thus were not "false alarms", but rather early cancellations.

4.3.6 *Questionnaire*

We also used a questionnaire after each stage in order to assess subjects' experiences and strategies during the different sections of the experiment. Subjects where asked two questions: "Did you use a particular strategy during the last round?" and "Did you feel there was a connection between your actions and the appearance of an interruption?". Detailed information about the participants' responses are given in Appendix A in Tables 3 and 4. During stage I 4/10 participants reported trying to "wait as long as possible" before an interruption, which they described as a "risky" strategy. Another 4/10 reported waiting until they "felt an interruption would come". Furthermore, 4/10 participants said that they modified their strategy dynamically and "pressed earlier [on trials] after interruptions". After stage II all participants reported that they made changes to how or when they chose to move. Notably, 4/10 participants reported acting more "unpredictably" or more "spontaneously" than during stage I and 1/10 participants reported ignoring the "urge" to move in favor of a deliberate strategy. After stage III 5/10 participants reported acting unpredictably or not thinking about their actions. Nine out of ten

participants reported that they felt predicted while the remaining participant reported that s/he could not rule out the possibility. Seven out of ten participants reported that something related to foot movements caused the interruptions. Among these two participants reported that "everything" caused interruptions, 2/10 specifically mentioned "thinking about pressing", 2/10 mentioned the change from being relaxed to preparing to move, and 1/10 mentioned movement onset. The remaining 3/10 participants reported feeling predicted but did not identify a specific event as being tied to predictions. As mentioned above, the changes revealed by the behavioral analyses did not result in a modification of the recorded readiness potential.

4.4 DISCUSSION

In our experiment we used a brain-computer interface (BCI) that was designed to detect the occurrence of a readiness potential in real-time. Subjects were challenged to press a button while at the same time avoiding being predicted by the BCI. If a light was green they were allowed to press a button to win the trial, if the light turned red they were not allowed to press the button. In some cases this might involve subjects having to cancel a movement upon seeing the red stop signal. Our study thus combined aspects of interruption studies (Hughes et al., 2011; Schurger et al., 2012) with aspects of cancellation studies (Brass and Haggard, 2007; Verbruggen and Logan, 2008). This experiment allowed us to test the two proposed hypotheses of conscious control. In the following sections, we first present a model that summarizes the obtained results and subsequently assess the hypotheses in the light of our findings and discuss the implications.

4.4.1 *Model of Results*

From the results obtained in our experiment, a hypothetical time line of events and stages leading up to a button press can be described as follows (Figure 22):

Baseline: In a first stage a person has not yet engaged in preparing for a movement. If a readiness potential is detected at this stage it is due to a false positive: a similarity between the RP shape and random fluctuations in brain activity. If a stop signal is elicited during this stage this constitutes a false alarm. Please note that our data are agnostic as to whether the onset of the readiness potential occurs prior to the preparation or not.

Movement preparation: At some point a person decides to move and starts movement preparation. If a stop signal is presented during this period, movement preparatory signals can be observed, for example a RP or ERD, but there are no overt signs of movement (as indicated by the EMG). However, an explanation is needed to clarify why people cannot prevent themselves from moving if the stop signal is presented later than 200 ms before movement onset. This cannot reflect the conduction delay between primary motor cortex and the

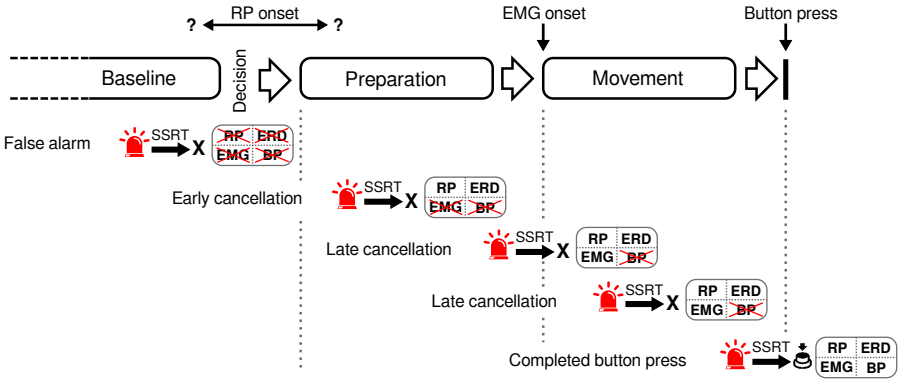

Figure 22: Summary model of results (see text for details). Abbreviations: SSRT, stop signal reaction time; RP, readiness potential; ERD, event-related desynchronization; EMG, electromyogram; BP, button press

calf muscles controlling the movement of the foot, because this delay is much shorter, around 25-30 ms (Morita et al., 2000). Instead, it presumably reflects the time it takes between the physical onset of the stop signal and the time the stop signal can catch up with and cancel a prepared movement (indicated by the X symbol in Figure 22). This so-called stop signal reaction time has been reported to be around 200 ms (Logan and Cowan, 1984), which is compatible with our data. So the time around 200 ms prior to movement onset constitutes a *point of no return* (De Jong et al., 1990) after which the initiation of a movement cannot be cancelled, even if it might still be possible to abort the completion of the movement.

Movement execution: Once the efferent motor signals have reached the peripheral muscles, the person begins to move. In the early stages of this phase it is still possible to abort the movement. As the movement progresses towards completion this becomes less possible due to the stop signal reaction time. Aborting a movement at this stage constitutes a "late cancellation" because it occurs in time to prevent pressing the button but not in time to cancel signs of overt movement. Once a second, late point of no return that divides controlled and ballistic phases of movement processing is reached, the stop-process cannot catch up with the go-process in time to abort the completion of the movement and thus the button will be pressed.

4.4.2 *Assessment of Hypotheses*

The Non-Overridable Readiness Potential

We found that the shape of the readiness potential was not affected by whether subjects were actively trying to evade being predicted or not (Figure 15). When they were actively being predicted by the BCI, subjects "lost" the trial 50% more often, due to pressing the button after a stop signal had been shown (Figure 18). Importantly, this rate was the same in stages II and III.

It is important to note that the roughly 30% unsuccessfully predicted movements are expected because the BCI predictor was adjusted conservatively to avoid false positives in the long waiting period before a movement is finally elicited. They do not reflect an ability of subjects to deliberately change or suppress their readiness potential when they move. On the other hand, they don't allow the conclusion that the RP is an unavoidable – or necessary – part of movement preparation. Such a conclusion would necessarily require a single trial analysis showing that every single button press was preceded by a RP, irrespective of whether it was predicted by the BCI or not.

We can, however, conclude that people are not able to exert any control over their readiness potential, which would have allowed them to act unpredictably when asked to do so. It is, however, possible that our experimental protocol is not sufficient to fully refute this possibility. When participants were informed about the predictor after stage II and instructed to move unpredictably during stage III, they performed each about 100 more movements. It could still be possible that they would have been able to "train" an unpredictable behavior given more time and trials. Furthermore, our choices pertained to decisions "when" to move and "whether" to move, but it did not involve a choice between different responses ("what" choices) (Brass and Haggard, 2008). It remains therefore unclear, whether people are able to "fool" a predictor that has been trained to detect such "what" choices from brain signals, for instance to move either the left or the right hand (Haggard and Eimer, 1999; Soon et al., 2008).

The Late Point of no Return

Despite the stereotypical shape of the readiness potential and its early onset at around 1000 ms before EMG activity, several aspects of our data suggest that subjects were able to cancel an upcoming movement until a point of no return was reached around 200 ms before movement onset. If the stop signal occurs later than 200 ms before EMG onset the subject cannot avoid moving. However, up until a second point of no return is reached (after movement onset) participants can still avoid completing the movement. For this it is necessary to consider the possible outcomes of our study. One possibility is that the onset of the readiness potential triggers a causal chain of events that unfolds in time and cannot be controlled, as in the domino analogy. This would be a ballistic stage of processing (Logan and Cowan, 1984; De Jong et al., 1990).

Alternatively, participants may be able to cancel a movement at later stages of movement preparation or even during execution. If the process initiated by the readiness potential were indeed ballistic and the readiness potential can be detected several hundred ms before the movement, some of the stop signals should occur several hundred ms before EMG onset. If however the subjects can still inhibit the chain of events from eliciting a movement, akin to taking out a domino

somewhere down the chain, the result would be an absence of such early predictions.

This is exactly what we find (Figure 19). The "successful" stop signals (i.e. those where subjects press a button despite the stop signal) only occur at a late stage after onset of the peripheral EMG signal. This suggests that once the motor command has reached the peripheral muscle there is a very low chance of cancelling the movement before the button is pressed (compare the red and green distributions in Figure 19c). If the stop signal occurs within 200 ms before EMG onset the subject begins a movement but can still cancel its completion and avert the button press. Thus, there appear to be two points of no return, meaning a stage of processing in the brain after which movements cannot be cancelled. Our data therefore refutes the assumption that there is no final ballistic stage in the brain and in contrast suggest that there is indeed a point of no return around 200 ms before a movement after which the onset of a movement cannot be cancelled (even if it is still possible to alter the movement) (De Jong et al., 1990).

5

GENERAL DISCUSSION AND CONCLUSIONS

Findings from cognitive neuroscience have repeatedly shown that mental states and intentions of humans – whether directly reflected in behavior, or hidden in the mind of a person – are associated with specific brain signals (Gazzaniga, 2004). The ability of modern brain-computer interfaces to study this relationship in *real-time* and provide *immediate feedback* to the person has put forth novel application possibilities for such BCIs. The work presented in this thesis aims to engage in the intriguing endeavor to study the "brain at work" by exploring the real-time assessment and detection of covert mental states and intentions from the ongoing EEG. The two contributions demonstrate how such BCIs can be used for completely different purposes, while exploiting the virtues that they bring about.

5.1 CHARACTERISTICS OF BCIS FOR APPLICATIONS BEYOND CONTROL

It has been suggested to refer to brain-computer interfaces that go beyond the traditional goal of communication and control as BCIs for "mental state monitoring" (Müller et al., 2008) or "passive BCIs" (Zander and Kothe, 2011), in the latter case because, from the point of view of the person, no active effort occurs towards an interaction with the BCI. However, such a labeling implies a passivity among such BCIs that is inconsistent with their multifaceted scope of applications. For instance, while the concept of traditional BCIs for communication and control is akin to two partners talking to each other and working on the same goal (establishing the communication channel), by contrast the concept of non-control BCIs is akin to one person (the user/human) "minding their own business", while the other person (the BCI), sits aloof, observes the former and decides whether, when and how to interact. The human may not even be aware of the presence of the BCI (as is the case during one experimental stage in the work presented in Chapter 4).

Hence, instead of contrasting active vs. passive BCIs, a more fitting comparison would be that of "bilateral" vs. "unilateral" BCIs. By decoding information from the ongoing EEG, unilateral BCIs can infer covert mental or cognitive states and intentions from the user, while retaining full control over the interaction with the behavior of the user. This interaction can range from very occasional (as targeted by the envisioned application in Chapter 3) to very frequent (as implemented in the BCI predictor in Chapter 4). Furthermore, unilateral BCIs allow the user to focus on the primary task – which in both presented studies was to win a game – without being imperatively interfered with.

Control-directed BCIs have been characterized by their closed-loop nature (Blankertz et al., 2005), because the establishing of the communication channel relies on feeding the user's decoded intentions back to the user in real-time. Aside from a few studies aiming for adaptive automation (Prinzel et al., 2000; Prinzel et al., 2003; Scerbo et al., 2003), non-control BCIs have been predominantly open-loop systems, since their primary goal has been the "monitoring" of mental states (Kohlmorgen et al., 2007; Müller et al., 2008), or the exploration of future closed-loop systems (Haufe et al., 2011; Haufe et al., 2014b), however without employing a direct interaction with the user. While the work presented in Chapter 3 falls into this latter category, the work in Chapter 4 represents an instance of a BCI that is at its very core a closed-loop system, relying on its ability for fast responsive feedback.

5.2 A BCI FOR ADVANCED ASSESSMENT OF OPERATOR WORKLOAD

In the work presented in Chapter 3, we aimed to advance the assessment of operator workload from ongoing EEG. For this purpose, we presented an approach that builds on findings from previous work in this field (Gevins and Smith, 2003; Kohlmorgen et al., 2007) and incorporated newly developed methods from machine learning (Dähne et al., 2014a; Dähne et al., 2014b), thus allowing to pursue the implementation of several challenges which address the ultimate areas of application in which such a BCI might be of use. One of the challenges was to depart from the prevailing focus on purely mental workload in laboratory conditions, and rather assess workload as it is expected in many real-life situations, such as in an industrial work environment. This entailed an experiment that required not only cognitive effort but also an increased visuomotor coordination, thereby inducing workload on multiple modalities. Tightly linked to this was the challenge to implement a "true" BCI in the sense that only EEG signals with cerebral origin are used as features. We intended to achieve this by either removing or avoiding confounding non-cerebral signals from the EEG, the success of which was eventually verified by assessing the neurophysiological plausibility of the signal sources.

The fact that the level of cognitive workload modulates the power of theta and alpha oscillations with contrary direction (Gevins and Smith, 2003; Holm et al., 2009), offers the unique possibility to employ the novel cSPoC method, which finds spatial EEG filters such that the correlation of the power between those two bands is maximally anti-correlated (Dähne et al., 2014b). Using cSPoC, a sufficient requirement for training is to provide the BCI with segments of EEG data with varying theta to alpha power contrast (induced by varying levels of workload), thus eliminating the need for a supervision signal. We hereby demonstrated for the first time the feasibility to employ an unsupervised approach for the assessment of workload from ongoing EEG. However, also the use of the spatial filtering method

SPoC (Dähne et al., 2014a) represents an advance in workload assessment by demonstrating the feasibility of using a continuous rather than a binary supervision signal, which has so far been the prevalent research direction (Kohlmorgen et al., 2007; Brouwer et al., 2012; Dijksterhuis et al., 2013).

Although in our experiment we did not induce workload levels from a continuous spectrum but rather used a performance measure as a continuous supervision signal that was tightly linked to the binary workload levels, one can assume this approach to be also applicable to the former case. This assumption was confirmed in a recent study, where participants played a video game whose difficulty was changed every 60 seconds from a set of 10 levels (Naumann et al., 2016). Because the difficulty levels were expected to directly reflect the mental workload induced by the game, a SPoC analysis was applied to the theta and alpha EEG bands and the resulting component signals combined with regression in order to predict the levels. A mean correlation between true and predicted levels of 0.85 was achieved, thus showing the suitability of using SPoC for assessing workload from a continuum of levels.

Our approach furthermore allows for a continuous measurement of workload from ongoing EEG activity without intervening with the user's primary task. This is in contrast to alternative approaches that rely on the evocation of event-related potentials by means of secondary stimuli (Allison and Polich, 2008). Furthermore, since the predictive models were employed in a cross-validation, the basic requirements for their application in an online scenario are existent. In this context, it is noteworthy that the long-term stability of parameters in an online workload detection system has been demonstrated (Arico et al., 2014). In order to fully achieve an online applicability, some preprocessing steps need to be adapted first, such as the dimensionality reduction via SSD and removal of EOG activity. Our work ultimately paves the way for real-world applications of operator workload assessment in which label information may be noisy or entirely unavailable. According to the neuroergonomical approach (Parasuraman and Wilson, 2008), a system is envisioned that enhances the interaction between a human operator and a work environment. This enhancement can for instance amount to adapting the task difficulty or to instructing the operator to take a break, thereby mitigating the consequences of excessive workload.

5.3 A CLOSED-LOOP BCI FOR COGNITIVE NEUROSCIENCE

With the work presented in Chapter 4 we broke new ground by using a brain-computer interface as a research tool for cognitive neuroscience. We trained a BCI to detect the occurrence of readiness potentials and provide immediate feedback to participants in real-time, thus allowing us to address questions concerning the nature of the readiness potential in an unprecedented way. Given the early onset of the RP at more than one second before voluntary movements (Ko-

rnhuber and Deecke, 1965), allegedly much earlier than the time of perceived intention (Libet, 1985), the question arises how much the presence of the RP undermines the degree of control that a person exerts over their decision. Does the onset of the RP trigger a ballistic process that *necessarily* leads to a movement and cannot be consciously terminated? And if not, does the process become ballistic at a later stage of movement preparation? We investigated these questions by testing whether participants were able to stop an intended movement *after* onset of the RP. Our findings suggest that there exists indeed a point of no return after which movement execution becomes ballistic, reflected by an increasing difficulty of participants to completely withhold the intended movement or, if already started, to stop its completion. However, we identified this point of no return occurring not with the onset of the RP but much later, around 200 milliseconds before movement onset.

5.3.1 *The Role of the Readiness Potential*

In a seminal experiment, Libet et al. (1983) used an experimental setup to determine the time when participants consciously formed their intention to perform spontaneous, voluntary movements. They found this time to be around 200 ms before movement onset, while the mean onset time of the RP occurred about 550 ms before movement onset. This temporal precedence of brain activity over the perceived time of intention was also found in subsequent experiments using the lateralized readines potential (Haggard and Eimer, 1999) and single neuron recordings (Fried et al., 2011). Two further studies used a pattern-based analysis on fMRI data in order to assess which brain regions had predictive information about a subject's decision and found that regions of the frontopolar cortex and precuneus/posterior cingulate cortex coded predictive information seven seconds before the decision was made (Soon et al., 2008; Soon et al., 2013). Together, these findings seem to demonstrate that our decisions are determined by unconscious neural processes while consciousness is merely a late byproduct of those neural processes with no influence on its own (Roskies, 2010; Smith, 2011; Lavazza, 2016) and continue to be used as one of the main arguments against the existence of a free will (Pockett, 2004).

However, not only has the Libet experiment met several criticisms, focusing on the feeling of volition (Lau et al., 2007; Matsuhashi and Hallett, 2008), on attentional effects (Keller and Heckhausen, 1990), on the influence of priming effects (Taylor and McCloskey, 1990; Taylor and McCloskey, 1996), and showing that movement preceding brain signals do not specifically determine behavior (Herrmann et al., 2008; Trevena and Miller, 2010). More importantly, recent studies have put forward a reinterpretation of the RP, suggesting that the early RP is the result of autocorrelated, stochastic fluctuations in brain activity in the decision network (Schurger et al., 2016), a mechanism that has been shown to account for observed reaction times (Hanes

and Schall, 1996; Brown and Heathcote, 2005) and perceptual choices (Usher and McClelland, 2001; Deco et al., 2007). Regarding the RP, it has been suggested that an accumulator integrates autocorrelated neuronal fluctuations until a decision threshold is reached (Schurger et al., 2012), or that the early RP emerges through an unequal ratio of negative and positive potential shifts (Jo et al., 2013). In this view, the time of intention and the neural commitment to act are identified as the moment of threshold crossing, which is consistently reported as being around 200 ms before the movement (Schurger et al., 2012; Murakami et al., 2014). The preceding neural activity (i.e. the early RP) would be the result of averaging trials that end with a movement and only reflects the threshold crossing of the accumulated noise or the unequal ratio of negative and positive potential shifts (Schurger et al., 2012; Jo et al., 2013).

In order to further shed light on the disagreement between these opposing views, it seems appropriate to probe how tight the causal relationship is between the readiness potential and the intended movement. How can the findings presented in Chapter 4 contribute to this controversy? First of all, it is important to note that the interpretation of our data is in general agnostic as to whether the decision to move occurred 1000 or 200 ms before the movement. However – in line with previous work – it suggests that the "neural commitment to move" (Schurger et al., 2016) cannot be identified with the early onset of the readiness potential, because movements could be cancelled until a late point of no return. Interestingly, this point of no return at 200 ms before movement onset is in line with the reported onset time of perceived intention (Libet et al., 1983). Thus, if one identifies this time point as the time point of both the neural *and* the conscious commitment to move, it could be considered as corresponding to the elicitation of the "internal go signal", analogous to the external go signal in stop signal studies. This would explain why stop signals presented *after* this point of no return are less and less successful in inhibiting the movement, as reflected in the stop signal reaction time in the race model (Logan and Cowan, 1984; De Jong et al., 1990). Regarding the domino analogy, it would mean that its very premise – that the early onset of the RP is akin to tipping the first in a row of dominoes – is faulty, and that the first domino is in fact tipped over much later, at the identified point of no return.

5.3.2 *The Ability to "Veto" Voluntary Movements*

Libet himself found that subjects could "veto" motor performance during a 100 - 200 ms period before a prearranged time to act (Libet, 1985). Thus, while the commitment to act might be initiated unconsciously, Libet argued that the ability to consciously veto the action reconstituted the free will – although he saw the necessity to explain the ability to veto with a dualistic mechanism, that is without requiring a neural correlate. A few other studies exist that have examined the spontaneous cancellations of self-initiated movements.

In contrast to Libet's view, recent studies found that last-moment decisions to delay voluntary movements may depend on unconscious preparatory neural activity (Filevich et al., 2013), and that inhibition of an impending motor action can be initiated by unconscious stimuli (Hughes et al., 2009). Furthermore, using fMRI with a Libet-like paradigm where participants were asked to perform self-paced movements, but to withhold the action at the last possible moment in some trials, studies have identified the dorso fronto-median cortex as the brain area associated with the endogenous cancellation process (Brass and Haggard, 2007; Kühn et al., 2009).

In contrast to our *externally* triggered stop signals, those studies used *internally* triggered, "voluntary" vetoes. While such experiments allow to study the mechanisms of self-control, they don't seem appropriate for the search of a point of no return in vetoing self-initiated movements. First, such veto paradigms rely on trusting a person to make up their mind to perform a movement and then to rapidly choose to terminate that movement, a task that seems highly unnatural. And second, combining findings that suggest that voluntary inhibition is influenced by early neural activity (Hughes et al., 2009; Filevich et al., 2013) with the thresholded accumulator model (Schurger et al., 2012; Schurger et al., 2016), makes it reasonable to assume that the decision to either veto or not to veto a voluntary movement is as much effected or initiated by early brain activity as the decision to move itself. Thus, in order to assess whether potentially preconsciously generated decisions undermine the degree of control of an individual, it seems necessary to use *externally* triggered stop signals.

While the study of externally triggered movement cancellations has so far been conducted in the context of stop-signal paradigms (Logan and Cowan, 1984; De Jong et al., 1990), the study of externally triggered stopping of voluntary movements is a per se challenging endeavor because it requires an online detection of covert movement preparation signals like the RP. To date, only one study has adopted the approach of interrupting voluntary movements, however depending on occasional coincidences of movement intentions and auditory stop signals presented at random times (Matsuhashi and Hallett, 2008). To the best of our knowledge, the findings reported in Chapter 4 represent the first instance of a "true" veto experiment where the probability was maximized for stop signals to be elicited *after* onset of the RP but *before* any sign of overt behavior.

5.3.3 *BCIs for Movement Prediction*

The first attempts on single-trial EEG aimed at predicting the laterality of finger movements from the lateralized readiness potential with the goal to improve the responsiveness of control-based BCIs (Dornhege et al., 2002; Blankertz et al., 2003; Krauledat et al., 2004; Blankertz et al., 2006). This work led to the development of a system capable of online predictions of externally evoked actions such as in an emergency braking situation (Haufe et al., 2011; Haufe et al.,

2014b). To the best of our knowledge, using ERD features only one study has so far aimed at using EEG to predict voluntary movements in real-time, however reporting very few successful predictions (Bai et al., 2011).

There is a general trade-off between sensitivity and specificity when calibrating a BCI for movement detection. A low classifier threshold increases the probability of early predictions but comes at the expense of a higher rate of false alarms, while a high threshold minimizes the false alarm rate. The specific choice thus depends on the purpose of the study. One such purpose is the development of asynchronous BCIs, which allow individuals to control a device at their own pace (Borisoff et al., 2004; Fatourechi et al., 2008; Hasan and Gan, 2010). For such systems a very low false positive rate is essential, while the temporal resolution of detections is negligible. In contrast, in Chapter 4 a detailed investigation of the timing of potential cancellations of movements required that we predict and interrupt subjects as early as possible. Consequently, our choice of the threshold resulted in a false alarm rate that was appropriate for our goals but higher than in other BCI studies (Bai et al., 2011).

5.4 CONCLUSIONS

Brain-computer interfaces have continuously evolved over time and created new application areas – not unlike the tree of life of species. Ever since the first proposal by Vidal (1973), the main branch of BCIs has dealt with establishing a communication channel between a user and a computer program (Birbaumer et al., 1999; Wolpaw et al., 2002; Dornhege, 2007). Later, another branch of BCIs emerged that did not rely on the ability of people to willfully alter brain states to express intentions (Sutton et al., 1965; Pfurtscheller and Da Silva, 1999), but rather on ongoing brain activity related to particular mental states (Müller et al., 2008; Schubert et al., 2008; Sturm et al., 2015; Wenzel et al., 2016).

One of the sub-branches sought to develop BCIs for the monitoring and assessment of cognitive workload (Scerbo et al., 2003; Kohlmorgen et al., 2007; Abbass et al., 2014). The work presented in Chapter 3 followed up on this line of experimental work and strived for its advancement. Given the noisy and convoluted characteristics of brain signals contained in the EEG, BCI research has ever since been dependent on intelligent data analysis techniques for the robust extraction of such signals (Dornhege et al., 2007; Blankertz et al., 2008; Blankertz et al., 2011). Therefore, one of the paramount ingredients in Chapter 3 was the integration of state-of-the-art machine learning methods (Dähne et al., 2014a; Dähne et al., 2014b), which allowed to pursue the implementation of approaches that had hitherto not been possible – most notably, abandoning the necessity for a supervision signal.

The work presented in Chapter 4 entered uncharted waters and could be considered as establishing a new branch in BCI research,

namely the use of a real-time, closed-loop BCI as a research tool. This approach emerged from linking the ability of BCIs to detect and feed back event-related potentials with high temporal precision (Krauledat et al., 2004; Haufe et al., 2011) with the decade-long controversy regarding the role of the early readiness potential (Kornhuber and Deecke, 1965; Libet, 1985; Schurger et al., 2016). While the cognitive neuroscience community has contributed considerable insights into this controversy with numerous studies (Keller and Heckhausen, 1990; Haggard and Eimer, 1999; Matsuhashi and Hallett, 2008; Schurger et al., 2012; Jo et al., 2013), the investigation of questions regarding the conscious control of individuals during the build-up of the RP has so far eluded a forthright investigation with prevalent experimental paradigms. It is only by implementing a closed-loop BCI that it becomes possible to address such questions (Haynes, 2011).

The success of the experimental approach presented in Chapter 4 in addressing questions from cognitive neuroscience paves the way for future applications of BCIs in this field. Not only can the experiment in Chapter 4 be modified in order to further shed light on the exact role of the RP, for instance by presenting stop signals at different time points of movement preparation (Marks, 1985), or by applying transcranial magnetic stimulation (TMS) to subjects instead of stop signals (Lau et al., 2007). Experiments can be also designed to address questions regarding value-based decisions (Maoz et al., 2012), or even combine several brain imaging modalities, such as with simultaneous EEG-fMRI (Ritter and Villringer, 2006; Dähne et al., 2015).

With this thesis we thus demonstrated how research needs, such as advancements of existing technologies or the emergence of novel scientific tools, can be approached by the continuous evolution of brain-computer interfaces, a process that – not unlike the evolution of life – is fostered by linking previously unrelated research.

APPENDIX

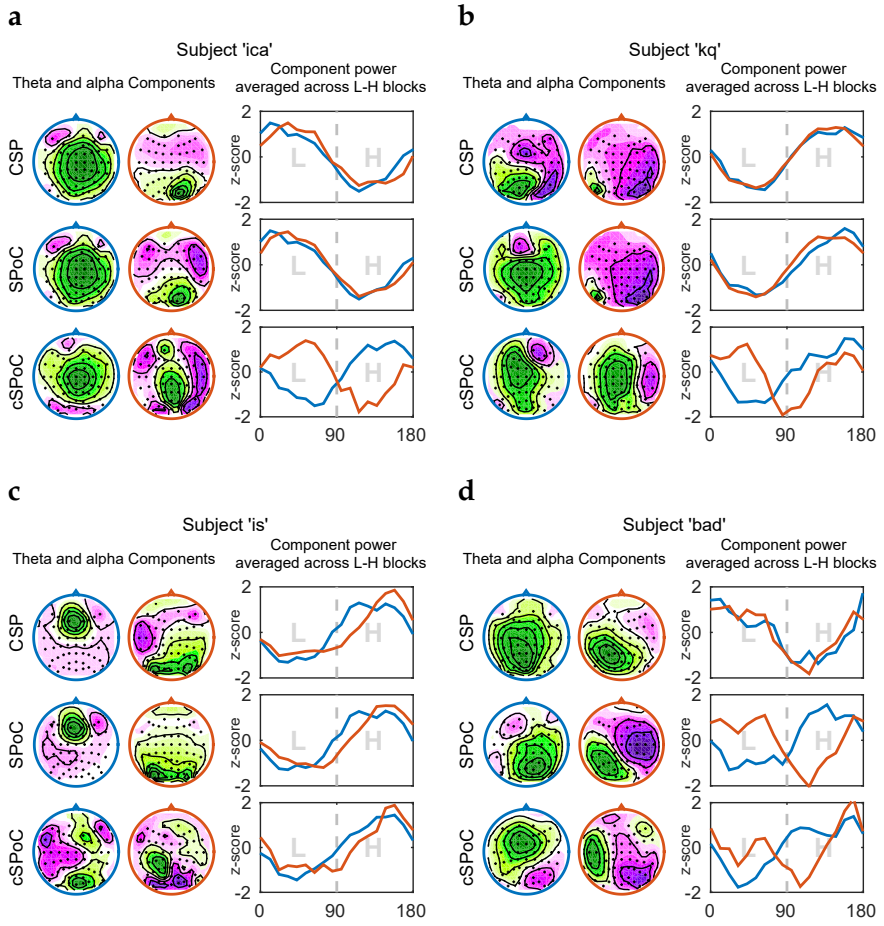

Figure 23: Spatial activation patterns and power envelopes of components extracted by the three EEG spatial filtering methods from subjects *ica* (**a**), *kq* (**b**), *is* (**c**) and *bad* (**d**). The shown activation patterns (scalp maps) and power envelopes correspond to the components with the *highest* value of the optimization criterion of the respective method.

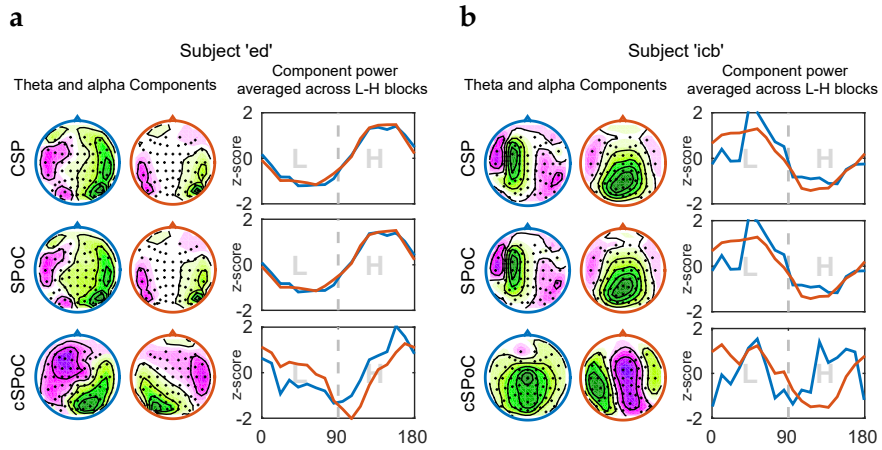

Figure 24: Like Figure 23, but for subjects *ed* (**a**) and *icb* (**b**).

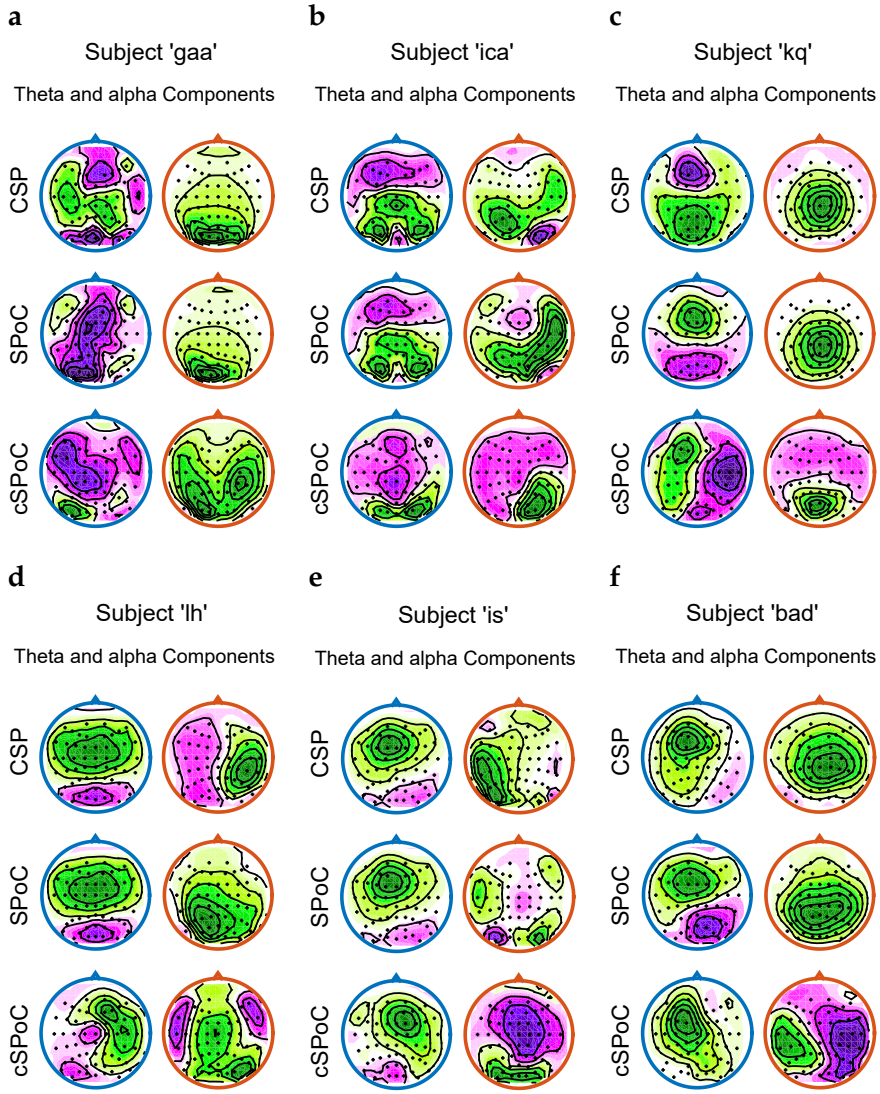

Figure 25: Spatial activation patterns extracted by the three EEG spatial filtering methods from subjects *gaa* (**a**), *ica* (**b**), *kq* (**c**), *lh* (**d**), *is* (**e**) and *bad* (**f**). The shown activation patterns (scalp maps) and power envelopes correspond to the components with the *second highest* value of the optimization criterion of the respective method.

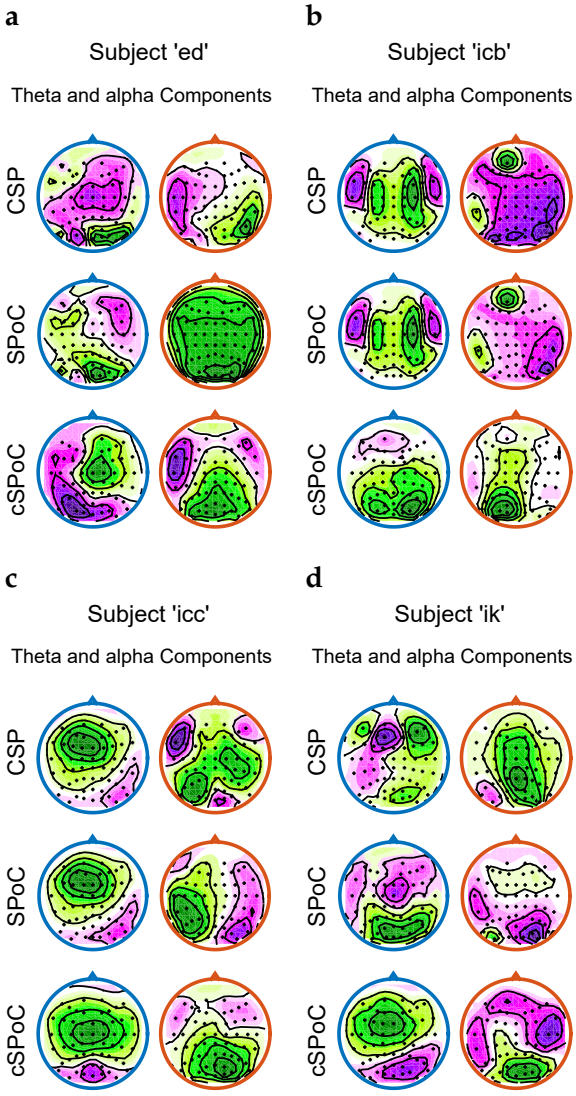

Figure 26: Like Figure 25, but for subjects *ed* (**a**), *icb* (**b**), *icc* (**c**) and *ik* (**d**).

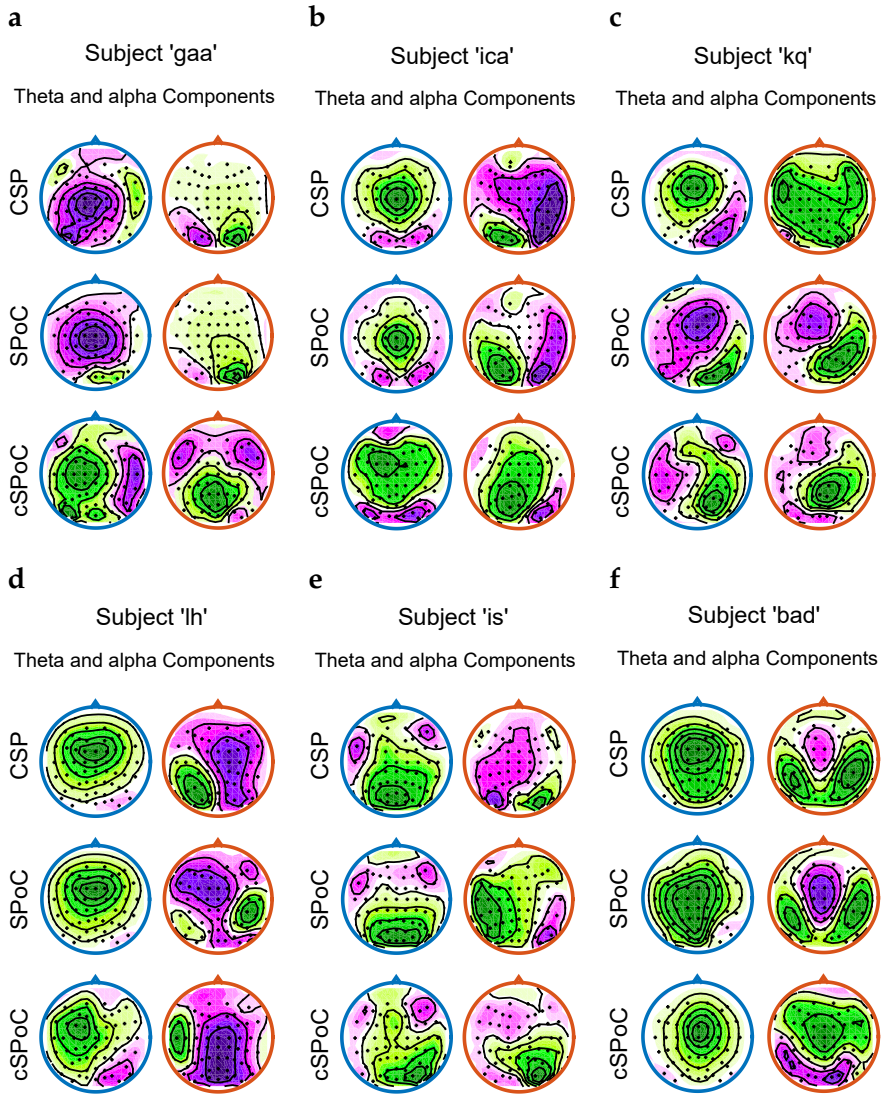

Figure 27: Like Figure 25, but showing components with the *third highest* value of the optimization criterion of the respective method.

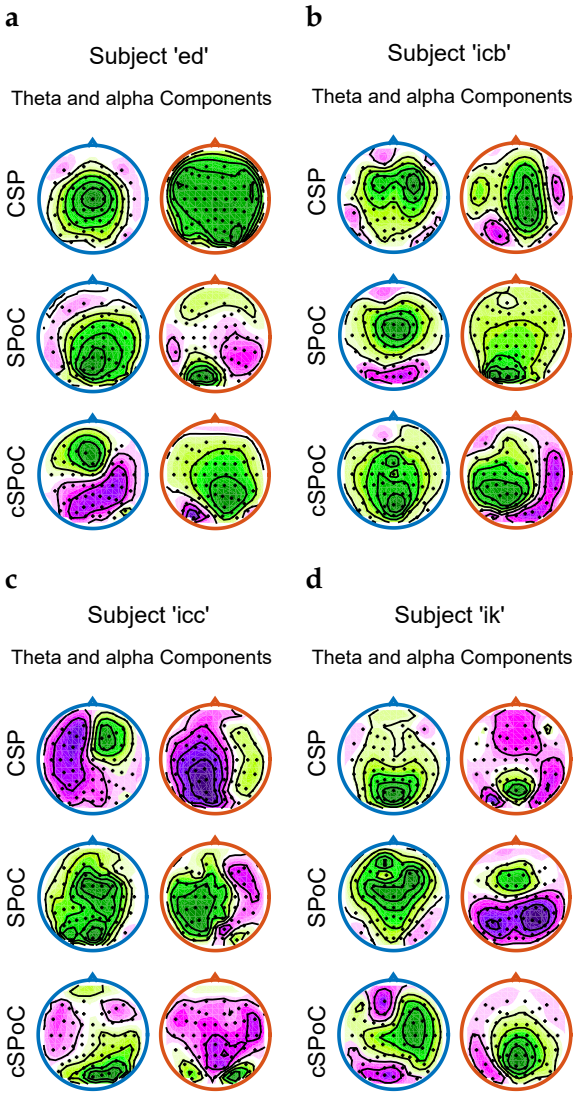

Figure 28: Like Figure 26, but showing components with the *third highest* value of the optimization criterion of the respective method.

	Analysis 1	**Analysis 2**	**Analysis 3**
Training set	Missed(I)	Missed(I), Silent(II,III)	
Features	signal downsampled to 10 Hz		log-var features: α_1 (8 - 10 Hz), α_2 (11 - 14 Hz), β_1 (15 - 19 Hz), β_2 (20 - 27 Hz)
"Movement" window	[-1200 0]ms w.r.t. EMG onset		[-500 0]ms w.r.t. EMG onset
"No Movement" window	[-1200 0]ms w.r.t. trial start		[-1500 -1000]ms w.r.t. EMG onset
Test set	Silent(II,III)	Predicted(II,III), Aborted(II,III), Early/FA(I,II,III)	
Applied to	[-1200 0]ms w.r.t. EMG onset	whole trial (1200ms sliding window)	[-500 0]ms w.r.t. stop signal

Table 2: Detailed overview of the three offline analyses performed after EEG recording. The analyses used different trial types (Silent, Missed, Predicted, Aborted and Early/FA, see Section 4.3.3) from different stages (I, II and III) as training and test set, respectively. In analyses 1 and 2, features were extracted in analogy to the BCI predictor described in Section 4.2.3. In analysis 2, the classifier was applied to the whole trial with a sliding window. In analysis 3, a classifier was trained on concatenated log-var features from four frequency bands. Therefore, for each band individually, Common Spatial Pattern (CSP) filters were defined that maximize the power contrast between "movement" and "no movement" windows (Blankertz et al., 2008). The trained classifier was applied to 500 ms EEG segments preceding a stop signal.

"Did you use a particular strategy during the last round?"

Stage I	Stage II	Stage III
Pressed earlier on trials following interruptions. (4)	Got interrupted more often, so pressed earlier overall. (4)	Tried to be unpredictable [or] didn't think about movements. (5)
Tried to wait as long as possible [or] played riskier. (4)	Tried to be more spontaneous [or] didn't think [or] tried to be unpredictable. (4)	"I pressed faster." (3)
Waited until "I felt an interruption would come" and then pressed. (4)	"I didn't wait for the interruptions, I played safer." (3)	"I was more relaxed [or] meditative." (2)
Pressed randomly (avoided rhythms, heart rate, breathing) (2)	"I tried to be less tense just before movements." (2)	Ignored the "feeling" or "urge" to move. (2)
Pressed faster or "I tried to play it safe." (2)	"I had more of a strategy, it was less of an 'urge'." (1)	"I tried to ignore when I was interrupted." (1)
Thought about other things, pressed when the 'urge' came.		"I tried harder." (1)
"I don't know." (1)		

Table 3: Summary of Responses to Question 1. Each participant was questioned at the end of every ten minute block (two per stage) during the experiment. Participants were not prompted but openly volunteered different strategies that they felt they had followed intentionally or unintentionally. Because many responses overlapped this table includes quotes and paraphrased quotes without quotations grouped together with other similar answer types. Each group includes the number of participants, in parentheses, who volunteered the quoted information. Because participants could mention multiple strategies, the total for each stage can add up to more than 10.

"Did you feel there was a connection between your actions and the appearance of an interruption?"

Stage I	Stage II	Stage III
"There was no consistent connection." (n=6)	Moving the foot caused interruptions. (4)	"There was no consistent connection." (3)
"I saw a pattern in the timing" of interruptions. (4)	"Thinking about pressing [or] the 'feeling/urge' to press" caused interruptions. (3)	"The switch from being 'relaxed' to 'going to push'" caused interruptions. (2)
"If I wait too long then an interruption comes." (3)	"There was no consistent connection." (2)	"Everything" related to foot movement caused interruptions. (2)
	"The moment of choice." (1)	"Thinking about pressing [or] the 'feeling/urge' to press" (2)
		"Heart rate" (1)
		Moving the foot caused interruptions (1)
		"I have no idea." (1)

Table 4: Summary of Responses to Question 2. See Table 3

REFERENCES

Abbass, H. A., J. Tang, R. Amin, M. Ellejmi, and S. Kirby (2014). „Augmented cognition using real-time EEG-based adaptive strategies for air traffic control." In: *Proceedings of the human factors and ergonomics society annual meeting*. Vol. 58. 1. SAGE Publications, pp. 230–234.

Acqualagna, L., S. Bosse, A. K. Porbadnigk, G. Curio, K.-R. Müller, T. Wiegand, and B. Blankertz (2015). EEG-based classification of video quality perception using steady state visual evoked potentials (SSVEPs). *Journal of Neural Engineering* 12.2, p. 026012.

Alexander, P., A. Schlegel, W. Sinnott-Armstrong, A. L. Roskies, T. Wheatley, and P. U. Tse (2016). Readiness potentials driven by non-motoric processes. *Consciousness and cognition* 39, pp. 38–47.

Allison, B. Z., D. J. McFarland, G. Schalk, S. D. Zheng, M. M. Jackson, and J. R. Wolpaw (2008). Towards an independent brain–computer interface using steady state visual evoked potentials. *Clinical neurophysiology* 119.2, pp. 399–408.

Allison, B. Z. and J. Polich (2008). Workload assessment of computer gaming using a single-stimulus event-related potential paradigm. *Biological Psychology* 77.3, pp. 277–283.

Aoki, F., E. Fetz, L. Shupe, E. Lettich, and G. Ojemann (2001). Changes in power and coherence of brain activity in human sensorimotor cortex during performance of visuomotor tasks. *Biosystems* 63.1, pp. 89–99.

Arico, P., G. Borghini, I. Graziani, F. Taya, Y. Sun, A. Bezerianos, N. Thakor, F. Cincotti, and F. Babiloni (2014). „Towards a multimodal bioelectrical framework for the online mental workload evaluation." In: *Engineering in Medicine and Biology Society (EMBC), 2014 36th Annual International Conference of the IEEE*, pp. 3001–3004.

Babiloni, C., F. Carducci, F. Cincotti, P. M. Rossini, C. Neuper, G. Pfurtscheller, and F. Babiloni (1999). Human movement-related potentials vs desynchronization of EEG alpha rhythm: a high-resolution EEG study. *Neuroimage* 10.6, pp. 658–665.

Babiloni, C., F. Babiloni, F. Carducci, F. Cincotti, G. Cocozza, C. Del Percio, D. V. Moretti, and P. M. Rossini (2002). Human cortical electroencephalography (EEG) rhythms during the observation of simple aimless movements: a high-resolution EEG study. *Neuroimage* 17.2, pp. 559–572.

Bai, O., Z. Mari, S. Vorbach, and M. Hallett (2005). Asymmetric spatiotemporal patterns of event-related desynchronization preceding voluntary sequential finger movements: a high-resolution EEG study. *Clinical Neurophysiology* 116.5, pp. 1213–1221.

Bai, O., V. Rathi, P. Lin, D. Huang, H. Battapady, D.-Y. Y. Fei, L. Schneider, E. Houdayer, X. Chen, and M. Hallett (2011). Prediction of human voluntary movement before it occurs. *Clinical neurophysiology* 122.2, pp. 364–372.

Bai, O., S. Vorbach, M. Hallett, and M. K. Floeter (2006). Movement-related cortical potentials in primary lateral sclerosis. *Annals of Neurology* 59.4, pp. 682–690.

Baillet, S., J. Mosher, and R. Leahy (2001). Electromagnetic Brain Mapping. *IEEE Signal Processing Magazine* 18 (6), pp. 14–30.

Bartz, D. and K.-R. Müller (2013). „Generalizing analytic shrinkage for arbitrary covariance structures." In: *Advances in Neural Information Processing Systems*, pp. 1869–1877.

Bauer, M., R. Oostenveld, M. Peeters, and P. Fries (2006). Tactile spatial attention enhances gamma-band activity in somatosensory cortex and reduces low-frequency activity in parieto-occipital areas. *The Journal of Neuroscience* 26.2, pp. 490–501.

Beatty, J., A. Greenberg, W. P. Deibler, and J. F. O'Hanlon (1974). Operant control of occipital theta rhythm affects performance in a radar monitoring task. *Science* 183.4127, pp. 871–873.

Bell, A. J. and T. J. Sejnowski (1995). An information-maximization approach to blind separation and blind deconvolution. *Neural computation* 7.6, pp. 1129–1159.

Berger, H. (1929). Üeber das Elektroenkephalogramm des Menschen. *Archiv für Psychiatrie und Nervenkrankheiten* 87.1, pp. 527–570.

Berka, C., D. J. Levendowski, M. N. Lumicao, A. Yau, G. Davis, V. T. Zivkovic, R. E. Olmstead, P. D. Tremoulet, and P. L. Craven (2007). EEG Correlates of Task Engagement and Mental Workload in Vigilance, Learning, and Memory Tasks. *Aviation, Space, and Environmental Medicine* 78.5, pp. 231–244.

Bin, G., X. Gao, Y. Wang, Y. Li, B. Hong, and S. Gao (2011). A high-speed BCI based on code modulation VEP. *Journal of Neural Engineering* 8.2, p. 025015.

Birbaumer, N., N. Ghanayim, T. Hinterberger, I. Iversen, B. Kotchoubey, A. Kübler, J. Perelmouter, E. Taub, and H. Flor (1999). A spelling device for the paralysed. *Nature* 398.6725, pp. 297–298.

Bishop, C. M. (2007). *Pattern Recognition and Machine Learning (Information Science and Statistics)*. Springer US.

Blankertz, B., G. Dornhege, M. Krauledat, K. R. Müller, and G. Curio (2007a). The non-invasive Berlin Brain-Computer Interface: fast acquisition of effective performance in untrained subjects. *NeuroImage* 37.2, pp. 539–550.

Blankertz, B., G. Curio, and K.-R. Müller (2002). Classifying single trial EEG: Towards brain computer interfacing. *Advances in Neural information processing systems* 1, pp. 157–164.

Blankertz, B., G. Dornhege, M. Krauledat, K.-R. Müller, and G. Curio (2005). The Berlin brain-computer interface: Report from the feedback sessions. *FIRST Reports*.

Blankertz, B., G. Dornhege, M. Krauledat, K.-R. Müller, and G. Curio (2007b). The non-invasive Berlin brain–computer interface: fast acquisition of effective performance in untrained subjects. *NeuroImage* 37.2, pp. 539–550.

Blankertz, B., G. Dornhege, S. Lemm, M. Krauledat, G. Curio, and K.-R. Müller (2006). The Berlin Brain-Computer Interface: Machine

Learning Based Detection of User Specific Brain States. *J. UCS* 12.6, pp. 581–607.

Blankertz, B., G. Dornhege, C. Schäfer, R. Krepki, J. Kohlmorgen, K.-R. Müller, V. Kunzmann, F. Losch, and G. Curio (2003). Boosting bit rates and error detection for the classification of fast-paced motor commands based on single-trial EEG analysis. *Neural Systems and Rehabilitation Engineering, IEEE Transactions on* 11.2, pp. 127–131.

Blankertz, B., S. Lemm, M. Treder, S. Haufe, and K.-R. Müller (2011). Single-trial analysis and classification of ERP components – A tutorial. *NeuroImage* 56.2, pp. 814–825.

Blankertz, B., M. Tangermann, C. Vidaurre, S. Fazli, C. Sannelli, S. Haufe, C. Maeder, L. E. Ramsey, I. Sturm, G. Curio, and K. R. Müller (2010). The Berlin Brain-Computer Interface: Non-Medical Uses of BCI Technology. *Frontiers in Neuroscience* 4.198. DOI: 10.3389/fnins.2010.00198.

Blankertz, B., R. Tomioka, S. Lemm, M. Kawanabe, and K.-R. Müller (2008). Optimizing Spatial Filters for Robust EEG Single-Trial Analysis. *IEEE Signal Processing Magazine* 25.1, pp. 41–56.

Bode, S., D. K. Sewell, S. Lilburn, J. D. Forte, P. L. Smith, and J. Stahl (2012). Predicting perceptual decision biases from early brain activity. *The Journal of neuroscience* 32.36, pp. 12488–12498.

Borghini, G., L. Astolfi, G. Vecchiato, D. Mattia, and F. Babiloni (2014). Measuring neurophysiological signals in aircraft pilots and car drivers for the assessment of mental workload, fatigue and drowsiness. *Neuroscience & Biobehavioral Reviews* 44, pp. 58–75.

Borisoff, J. F., S. G. Mason, A. Bashashati, and G. E. Birch (2004). Brain-computer interface design for asynchronous control applications: improvements to the LF-ASD asynchronous brain switch. *Biomedical Engineering, IEEE Transactions on* 51.6, pp. 985–992.

Brass, M. and P. Haggard (2007). To do or not to do: the neural signature of self-control. *The Journal of Neuroscience* 27.34, pp. 9141–9145.

Brass, M. and P. Haggard (2008). The what, when, whether model of intentional action. *The Neuroscientist* 14.4, pp. 319–325.

Brookings, J. B., G. F. Wilson, and C. R. Swain (1996). Psychophysiological responses to changes in workload during simulated air traffic control. *Biological Psychology* 42.3, pp. 361–377.

Brouwer, A.-M., M. A. Hogervorst, J. B. F. van Erp, T. Heffelaar, P. H. Zimmerman, and R. Oostenveld (2012). Estimating workload using EEG spectral power and ERPs in the n-back task. *Journal of Neural Engineering* 9 (4).

Brown, S. and A. Heathcote (2005). A ballistic model of choice response time. *Psychological review* 112.1, p. 117.

Brunia, C. H., F. J. Voorn, and B. M. P. (1985). Movement related slow potentials. II. A contrast between finger and foot movements in left-handed subjects. *Electroencephalogr Clin Neurophysiol* 60, pp. 135–145.

Buzsaki, G. and A. Draguhn (2004). Neuronal Oscillations in Cortical Networks. *Science* 304.5679, pp. 1926–1938.

Calancie, B., M. Nordin, U. Wallin, and K. E. Hagbarth (1987). Motor-unit responses in human wrist flexor and extensor muscles to tran-

scranial cortical stimuli. *Journal of Neurophysiology* 58.5, pp. 1168–1185.

Cavanagh, J. F. and M. J. Frank (2014). Frontal theta as a mechanism for cognitive control. *Trends in Cognitive Sciences* 18.8, pp. 414–421.

Chen, Y., M. Ding, and S. J. Kelso (2003). Task-related power and coherence changes in neuromagnetic activity during visuomotor coordination. *Experimental Brain Research* 148.1, pp. 105–116.

Chiang, T. (2005). What's expected of us. *Nature* 436.7047, pp. 150–150.

Christensen, J. C., J. R. Estepp, G. F. Wilson, and C. A. Russell (2012). The effects of day-to-day variability of physiological data on operator functional state classification. *NeuroImage* 59.1, pp. 57–63.

Classen, J., C. Gerloff, M. Honda, and M. Hallett (1998). Integrative visuomotor behavior is associated with interregionally coherent oscillations in the human brain. *Journal of Neurophysiology* 79.3, pp. 1567–1573.

Cohen, D. et al. (1968). Magnetoencephalography: evidence of magnetic fields produced by alpha-rhythm currents. *Science* 161.3843, pp. 784–786.

Coles, M. G., G. Gratton, and E. Donchin (1988). Detecting early communication: Using measures of movement-related potentials to illuminate human information processing. *Biological Psychology* 26.1, pp. 69–89.

Comstock Jr, J. R. and R. J. Arnegard (1992). The multi-attribute task battery for human operator workload and strategic behavior research.

Cooper, N. R., R. J. Croft, S. J. Dominey, A. P. Burgess, and J. H. Gruzelier (2003). Paradox lost? Exploring the role of alpha oscillations during externally vs. internally directed attention and the implications for idling and inhibition hypotheses. *International Journal of Psychophysiology* 47.1, pp. 65–74.

Coyle, S., T. Ward, C. Markham, and G. McDarby (2004). On the suitability of near-infrared (NIR) systems for next-generation brain–computer interfaces. *Physiological measurement* 25.4, p. 815.

Cui, R. Q., D. Huter, W. Lang, and L. Deecke (1999). Neuroimage of voluntary movement: topography of the Bereitschaftspotential, a 64-channel DC current source density study. *NeuroImage* 9.1, pp. 124–134.

Cunnington, R., R. Iansek, J. L. Bradshaw, and J. G. Phillips (1996). Movement-related potentials associated with movement preparation and motor imagery. *Exp Brain Res* 111.3, pp. 429–436.

Dähne, S., F. Biessmann, W. Samek, S. Haufe, D. Goltz, C. Gundlach, A. Villringer, S. Fazli, and K.-R. Müller (2015). Multivariate machine learning methods for fusing multimodal functional neuroimaging data. *Proceedings of the IEEE* 103.9, pp. 1507–1530.

Dähne, S., F. C. Meinecke, S. Haufe, J. Höhne, M. Tangermann, K.-R. Müller, and V. V. Nikulin (2014a). SPoC: a novel framework for relating the amplitude of neuronal oscillations to behaviorally relevant parameters. *NeuroImage* 86, pp. 111–122.

Dähne, S., V. V. Nikulin, D. Ramírez, P. J. Schreier, K.-R. Müller, and S. Haufe (2014b). Finding brain oscillations with power dependencies in neuroimaging data. *NeuroImage* 96, pp. 334–348.

Davis, P. A. (1939). Effects of acoustic stimuli on the waking human brain. *Journal of Neurophysiology* 2.6, pp. 494–499.

De Jong, R., M. G. Coles, G. D. Logan, and G. Gratton (1990). In search of the point of no return: The control of response processes. *Journal of Experimental Psychology: Human Perception and Performance* 16.1, pp. 164–182.

Deco, G., M. Pérez-Sanagustín, V. de Lafuente, and R. Romo (2007). Perceptual detection as a dynamical bistability phenomenon: a neurocomputational correlate of sensation. *Proceedings of the National Academy of Sciences* 104.50, pp. 20073–20077.

Deecke, L., P. Scheid, and H. Kornhuber (1969). Distribution of readiness potential, pre-motion positivity, and motor potential of the human cerebral cortex preceding voluntary finger movements. *Experimental Brain Research* 7.2, pp. 158–168.

Dennett, D. C. (1993). *Consciousness explained*. Penguin UK.

Dijksterhuis, C., D. de Waard, K. Brookhuis, B. Mulder, and R. de Jong (2013). Classifying visuomotor workload in a driving simulator using subject specific spatial brain patterns. *Frontiers in Neuroscience* 7.149. DOI: 10.3389/fnins.2013.00149.

Dornhege, G. (2007). *Toward brain-computer interfacing*. MIT press.

Dornhege, G., B. Blankertz, G. Curio, and K.-R. Müller (2002). „Combining features for BCI." In: *Advances in Neural Information Processing Systems*, pp. 1115–1122.

Dornhege, G., M. Krauledat, and K.-R. M. and Benjamin Blankertz (2007). General signal processing and machine learning tools for BCI. In: *Toward Brain-Computer Interfacing*. Ed. by G. Dornhege, J. del R. Millán, D. Hinterberger Thilo and McFarland, and K.-R. Müller. Cambridge, MA: MIT Press, pp. 207–233.

Duda, R. O., P. E. Hart, and D. G. Stork (2001). *Pattern Classification*. 2nd edition. Wiley & Sons.

Eimer, M. (1998). The lateralized readiness potential as an on-line measure of central response activation processes. *Behavior Research Methods, Instruments, & Computers* 30.1, pp. 146–156.

Erp, J. van, F. Lotte, and M. Tangermann (2012). Brain-computer interfaces: beyond medical applications. *Computer*, pp. 26–34.

Fabiani, M., G. Gratton, and M. Coles (2000). Event-related brain potentials: methods, theory. *Handbook of psychophysiology*, pp. 53–84.

Falkenstein, M., J. Hoormann, S. Christ, and J. Hohnsbein (2000). ERP components on reaction errors and their functional significance: a tutorial. *Biological psychology* 51.2, pp. 87–107.

Farwell, L. A. and E. Donchin (1988). Talking off the top of your head: toward a mental prosthesis utilizing event-related brain potentials. *Electroencephalography and clinical Neurophysiology* 70.6, pp. 510–523.

Fatourechi, M., R. K. Ward, and G. E. Birch (2008). A Self-Paced Brain-Computer Interface System with a Low False Positive Rate. *Journal of Neural Engineering* 5.1, pp. 9–23.

Fazli, S., S. Dähne, W. Samek, F. Bießmann, and K.-R. Müller (2015). Learning from more than one data source: data fusion techniques for sensorimotor rhythm-based Brain-Computer Interfaces. *Proceedings of the IEEE* 103.6, pp. 891–906.

Fazli, S., J. Mehnert, J. Steinbrink, G. Curio, A. Villringer, K.-R. Müller, and B. Blankertz (2012). Enhanced performance by a hybrid NIRS–EEG brain computer interface. *Neuroimage* 59.1, pp. 519–529.

Filevich, E., S. Kühn, and P. Haggard (2013). There is no free won't: antecedent brain activity predicts decisions to inhibit. *PloS one* 8.2, e53053.

Fink, A., R. Grabner, C. Neuper, and A. Neubauer (2005). EEG alpha band dissociation with increasing task demands. *Cognitive Brain Research* 24.2, pp. 252–259.

Fried, I., R. Mukamel, and G. Kreiman (2011). Internally generated preactivation of single neurons in human medial frontal cortex predicts volition. *Neuron* 69.3, pp. 548–562.

Friedman, J. H. (1989). Regularized discriminant analysis. *Journal of the American statistical association* 84.405, pp. 165–175.

Galán, F., M. Nuttin, E. Lew, P. W. Ferrez, G. Vanacker, J. Philips, and J. d. R. Millán (2008). A brain-actuated wheelchair: asynchronous and non-invasive brain–computer interfaces for continuous control of robots. *Clinical Neurophysiology* 119.9, pp. 2159–2169.

Galgano, J. and K. Froud (2008). Evidence of the voice-related cortical potential: an electroencephalographic study. *Neuroimage* 41.4, pp. 1313–1323.

Galin, D., J. Johnstone, and J. Herron (1978). Effects of task difficulty on EEG measures of cerebral engagement. *Neuropsychologia* 16.4, pp. 461–472.

Gazzaniga, M. S. (2004). *The cognitive neurosciences*. MIT press.

Gevins, A. S., S. L. Bressler, B. A. Cutillo, J. Illes, J. C. Miller, J. Stern, and H. R. Jex (1990). Effects of prolonged mental work on functional brain topography. *Electroencephalography and Clinical Neurophysiology* 76.4, pp. 339–350.

Gevins, A. and B. Cutillo (1993). Spatiotemporal dynamics of component processes in human working memory. *Electroencephalography and Clinical Neurophysiology* 87.3, pp. 128–143.

Gevins, A., H. Leong, R. Du, M. E. Smith, J. Le, D. DuRousseau, J. Zhang, and J. Libove (1995). Towards measurement of brain function in operational environments. *Biological Psychology* 40.1, pp. 169–186.

Gevins, A. and M. E. Smith (2003). Neurophysiological measures of cognitive workload during human-computer interaction. *Theoretical Issues in Ergonomics Science* 4.1-2, pp. 113–131.

Guo, F., B. Hong, X. Gao, and S. Gao (2008). A brain–computer interface using motion-onset visual evoked potential. *Journal of Neural Engineering* 5.4, p. 477.

Haggard, P. and M. Eimer (1999). On the relation between brain potentials and the awareness of voluntary movements. *Experimental Brain Research* 126.1, pp. 128–133.

Haggard, P. (2008). Human volition: towards a neuroscience of will. *Nature Reviews Neuroscience* 9.12, pp. 934–946.

Hanes, D. P. and J. D. Schall (1996). Neural Control of Voluntary Movement Initiation. *Science* 274.5286, pp. 427–430.

Hankins, T. C. and G. F. Wilson (1998). A comparison of heart rate, eye activity, EEG and subjective measures of pilot mental workload during flight. *Aviat Space Environ Med* 69.4, pp. 360–367.

Harmony, T., T. Fernández, J. Silva, J. Bernal, L. Díaz-Comas, A. Reyes, E. Marosi, M. Rodríguez, and M. Rodríguez (1996). EEG delta activity: an indicator of attention to internal processing during performance of mental tasks. *International journal of psychophysiology* 24.1, pp. 161–171.

Hart, S. G. and L. E. Staveland (1988). Development of NASA-TLX (Task Load Index): Results of empirical and theoretical research. *Advances in psychology* 52, pp. 139–183.

Hasan, B. A. S. and J. Q. Gan (2010). Unsupervised movement onset detection from EEG recorded during self-paced real hand movement. *Med Biol Engineering and Computing* 48.3, pp. 245–253.

Haufe, S., S. Dähne, and V. V. Nikulin (2014a). Dimensionality reduction for the analysis of brain oscillations. *NeuroImage* 101, pp. 583–597.

Haufe, S., J.-W. Kim, I.-H. Kim, A. Sonnleitner, M. Schrauf, G. Curio, and B. Blankertz (2014b). Electrophysiology-based detection of emergency braking intention in real-world driving. *Journal of Neural Engineering* 11.5, p. 056011.

Haufe, S., F. Meinecke, K. Görgen, S. Dähne, J.-D. Haynes, B. Blankertz, and F. Bießmann (2014c). On the interpretation of weight vectors of linear models in multivariate neuroimaging. *NeuroImage* 87, pp. 96–110.

Haufe, S., M. S. Treder, M. F. Gugler, M. Sagebaum, G. Curio, and B. Blankertz (2011). EEG potentials predict upcoming emergency brakings during simulated driving. *Journal of Neural Engineering* 8.5, pp. 056001+.

Haynes, J.-D. (2011). Decoding and predicting intentions. *Annals of the New York Academy of Sciences* 1224.1, pp. 9–21.

Hebb, D. O. (2005). *The organization of behavior: A neuropsychological theory*. Psychology Press.

Herrmann, C. S., M. Pauen, B.-K. Min, N. A. Busch, and J. W. Rieger (2008). Analysis of a choice-reaction task yields a new interpretation of Libet's experiments. *International journal of psychophysiology* 67.2, pp. 151–157.

Hillyard, S. A., R. Hink, V. L. Schwent, and T. W. Picton (1973). Electrical Signs of Selective Attention in the Human Brain. *Science* 182.4108, pp. 177–182.

Hockey, G. R. J. (2003). *Operator functional state: the assessment and prediction of human performance degradation in complex tasks*. Vol. 355. IOS Press.

Hodgkin, A. L. and A. F. Huxley (1952). A quantitative description of membrane current and its application to conduction and excitation in nerve. *The Journal of physiology* 117.4, p. 500.

Hogervorst, M. A., A.-M. Brouwer, and J. B. F. Van Erp (2014). Combining and comparing EEG, peripheral physiology and eye-related measures for the assessment of mental workload. *Frontiers in Neuroscience* 8.322.

Holm, A., K. Lukander, J. Korpela, M. Sallinen, and K. M. I. Müller (2009). Estimating brain load from the EEG. *TheScientificWorldJournal* 9, pp. 639–51.

Hughes, G., S. Schütz-Bosbach, and F. Waszak (2011). One Action System or Two? Evidence for Common Central Preparatory Mechanisms in Voluntary and Stimulus-Driven Actions. *The Journal of Neuroscience* 31.46, pp. 16692–16699.

Hughes, G., M. Velmans, and J. De Fockert (2009). Unconscious priming of a no-go response. *Psychophysiology* 46.6, pp. 1258–1269.

Hyvarinen, A. (1999). Fast and robust fixed-point algorithms for independent component analysis. *IEEE Transactions on Neural Networks* 10.3, pp. 626–634.

Jeffreys, D. and J. Axford (1972). Source locations of pattern-specific components of human visual evoked potentials. I. Component of striate cortical origin. *Experimental Brain Research* 16.1, pp. 1–21.

Jensen, O. and L. L. Colgin (2007). Cross-frequency coupling between neuronal oscillations. *Trends in cognitive sciences* 11.7, pp. 267–269.

Jensen, O., J. Gelfand, J. Kounios, and J. E. Lisman (2002). Oscillations in the Alpha Band (9-12 Hz) Increase with Memory Load during Retention in a Short-term Memory Task. *Cerebral Cortex* 12.8, pp. 877–882.

Jensen, O. and C. D. Tesche (2002). Frontal theta activity in humans increases with memory load in a working memory task. *European Journal of Neuroscience* 15.8, pp. 1395–1399.

Jo, H.-G., T. Hinterberger, M. Wittmann, T. L. Borghardt, and S. Schmidt (2013). Spontaneous EEG fluctuations determine the readiness potential: is preconscious brain activation a preparation process to move? *Experimental brain research* 231.4, pp. 495–500.

Jobsis, F. F. (1977). Noninvasive, infrared monitoring of cerebral and myocardial oxygen sufficiency and circulatory parameters. *Science* 198.4323, pp. 1264–1267.

Jung, T.-P., S. Makeig, M. Stensmo, and T. Sejnowski (1997). Estimating alertness from the EEG power spectrum. *IEEE Transactions on Biomedical Engineering* 44.1, pp. 60–69.

Jung, T.-P., S. Makeig, C. Humphries, T.-W. Lee, M. J. Mckeown, V. Iragui, and T. J. Sejnowski (2000). Removing electroencephalographic artifacts by blind source separation. *Psychophysiology* 37.02, pp. 163–178.

Kahneman, D. (1973). *Attention and effort*. Englewood Cliffs, NJ: Prentice-Hall.

Kandel, E. R., J. H. Schwartz, T. M. Jessell, S. A. Siegelbaum, and A. Hudspeth (2000). *Principles of Neural Science*. Vol. 4. McGraw-hill New York.

Karavidas, M. K., P. M. Lehrer, S.-E. Lu, E. Vaschillo, B. Vaschillo, and A. Cheng (2010). The effects of workload on respiratory variables

in simulated flight: A preliminary study. *Biological Psychology* 84.1, pp. 157–160.

Kecklund, G. and T. Åkerstedt (1993). Sleepiness in long distance truck driving: an ambulatory EEG study of night driving. *Ergonomics* 36.9, pp. 1007–1017.

Keil, A., T. Mussweiler, and K. Epstude (2006). Alpha-band activity reflects reduction of mental effort in a comparison task: A source space analysis. *Brain Research* 1121.1, pp. 117–127.

Keller, I. and H. Heckhausen (1990). Readiness potentials preceding spontaneous motor acts: voluntary vs. involuntary control. *Electroencephalography and clinical Neurophysiology* 76.4, pp. 351–361.

Kitamura, J., H. Shibasaki, A. Takagi, H. Nabeshima, and A. Yamaguchi (1993). Enhanced negative slope of cortical potentials before sequential as compared with simultaneous extensions of two fingers. *Electroencephalogr Clin Neurophysiol* 86.3, pp. 176–182.

Klimesch, W., M. Doppelmayr, J. Schwaiger, P. Auinger, and T. Winkler (1999). 'Paradoxical' alpha synchronization in a memory task. *Cognitive Brain Research* 7.4, pp. 493–501.

Klimesch, W. (1999). EEG alpha and theta oscillations reflect cognitive and memory performance: a review and analysis. *Brain Research Reviews* 29.2, pp. 169–195.

Klimesch, W., M. Doppelmayr, H. Russegger, T. Pachinger, and J. Schwaiger (1998). Induced alpha band power changes in the human EEG and attention. *Neuroscience letters* 244.2, pp. 73–76.

Kohlisch, O. and F. Schaefer (1996). Physiological changes during computer tasks: responses to mental load or to motor demands? *Ergonomics* 39.2, pp. 213–224.

Kohlmorgen, J., G. Dornhege, M. Braun, B. Blankertz, K.-R. Müller, G. Curio, K. Hagemann, A. Bruns, M. Schrauf, and W. Kincses (2007). Improving human performance in a real operating environment through real-time mental workload detection. In: *Toward Brain-Computer Interfacing*. Ed. by G. Dornhege, J. del R. Millán, T. Hinterberger, D. McFarland, and K.-R. Müller. Cambridge, MA: MIT press, pp. 409–422.

Koles, Z. J. (1991). The quantitative extraction and topographic mapping of the abnormal components in the clinical EEG. *Electroencephalography and clinical neurophysiology* 79.6, pp. 440–447.

Kornhuber, H. H. and L. Deecke (1965). Hirnpotentialänderungen bei Willkürbewegungen und passiven Bewegungen des Menschen: Bereitschaftspotential und reafferente Potentiale. *Pflügers Arch* 284, pp. 1–17.

Krauledat, M., G. Dornhege, B. Blankertz, F. Losch, G. Curio, and K.-R. Müller (2004). „Improving speed and accuracy of brain-computer interfaces using readiness potential features." In: *Engineering in Medicine and Biology Society, 2004. IEMBS '04. 26th Annual International Conference of the IEEE*. Vol. 2, pp. 4511–4515.

Kübler, A., N. Neumann, J. Kaiser, B. Kotchoubey, T. Hinterberger, and N. P. Birbaumer (2001). Brain-computer communication: Self-regulation of slow cortical potentials for verbal communication. *Archives of Physical Medicine and Rehabilitation* 82.11, pp. 1533–1539.

Kühn, S., P. Haggard, and M. Brass (2009). Intentional inhibition: How the "veto-area" exerts control. *Human brain mapping* 30.9, pp. 2834–2843.

Kwong, K. K., J. W. Belliveau, D. A. Chesler, I. E. Goldberg, R. M. Weisskoff, B. P. Poncelet, D. N. Kennedy, B. E. Hoppel, M. S. Cohen, and R. Turner (1992). Dynamic magnetic resonance imaging of human brain activity during primary sensory stimulation. *Proceedings of the National Academy of Sciences* 89.12, pp. 5675–5679.

Lang, W., D. Cheyne, R. Kristeva, R. Beisteiner, G. Lindinger, and L. Deecke (1991). Three-dimensional localization of SMA activity preceding voluntary movement. A study of electric and magnetic fields in a patient with infarction of the right supplementary motor area. *Exp Brain Res* 87.3, pp. 688–695.

Lau, H. C., R. D. Rogers, P. Haggard, and R. E. Passingham (2004). Attention to intention. *science* 303.5661, pp. 1208–1210.

Lau, H. C., R. D. Rogers, and R. E. Passingham (2007). Manipulating the experienced onset of intention after action execution. *Journal of cognitive neuroscience* 19.1, pp. 81–90.

Lavazza, A. (2016). Free Will and Neuroscience: From Explaining Freedom Away to New Ways of Operationalizing and Measuring It. *Frontiers in Human Neuroscience* 10, p. 262.

Ledoit, O. and M. Wolf (2004). A well-conditioned estimator for large-dimensional covariance matrices. *Journal of multivariate analysis* 88.2, pp. 365–411.

Lemm, S., B. Blankertz, T. Dickhaus, and K.-R. Müller (2011). Introduction to machine learning for brain imaging. *Neuroimage* 56.2, pp. 387–399.

Leuthardt, E. C., K. J. Miller, G. Schalk, R. P. Rao, and J. G. Ojemann (2006). Electrocorticography-based brain computer interface – the Seattle experience. *IEEE Transactions on Neural Systems and Rehabilitation Engineering* 14.2, pp. 194–198.

Leuthardt, E. C., G. Schalk, J. R. Wolpaw, J. G. Ojemann, and D. W. Moran (2004). A brain–computer interface using electrocorticographic signals in humansThe authors declare that they have no competing financial interests. *Journal of Neural Engineering* 1.2, p. 63.

Lew, E., R. Chavarriaga, S. Silvoni, and J. d. R. MillÃ¡n (2012). Detection of Self-Paced Reaching Movement Intention from EEG Signals. *Frontiers in Neuroengineering* 5.13. DOI: 10.3389/fneng.2012.00013.

Libet, B., C. A. Gleason, E. W. Wright, and D. K. Pearl (1983). Time of conscious intention to act in relation to onset of cerebral activity (readiness-potential). The unconscious initiation of a freely voluntary act. *Brain : a journal of neurology* 106 (Pt 3).3, pp. 623–642.

Libet, B. W. (1985). Unconscious Cerebral Initiative and the Role of Conscious Will in Voluntary Action. *Behavioral and Brain Sciences* 8.4, pp. 529–66.

Logan, G. D. and W. B. Cowan (1984). On the ability to inhibit thought and action: A theory of an act of control. *Psychological Review* 91.3, pp. 295–327.

Luck, S. J. (2014). *An introduction to the event-related potential technique*. MIT press.

Makeig, S., F. Elliott, and M. Postal (1994). *First demonstration of an alertness monitoring management system*. Tech. rep. DTIC Document.

Makeig, S. and T. P. Jung (1996). Tonic, phasic, and transient EEG correlates of auditory awareness in drowsiness. *Cognitive Brain Research* 4.1, pp. 15–25.

Makeig, S., M. Westerfield, T.-P. Jung, S. Enghoff, J. Townsend, E. Courchesne, and T. Sejnowski (2002). Dynamic brain sources of visual evoked responses. *Science* 295.5555, pp. 690–694.

Makeig, S., M. Westerfield, T.-P. Jung, J. Covington, J. Townsend, T. J. Sejnowski, and E. Courchesne (1999). Functionally independent components of the late positive event-related potential during visual spatial attention. *The Journal of Neuroscience* 19.7, pp. 2665–2680.

Makeig, S., A. J. Bell, T.-P. Jung, T. J. Sejnowski, et al. (1996). Independent component analysis of electroencephalographic data. *Advances in Neural Information Processing Systems*, pp. 145–151.

Manzey, D. (1998). Psychophysiologie mentaler Beanspruchung. *Ergebnisse und Anwendungen der Psychophysiologie. Enzyklopädie der Psychologie* 100, pp. 799–864.

Maoz, U., U. Rutishauser, S. Kim, X. Cai, D. Lee, and C. Koch (2013). Predeliberation activity in prefrontal cortex and striatum and the prediction of subsequent value judgment. *Frontiers in Neuroscience* 7.225. DOI: 10.3389/fnins.2013.00225.

Maoz, U., S. Ye, I. B. Ross, A. N. Mamelak, and C. Koch (2012). „Predicting Action Content On-Line and in Real Time before Action Onset - an Intracranial Human Study.“ In: *NIPS*. Ed. by P. L. Bartlett, F. C. N. Pereira, C. J. C. Burges, L. Bottou, and K. Q. Weinberger, pp. 881–889.

Markand, O. N. (1990). Alpha rhythms. *Journal of Clinical Neurophysiology* 7.2, pp. 163–190.

Marks, L. E. (1985). Toward a psychophysics of intention. *Behavioral and Brain Sciences* 8 (04), pp. 547–547.

Martel, A., S. Dähne, and B. Blankertz (2014). EEG Predictors of Covert Vigilant Attention. *Journal of Neural Engineering* 11.3, p. 035009.

Masaki, H., N. Takasawa, and K. Yamazaki (1998). Enhanced negative slope of the readiness potential preceding a target force production task. *Electroencephalogr Clin Neurophysiol* 108.4, pp. 390–397.

Mason, S., A. Bashashati, M. Fatourechi, K. Navarro, and G. Birch (2007). A comprehensive survey of brain interface technology designs. *Annals of biomedical Engineering* 35.2, pp. 137–169.

Matousek, M. and I. Petersén (1983). A method for assessing alertness fluctuations from EEG spectra. *Electroencephalography and clinical neurophysiology* 55.1, pp. 108–113.

Matsuhashi, M. and M. Hallett (2008). The timing of the conscious intention to move. *The European journal of neuroscience* 28.11, pp. 2344–2351.

Matthews, G., L. E. Reinerman-Jones, D. J. Barber, and J. Abich (2015). The Psychometrics of Mental Workload: Multiple Measures Are Sensitive but Divergent. *Human Factors* 57.1, pp. 125–143.

Mellinger, J., G. Schalk, C. Braun, H. Preissl, W. Rosenstiel, N. Birbaumer, and A. Kübler (2007). An MEG-based brain–computer interface (BCI). *Neuroimage* 36.3, pp. 581–593.

Morita, H., E. Olivier, J. Baumgarten, N. Petersen, L. Christensen, and J. B. Nielsen (2000). Differential changes in corticospinal and Ia input to tibialis anterior and soleus motor neurones during voluntary contraction in man. *Acta physiologica scandinavica* 170.1, pp. 65–76.

Mühl, C., C. Jeunet, and F. Lotte (2014). EEG-based Workload Estimation Across Affective Contexts. *Frontiers in Neuroscience* 8.114.

Müller, K.-R., M. Tangermann, G. Dornhege, M. Krauledat, G. Curio, and B. Blankertz (2008). Machine learning for real-time single-trial EEG-analysis: from brain–computer interfacing to mental state monitoring. *Journal of neuroscience methods* 167.1, pp. 82–90.

Müller, K.-R., S. Mika, G. Ratsch, K. Tsuda, and B. Schölkopf (2001). An introduction to kernel-based learning algorithms. *IEEE transactions on Neural networks* 12.2, pp. 181–201.

Müller-Putz, G. R., R. Scherer, C. Brauneis, and G. Pfurtscheller (2005). Steady-state visual evoked potential (SSVEP)-based communication: impact of harmonic frequency components. *Journal of Neural Engineering* 2.4, pp. 123–130.

Müller-Putz, G., R. Scherer, C. Neuper, and G. Pfurtscheller (2006). Steady-state somatosensory evoked potentials: suitable brain signals for brain-computer interfaces? *IEEE transactions on Neural systems and rehabilitation Engineering* 14.1, pp. 30–37.

Murakami, M., M. I. Vicente, G. M. Costa, and Z. F. Mainen (2014). Neural antecedents of self-initiated actions in secondary motor cortex. *Nature neuroscience* 17.11, pp. 1574–1582.

Nagamine, T., M. Kajola, R. Salmelin, H. Shibasaki, and R. Hari (1996). Movement-related slow cortical magnetic fields and changes of spontaneous MEG-and EEG-brain rhythms. *Electroencephalography and clinical neurophysiology* 99.3, pp. 274–286.

Naumann, L. B., M. Schultze-Kraft, S. Dähne, and B. Blankertz (2016). „Prediction of difficulty levels in video games from EEG." In: *6th International BCI Meeting in Asilomar*.

Nicolae, I., L. Acqualagna, and B. Blankertz (2015). „Neural indicators of the depth of cognitive processing for user-adaptive neurotechnological applications." In: *Engineering in Medicine and Biology Society (EMBC), 2015 37th Annual International Conference of the IEEE*. IEEE, pp. 1484–1487.

Nicolelis, M. A. (2003). Brain–machine interfaces to restore motor function and probe neural circuits. *Nature Reviews Neuroscience* 4.5, pp. 417–422.

Niedermeyer, E. (1997). Alpha rhythms as physiological and abnormal phenomena. *International Journal of Psychophysiology* 26.1, pp. 31–49.

Nikulin, V. V., G. Nolte, and G. Curio (2011). A novel method for reliable and fast extraction of neuronal EEG/MEG oscillations on the basis of spatio-spectral decomposition. *NeuroImage* 55.4, pp. 1528–1535.

Nunez, P. L. and R. Srinivasan (2005). *Electric Fields of the Brain: The Neurophysics of EEG*. 2nd ed. Oxford University Press, USA.

Onton, J., A. Delorme, and S. Makeig (2005). Frontal midline EEG dynamics during working memory. *NeuroImage* 27.2, pp. 341–356.

Osman, A., S. Kornblum, and D. E. Meyer (1986). The point of no return in choice reaction time: controlled and ballistic stages of response preparation. *Journal of Experimental Psychology: Human Perception and Performance* 12.3, p. 243.

Papadopoulou, M., I. Evdokimidis, E. Tsoukas, A. Mantas, and N. Smyrnis (2010). Event-related potentials before saccades and antisaccades and their relation to reaction time. *Exp Brain Res* 205.4, pp. 521–531.

Parasuraman, R. (2003). Neuroergonomics: Research and practice. *Theoretical Issues in Ergonomics Science* 4.1-2, pp. 5–20.

Parasuraman, R. and G. F. Wilson (2008). Putting the Brain to Work: Neuroergonomics Past, Present, and Future. *Human Factors* 50.3, pp. 468–474.

Parra, L. C., C. D. Spence, A. D. Gerson, and P. Sajda (2005). Recipes for the Linear Analysis of EEG. *NeuroImage* 28.2, pp. 326–341.

Penfield, W. and E. Boldrey (1937). Somatic motor and sensory representation in the cerebral cortex of man as studied by electrical stimulation. *Brain: A journal of neurology*.

Penttonen, M. and G. Buzsáki (2003). Natural logarithmic relationship between brain oscillators. *Thalamus & Related Systems* 2.02, pp. 145–152.

Pfurtscheller, G. and A. Aranibar (1979). Evaluation of event-related desynchronization (ERD) preceding and following voluntary self-paced movement. *Electroencephalography and clinical neurophysiology* 46.2, pp. 138–146.

Pfurtscheller, G. and F. L. Da Silva (1999). Event-related EEG/MEG synchronization and desynchronization: basic principles. *Clinical neurophysiology* 110.11, pp. 1842–1857.

Pfurtscheller, G., G. R. Müller, J. Pfurtscheller, H. J. Gerner, and R. Rupp (2003). 'Thought'–control of functional electrical stimulation to restore hand grasp in a patient with tetraplegia. *Neuroscience letters* 351.1, pp. 33–36.

Pockett, S. (2004). Does consciousness cause behaviour? *Journal of Consciousness Studies* 11.2, pp. 23–40.

Pockett, S. and S. Purdy (2010). Are voluntary movements initiated preconsciously? The relationships between readiness potentials, urges and decisions. *Conscious will and responsibility: A tribute to Benjamin Libet*, pp. 34–46.

Polich, J. (1989). Frequency, intensity, and duration as determinants of P300 from auditory stimuli. *Journal of Clinical Neurophysiology* 6.3, pp. 277–286.

Pope, A. T., E. H. Bogart, and D. S. Bartolome (1995). Biocybernetic system evaluates indices of operator engagement in automated task. *Biological Psychology* 40.1–2, pp. 187–195.

Porbadnigk, A. K., N. Görnitz, C. Sannelli, A. Binder, M. Braun, M. Kloft, and K.-R. Müller (2015). Extracting latent brain states – To-

wards true labels in cognitive neuroscience experiments. *NeuroImage* 120, pp. 225–253.

Porbadnigk, A. K., M. S. Treder, B. Blankertz, J.-N. Antons, R. Schleicher, S. Möller, G. Curio, and K.-R. Müller (2013). Single-trial analysis of the neural correlates of speech quality perception. *Journal of Neural Engineering* 10.5, p. 056003.

Pribram, K. H. and D. McGuinness (1975). Arousal, activation, and effort in the control of attention. *Psychological review* 82.2, p. 116.

Prinzel, L. J., F. G. Freeman, M. W. Scerbo, P. J. Mikulka, and A. T. Pope (2000). A Closed-Loop System for Examining Psychophysiological Measures for Adaptive Task Allocation. *The International Journal of Aviation Psychology* 10.4, pp. 393–410.

Prinzel, L. J., F. G. Freeman, M. W. Scerbo, P. J. Mikulka, and A. T. Pope (2003). Effects of a psychophysiological system for adaptive automation on performance, workload, and the event-related potential P300 component. *Human Factors: The Journal of the Human Factors and Ergonomics Society* 45.4, pp. 601–614.

Putze, F., J.-P. Jarvis, and T. Schultz (2010). „Multimodal recognition of cognitive workload for multitasking in the car." In: *Pattern Recognition (ICPR), 2010 20th International Conference on*, pp. 3748–3751.

Raichle, M. E. (2009). A brief history of human brain mapping. *Trends in neurosciences* 32.2, pp. 118–126.

Reimer, B. and B. Mehler (2011). The impact of cognitive workload on physiological arousal in young adult drivers: a field study and simulation validation. *Ergonomics* 54.10, pp. 932–942.

Ritter, P. and A. Villringer (2006). Simultaneous EEG–fMRI. *Neuroscience & Biobehavioral Reviews* 30.6, pp. 823–838.

Roskies, A. L. (2010). How does neuroscience affect our conception of volition? *Annual Review of Neuroscience* 33, pp. 109–130.

Salvaris, M. and P. Haggard (2014). Decoding Intention at Sensorimotor Timescales. *PLoS ONE* 9.2, e85100.

Sannelli, C., C. Vidaurre, K.-R. Müller, and B. Blankertz (2011). Common Spatial Pattern Patches - an Optimized Filter Ensemble for Adaptive Brain-Computer Interfaces. *Journal of Neural Engineering* 8.2, 025012 (7pp).

Sarter, N. B. and D. D. Woods (1995). How in the world did we ever get into that mode? Mode error and awareness in supervisory control. *Human Factors: The Journal of the Human Factors and Ergonomics Society* 37.1, pp. 5–19.

Sauseng, P., J. Hoppe, W. Klimesch, C. Gerloff, and F. Hummel (2007). Dissociation of sustained attention from central executive functions: local activity and interregional connectivity in the theta range. *European Journal of Neuroscience* 25.2, pp. 587–593.

Scanziani, M. and M. Häusser (2009). Electrophysiology in the age of light. *Nature* 461.7266, pp. 930–939.

Scerbo, M. W., F. G. Freeman, and P. J. Mikulka (2003). A brain-based system for adaptive automation. *Theoretical Issues in Ergonomics Science* 4.1-2, pp. 200–219.

Schäfer, J., K. Strimmer, et al. (2005). A shrinkage approach to large-scale covariance matrix estimation and implications for functional

genomics. *Statistical applications in genetics and molecular biology* 4.1, p. 32.

Schmidt, E. A., M. Schrauf, M. Simon, M. Fritzsche, A. Buchner, and W. E. Kincses (2009). Drivers' misjudgement of vigilance state during prolonged monotonous daytime driving. *Accident Analysis & Prevention* 41.5, pp. 1087–1093.

Scholler, S., S. Bosse, M. S. Treder, B. Blankertz, G. Curio, K.-R. Muller, and T. Wiegand (2012). Toward a direct measure of video quality perception using EEG. *IEEE transactions on Image Processing* 21.5, pp. 2619–2629.

Schreuder, M., B. Blankertz, and M. Tangermann (2010). A new auditory multi-class brain-computer interface paradigm: spatial hearing as an informative cue. *PloS one* 5.4, e9813.

Schreuder, M., T. Rost, and M. Tangermann (2011). Listen, you are writing! Speeding up online spelling with a dynamic auditory BCI. *Frontiers in neuroscience* 5, p. 112.

Schubert, R., S. Haufe, F. Blankenburg, A. Villringer, and G. Curio (2009). Now you'll feel it, now you won't: EEG rhythms predict the effectiveness of perceptual masking. *Journal of cognitive neuroscience* 21.12, pp. 2407–2419.

Schubert, R., M. Tangermann, S. Haufe, C. Sannelli, M. Simon, E. A. Schmidt, W. E. Kincses, and G. Curio (2008). „Parieto-occipital alpha power indexes distraction during simulated car driving." In: *International Journal of Psychophysiology*. Vol. 69. 3.

Schultze-Kraft, M., R. Becker, M. Breakspear, and P. Ritter (2011a). Exploiting the potential of three dimensional spatial wavelet analysis to explore nesting of temporal oscillations and spatial variance in simultaneous EEG-fMRI data. *Progress in biophysics and molecular biology* 105.1, pp. 67–79.

Schultze-Kraft, M., D. Birman, M. Rusconi, C. Allefeld, K. Görgen, S. Dähne, B. Blankertz, and J.-D. Haynes (2014a). „A man vs. machine shootout duel: Do we have control over our choice-predictive brain signals?" In: *12th International Conference on Cognitive Neuroscience (ICON), Brisbane, Australia*.

Schultze-Kraft, M., D. Birman, M. Rusconi, C. Allefeld, K. Görgen, S. Dähne, B. Blankertz, and J.-D. Haynes (2015). „Predicting and interrupting movement intentions with a closed loop BCI." In: *Annual Meeting of the Organization for Human Brain Mapping (OHBM), Honolulu, USA*.

Schultze-Kraft, M., D. Birman, M. Rusconi, C. Allefeld, K. Görgen, S. Dähne, B. Blankertz, and J.-D. Haynes (2016a). The point of no return in vetoing self-initiated movements. *Proceedings of the National Academy of Sciences* 113.4, pp. 1080–1085. DOI: 10.1073/pnas.1513569112.

Schultze-Kraft, M., S. Dähne, G. Curio, and B. Blankertz (2013a). „Temporal and spatial distribution of workload-induced power modulations of EEG rhythms." In: *5th International BCI Meeting, Asilomar, USA*.

Schultze-Kraft, M., S. Dähne, G. Curio, and B. Blankertz (2014b). „Classification of visuomotor workload: A comparison of state-of-the-art

spatial filtering methods.“ In: *Annual Meeting of the Organization for Human Brain Mapping (OHBM), Hamburg, Germany*.

Schultze-Kraft, M., S. Dähne, M. Gugler, G. Curio, and B. Blankertz (2016b). Unsupervised classification of operator workload from brain signals. *Journal of Neural Engineering* 13.3, p. 036008. DOI: 10.1088/1741-2560/13/3/036008.

Schultze-Kraft, M., M. Diesmann, S. Grün, and M. Helias (2011b). Correlation transmission of spiking neurons is boosted by synchronous input. *BMC Neuroscience* 12.1, p. 1.

Schultze-Kraft, M., M. Diesmann, S. Grün, and M. Helias (2011c). „How much synchrony would there be if there was no synchrony?“ In: *Ninth Göttingen Meeting of the German Neuroscience Society, Göttingen, Germany*.

Schultze-Kraft, M., M. Diesmann, S. Grün, and M. Helias (2013b). Noise suppression and surplus synchrony by coincidence detection. *PLoS Comput Biol* 9.4, e1002904.

Schurger, A., M. Mylopoulos, and D. Rosenthal (2016). Neural Antecedents of Spontaneous Voluntary Movement: A New Perspective. *Trends in Cognitive Sciences* 20.2, pp. 77–79.

Schurger, A., J. D. Sitt, and S. Dehaene (2012). An accumulator model for spontaneous neural activity prior to self-initiated movement. *Proceedings of the National Academy of Sciences* 109.42, E2904–E2913.

Sellers, E. W., D. J. Krusienski, D. J. McFarland, T. M. Vaughan, and J. R. Wolpaw (2006). A P300 event-related potential brain–computer interface (BCI): the effects of matrix size and inter stimulus interval on performance. *Biological psychology* 73.3, pp. 242–252.

Shibasaki, H. and M. Hallett (2006). What is the Bereitschaftspotential? *Clinical neurophysiology* 117.11, pp. 2341–2356.

Slobounov, S., M. Hallett, and K. M. Newell (2004). Perceived effort in force production as reflected in motor-related cortical potentials. *Clin Neurophysiol* 115.10, pp. 2391–2402.

Slobounov, S., K. Fukada, R. Simon, M. Rearick, and W. Ray (2000). Neurophysiological and behavioral indices of time pressure effects on visuomotor task performance. *Cognitive Brain Research* 9.3, pp. 287–298.

Smith, K. (2011). Neuroscience vs philosophy: Taking aim at free will. *Nature* 477.7362, p. 23.

Sochůrková, D., I. Rektor, P. Jurák, and A. Stančák (2006). Intracerebral recording of cortical activity related to self-paced voluntary movements: a Bereitschaftspotential and event-related desynchronization/synchronization. SEEG study. *Experimental Brain Research* 173.4, pp. 637–649.

Sonnleitner, A., M. Simon, W. E. Kincses, A. Buchner, and M. Schrauf (2012). Alpha spindles as neurophysiological correlates indicating attentional shift in a simulated driving task. *International Journal of Psychophysiology* 83.1, pp. 110–118.

Soon, C. S., A. H. He, S. Bode, and J.-D. Haynes (2013). Predicting free choices for abstract intentions. *Proceedings of the National Academy of Sciences*.

Soon, C. S., M. Brass, H.-J. Heinze, and J.-D. Haynes (2008). Unconscious determinants of free decisions in the human brain. *Nature Neuroscience* 11.5, pp. 543–545.

Spehlmann, R. (1965). The averaged electrical responses to diffuse and to patterned light in the human. *Electroencephalography and clinical neurophysiology* 19.6, pp. 560–569.

Stanney, K. M., D. D. Schmorrow, M. Johnston, S. Fuchs, D. Jones, K. S. Hale, A. Ahmad, and P. Young (2009). Augmented cognition: An overview. *Reviews of Human Factors and Ergonomics* 5.1, pp. 195–224.

Stikic, M., R. R. Johnson, D. J. Levendowski, D. P. Popovic, R. E. Olmstead, and C. Berka (2011). EEG-derived estimators of present and future cognitive performance. *Frontiers in Human Neuroscience* 5.70.

Sturm, I., M. Treder, D. Miklody, H. Purwins, S. Dähne, B. Blankertz, and G. Curio (2015). Extracting the neural representation of tone onsets for separate voices of ensemble music using multivariate EEG analysis. *Psychomusicology: Music, Mind, and Brain* 25.4, p. 366.

Sutton, S., M. Braren, J. Zubin, and E. John (1965). Evoked-potential correlates of stimulus uncertainty. *Science* 150.3700, pp. 1187–1188.

Taylor, J. L. and D. I. McCloskey (1990). Triggering of preprogrammed movements as reactions to masked stimuli. *Journal of Neurophysiology* 63.3, pp. 439–446.

Taylor, J. L. and D. I. McCloskey (1996). Selection of motor responses on the basis of unperceived stimuli. *Experimental Brain Research* 110.1, pp. 62–66.

Thut, G., A. Nietzel, S. A. Brandt, and A. Pascual-Leone (2006). α-Band electroencephalographic activity over occipital cortex indexes visuospatial attention bias and predicts visual target detection. *The Journal of Neuroscience* 26.37, pp. 9494–9502.

Tomioka, R. and K.-R. Müller (2010). A regularized discriminative framework for EEG analysis with application to brain–computer interface. *NeuroImage* 49.1, pp. 415–432.

Treder, M. S. and B. Blankertz (2010). (C)overt attention and visual speller design in an ERP-based brain-computer interface. *Behavioral and brain functions* 6.1, p. 1.

Trevena, J. and J. Miller (2010). Brain preparation before a voluntary action: evidence against unconscious movement initiation. *Consciousness and cognition* 19.1, pp. 447–456.

Ušćumlić, M. and B. Blankertz (2016). Active visual search in non-stationary scenes: coping with temporal variability and uncertainty. *Journal of Neural Engineering* 13.1, p. 016015.

Usher, M. and J. L. McClelland (2001). The time course of perceptual choice: the leaky, competing accumulator model. *Psychological review* 108.3, p. 550.

Veltman, J. and A. Gaillard (1996). Physiological indices of workload in a simulated flight task. *Biological Psychology* 42.3, pp. 323–342.

Venthur, B., B. Blankertz, M. F. Gugler, and G. Curio (2010a). „Novel applications of BCI technology: psychophysiological optimization of working conditions in industry.“ In: *Systems Man and Cybernetics (SMC), 2010 IEEE International Conference on*. IEEE, pp. 417–421.

Venthur, B., S. Scholler, J. Williamson, S. Dähne, M. S. Treder, M. T. Kramarek, K.-R. Müller, and B. Blankertz (2010b). Pyff—A Pythonic Framework for Feedback Applications and Stimulus Presentation in Neuroscience. *Frontiers in Neuroscience* 4.179.

Verbruggen, F. and G. Logan (2008). Response inhibition in the stop-signal paradigm. *Trends in cognitive sciences* 12.11, pp. 418–424.

Vidal, J. J. (1973). Toward direct brain-computer communication. *Annual review of Biophysics and Bioengineering* 2.1, pp. 157–180.

Vigário, R. N. (1997). Extraction of ocular artefacts from EEG using independent component analysis. *Electroencephalography and clinical neurophysiology* 103.3, pp. 395–404.

Vogt, J., T. Hagemann, and M. Kastner (2006). The Impact of Workload on Heart Rate and Blood Pressure in En-Route and Tower Air Traffic Control. *Journal of Psychophysiology* 20.4, pp. 297–314.

Von Stein, A. and J. Sarnthein (2000). Different frequencies for different scales of cortical integration: from local gamma to long range alpha/theta synchronization. *International Journal of Psychophysiology* 38.3, pp. 301–313.

Walter, W. G., R. Cooper, V. J. Aldridge, W. C. McCallum, and A. L. Winter (1964). Contingent Negative Variation: an electric sign of sensorimotor association and expectancy in the human brain. *Nature* 203, pp. 380–384.

Weiskopf, N., K. Mathiak, S. W. Bock, F. Scharnowski, R. Veit, W. Grodd, R. Goebel, and N. Birbaumer (2004). Principles of a brain-computer interface (BCI) based on real-time functional magnetic resonance imaging (fMRI). *IEEE transactions on biomedical Engineering* 51.6, pp. 966–970.

Wenzel, M. A., J.-E. Golenia, and B. Blankertz (2016). Classification of eye fixation related potentials for variable stimulus saliency. *Frontiers in neuroscience* 10.

Whitham, E. M., K. J. Pope, S. P. Fitzgibbon, T. Lewis, C. R. Clark, S. Loveless, M. Broberg, A. Wallace, D. DeLosAngeles, P. Lillie, A. Hardy, R. Fronsko, A. Pulbrook, and J. O. Willoughby (2007). Scalp electrical recording during paralysis: Quantitative evidence that EEG frequencies above 20 Hz are contaminated by EMG. *Clinical Neurophysiology* 118.8, pp. 1877–1888.

Wickens, C. D. (2002). Multiple resources and performance prediction. *Theoretical issues in ergonomics science* 3.2, pp. 159–177.

Wilde, G. J. (1982). The theory of risk homeostasis: implications for safety and health. *Risk analysis* 2.4, pp. 209–225.

Wilson, G. F. and C. A. Russell (2007). Performance Enhancement in an Uninhabited Air Vehicle Task Using Psychophysiologically Determined Adaptive Aiding. *Human Factors* 49.6, pp. 1005–1018.

Winkler, I., S. Haufe, and M. Tangermann (2011). Automatic classification of artifactual ICA-components for artifact removal in EEG signals. *Behavioral and Brain Functions* 7.1, p. 1.

Wolpaw, J. R., N. Birbaumer, D. J. McFarland, G. Pfurtscheller, and T. M. Vaughan (2002). Brain–computer interfaces for communication and control. *Clinical neurophysiology* 113.6, pp. 767–791.

Wolpaw, J. R. and D. J. McFarland (2004). Control of a two-dimensional movement signal by a noninvasive brain-computer interface in humans. *Proceedings of the National Academy of Sciences of the United States of America* 101.51, pp. 17849–17854.

Wolpaw, J. and E. W. Wolpaw (2012). *Brain-computer interfaces: principles and practice*. OUP USA.

Wolters, C. and J. C. de Munck (2007). Volume conduction. *Scholarpedia* 2.3, p. 1738.

Wyler, A. R., G. A. Ojemann, E. Lettich, and A. A. Ward Jr (1984). Subdural strip electrodes for localizing epileptogenic foci. *Journal of neurosurgery* 60.6, pp. 1195–1200.

Yazawa, S., A. Ikeda, T. Kunieda, S. Ohara, T. Mima, T. Nagamine, W. Taki, J. Kimura, T. Hori, and H. Shibasaki (2000). Human presupplementary motor area is active before voluntary movement: subdural recording of Bereitschaftspotential from medial frontal cortex. *Exp Brain Res* 131.2, pp. 165–177.

Zander, T. O. and C. Kothe (2011). Towards passive brain-computer interfaces: applying brain-computer interface technology to human-machine systems in general. *Journal of Neural Engineering* 8.2, p. 025005.

LIST OF FIGURES

Figure 1 Chapter 2: Estimation and Removal of EOG Activity 19
Figure 2 Chapter 3: Experimental task 28
Figure 3 Chapter 3: Experimental structure 28
Figure 4 Chapter 3: Schematic Representation of the Data Analysis Workflow 30
Figure 5 Chapter 3: Impact of the Experimental Paradigm on Task Performance and Peripheral Physiological Measures 36
Figure 6 Chapter 3: Performance of Spatial-Filtering-Based Models 37
Figure 7 Chapter 3: Performance of Spatial-Filtering-Based Models, Single Subjects 38
Figure 8 Chapter 3: Performance Comparison of Channel-Based Models vs. Spatial-Filtering-Based Models 39
Figure 9 Chapter 3: Spatial Activation Patterns and Power Envelopes of Components 41
Figure 10 Chapter 3: Spatial Activation Patterns for the Beta Band 42
Figure 11 Chapter 3: Added Value of Peripheral Physiological Measures 44
Figure 12 Chapter 4: The readiness potential as reported in Kornhuber and Deecke in 1965 53
Figure 13 Chapter 4: Experimental Design 56
Figure 14 Chapter 4: Behavioral Results 59
Figure 15 Chapter 4: Mean readiness potential, EMG activity and button press distribution 61
Figure 16 Chapter 4: Waiting Time and Movement Duration 62
Figure 17 Chapter 4: Possible Trial Outcomes 63
Figure 18 Chapter 4: Percentage of Trial Outcomes 63
Figure 19 Chapter 4: Distribution of BCI Predictions Time-locked to EMG Onset 64
Figure 20 Chapter 4: Time-resolved Output of a Classifier 67
Figure 21 Chapter 4: Classification Accuracies of ERD Classifier 68
Figure 22 Chapter 4: Summary Model of Results 70
Figure 23 Appendix A: Supplementary Results 1 81
Figure 24 Appendix A: Supplementary Results 2 82
Figure 25 Appendix A: Supplementary Results 3 83
Figure 26 Appendix A: Supplementary Results 4 84
Figure 27 Appendix A: Supplementary Results 5 85
Figure 28 Appendix A: Supplementary Results 6 86

LIST OF TABLES

Table 1 Chapter 3: Overview of the Six Models Used to Predict Workload 34

Table 2 Appendix A: Overview of the Three Offline Analyses 87

Table 3 Appendix A: Summary of Responses to Question 1 88

Table 4 Appendix A: Summary of Responses to Question 2 89